R-5061

FACILITY FORM 602

N64-29187
(ACCESSION NUMBER)

(THRU)

112
(PAGES)

1
(CODE)

CR-58035
(NASA CR OR TMX OR AD NUMBER)

27
(CATEGORY)

ROCKETDYNE • A DIVISION OF NORTH AMERICAN AVIATION INC

NASA CONTRACT: NAS 7-124
FINAL REPORT FEBRUARY 1963

OTS PRICE

XEROX $

MICROFILM $

# In Extraterrestrial Landing Environments

## VOLUME III - Appendices

R-5061

# Propulsion Requirements for Soft Landing in Extraterrestrial Environments

Volume 3 - Appendices

February 1963

NAS 7-124

Prepared for
National Aeronautics and Space Administration

NASA Headquarters
Mr. H. Burlage

Ames Research Center
Mr. H. Hornby

Prepared by
Advanced Systems Section

Martin S. Bensky
M. S. Bensky
Responsible Engineer

Approved by

S. F. Iacobellis
S. F. Iacobellis
Section Chief
Advanced Systems

## FOREWORD

This document was prepared in compliance with the requirement for the final report for National Aeronautics and Space Administration contract NAS 7-124, "Propulsion Requirements for Soft Landing in Extraterrestrial Environments."

## ABSTRACT

29187

Volume III, "Propulsion Requirements for Soft Landing in Extraterrestrial Environments-Appendices," presents supplementary investigations related to the analyses described in Volumes I and II. This volume contains a survey of extraterrestrial environments, a description of vehicle systems for several interplanetary missions, an investigation of start systems for extraterrestrial landing propulsion systems, a design study of lunar landing impact devices, and an analytical study of propellant storage on the lunar surface.

author



FORM 608-B (LEDGER) REV. 1-58

TABLE OF CONTENTS - VOLUME III

| | PAGE |
|---|---|
| FOREWORD | i |
| ABSTRACT | i |
| TABLE OF CONTENTS | ii |
| APPENDIX A | |
| Extraterrestrial Environments | 1 |
| APPENDIX B | |
| Vehicle Requirements for Interplanetary Missions | 14 |
| APPENDIX C | |
| Engine Start Techniques for Extraterrestrial Landing Engines | 44 |
| APPENDIX D | |
| Landing Gear Systems for Extraterrestrial Landing Vehicles | 67 |
| APPENDIX E | |
| Lunar Surface Storage of Liquid Propellants | 83 |
| REFERENCES | 112 |

# APPENDICES

## APPENDIX A

### EXTRATERRESTRIAL ENVIRONMENTS

#### Extraterrestrial Atmospheres and Surfaces

The data compiled from references 1 through 22 to describe the environmental conditions of the moon, Mars, Venus and Mercury are presented in Figures 1 and 2 and Tables 1 through 6. It should be noted that at present, wide disparities exist in the values of certain characteristics as measured by different researchers. Continued research, particularly that performed by unmanned interplanetary probes, will serve to clarify much of the data presented; however, these data currently represent the best available, and are employed for assistance in the design and analysis of landing propulsion systems.

The general characteristics of the planetary bodies of interest are presented in Tables 1 and 2. Atmosphere data for Earth, Mars and Venus are shown in Figures 1 and 2. Tables 3, 4, 5 and 6 present available versions of the atmospheric and topographical features of the Moon, Venus, Mars and Mercury. These tables include a review based on the available cross section of opinions.

#### Effects of Rocket Exhausts

Chemical Reactions. Several potential propellants were considered for engines performing soft landings on extraterrestrial bodies. Liquid rocket engines may employ bipropellants such as $O_2$/RP, $O_2H_2$, $F_2/H_2$, $F_2/N_2H_4$, CTF/$N_2H_4$, $N_2O_4/N_2H_4$, or CTF/$B_5H_9$. Liquid monopropellants may be $H_2O_2$, $N_2H_4$ and Cavea B. Solid rockets would probably employ PBAA/AL/AP and a hybrid, possibly CTF/LiH. These representative propellants were examined regarding compatibility with planet environment and surface conditions.

Moon and Mercury. The moon and planet Mercury have essentially vacuum conditions. If gases do exist, they are thought to be only traces which will present no problem to propellants or exhaust products. The surface conditions (considered to be essentially the same except Mercury probably being more crusty) are thought to consist of pumice, lava, silicates, rock, sandstone, and gypsum. The fluorine propellants are reactive with minerals but the absence of oxygen or water in the atmosphere precludes sustained combustion in the event of spillage.



FORM 608-B (LEDGER) REV. 1-58

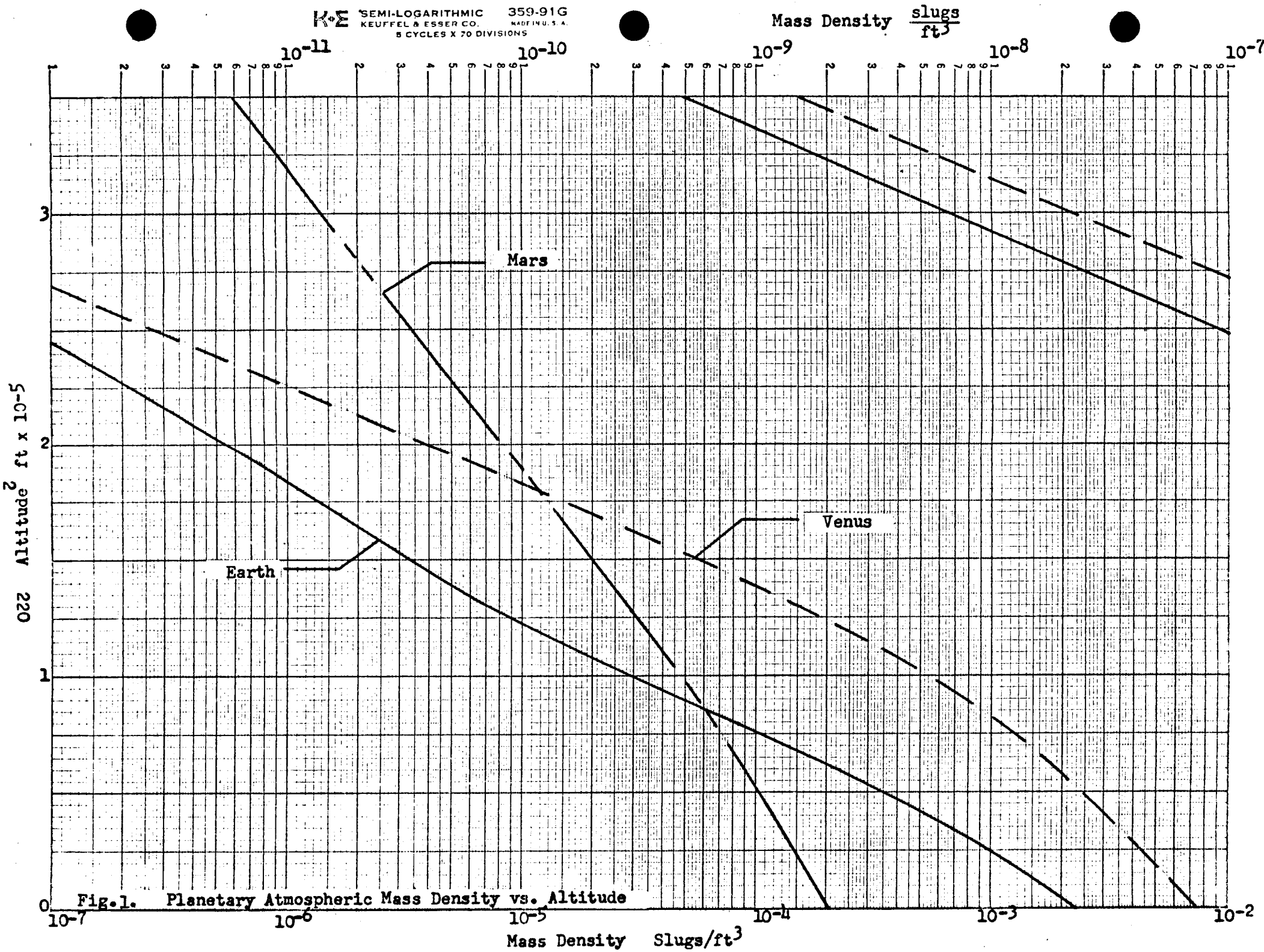


Fig.1. Planetary Atmospheric Mass Density vs. Altitude

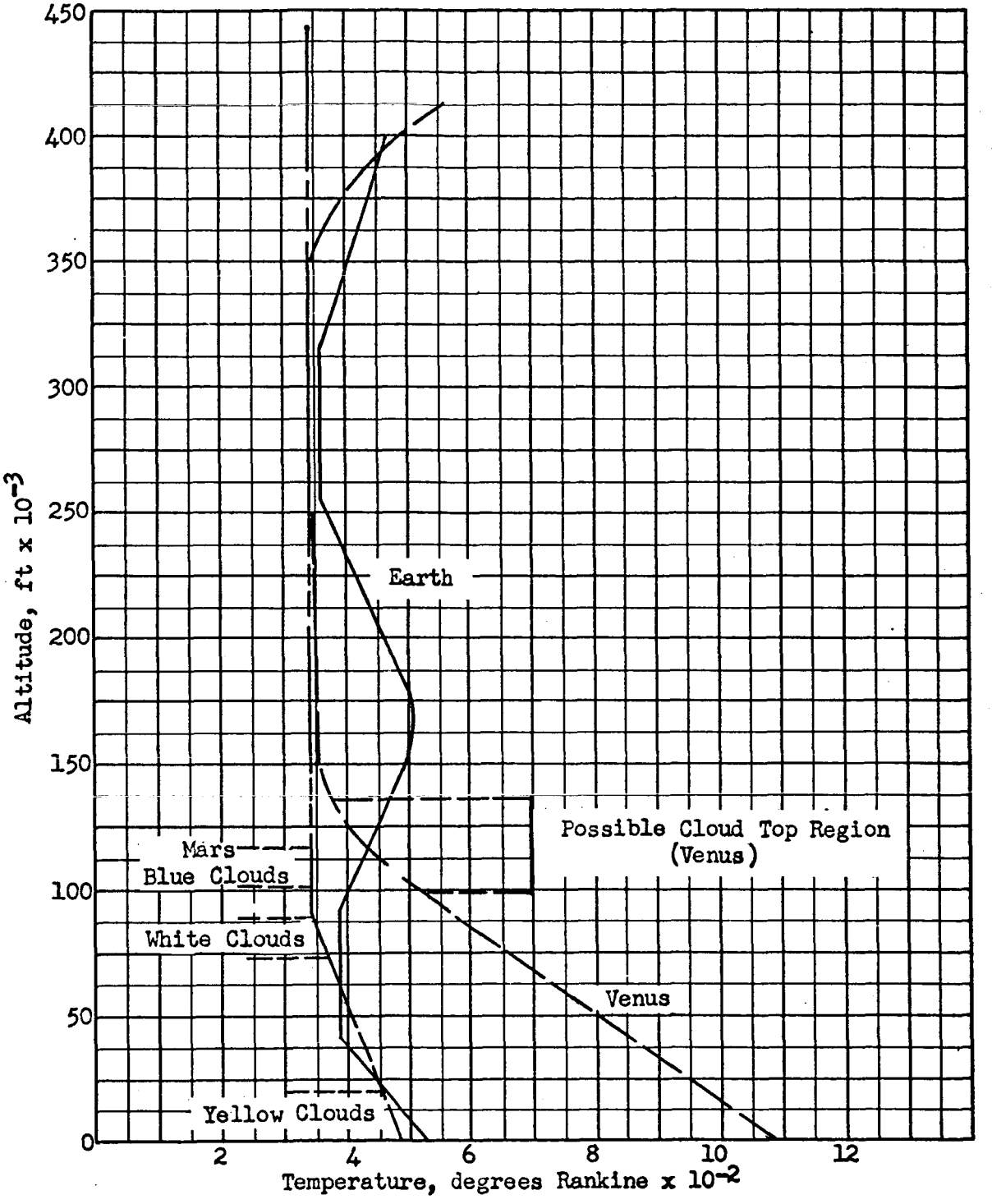


Figure 2. Planetary Temperature vs Altitude

TABLE 1

GENERAL PLANET INFORMATION GUIDE

| | EARTH | MOON | VENUS | MARS | MERCURY |
|---|---|---|---|---|---|
| Mean Distance From Sun, Millions of N.Mi. | 80.7 | 80.7 | 58.3 | 122.9 | 31.2 |
| Mean Distance From Earth, Millions of N.Mi. | ---- | 0.2074 | 22.6 Least<br>139 Greatest | 20.5 Least<br>26.9 Greatest | 43.4 Least<br>118 Greatest |
| Mean Diameter, N. Mi. | 6975.74 | 1880 | 6648.9 | 3596 | 2612.8 |
| Surface Gravity, ft/sec$^2$ | 32.2284 | 5.1565 | 28.387 | 12.5670 | 12.2447 |
| Escape Velocity, ft/sec | 36,700 | 7880 | 34,100 | 16,700 | 14,100 |
| Oblateness | 1/298.38 | 0 | 0 | 1/192 | 0 |
| Albedo | 0.39 | 0.07 | 0.64-0.71 | 0.148 | 0.058 |
| Moons | 1 | --- | 0 | 2 | 0 |
| Thermal Radiation | 444 BTU/FT$^2$ HR | Same as Earth | 848 BTU/FT$^2$ HR | 191 BTU/FT$^2$ HR | 3100 BTU/FT$^2$ HR |
| Nuclear Radiation | Van Allen Belts<br>Solar Flares | 4 REM/HR AVG<br>40 REM/HR MAX | More Severe Than Earth | ---- | ---- |
| Meteoroids | Yes | Yes | Yes | More Iron Meteoroids | ---- |
| Magnetic Fields | Yes | Weaker Than Earth | Stronger Than Earth | Weaker Than Earth | ---- |



ROCKETDYNE
A DIVISION OF NORTH AMERICAN AVIATION INC

TABLE 2

ENVIRONMENT DESIGN GUIDE

| | EARTH* | MOON | VENUS | MARS | MERCURY |
|---|---|---|---|---|---|
| ATMOSPHERE | OVER 500,000 FT | None | approx. 5000,000 ft Thick | approx. 1,500,000 ft Thick | None or ≈ 45 ft Thick |
| PRESSURE | $P_{SL}$ = 2116 lb/ft$^2$ | 2116 x $10^{-12}$ lb/ft$^2$ | $P_{SL}$ = 8800 lb/ft$^2$ | $P_{SL}$ = 178 lb/ft$^2$ | Same as Moon |
| TEMPERATURE | $T_{SL}$ = 519°R | -- | $T_{SL}$ = 1070°R | $T_{SL}$ = 490 °R | ---- |
| MASS DENSITY | $\rho_{SL}$ = 2.377 x $10^{-3}$ Slugs/Ft$^3$ | 2.377 x $10^{-15}$ Slugs/Ft$^3$ | $\rho_{SL}$ = 7.5 x $10^{-3}$ Slugs/Ft$^3$ | $\rho_{SL}$ = 2.1x$10^{-4}$ Slugs/ft$^3$ | Same as Moon |
| SPEED OF SOUND | $a_o$ = 1116.89 Ft/Sec @ S.L. STD | --- | 1.01 $a_{o\ Earth}$ | 0.81 $a_{o\ Earth}$ | -- |
| COMPOSITION | 21% $O_2$, 78% $N_2$, Rare Gases | Possibly Some Unknown Proportions of A, Kr, Xe, $SO_2$, $CO_2$, $H_2S$, $O_3$ | 90% $CO_2$, 10% $N_2$ By Weight | 95% $N_2$, 5% A By Volume | Possibly $CO_2$ |
| WIND | YES | None | Windy With Gusts | Up to 20 MPH - Possibly Higher | None |
| CLOUDS | YES | None | Opaque 98,000 ft to 132,000 ft Cloud Top | White<br>Yellow<br>Blue | None |
| HUMIDITY; RAIN | YES | None | --- | --- | None |
| LIGHTNING | YES | None | Possible | --- | None |
| ECLIPSE EFFECT | YES | Rapid Change of 340 R° | --- | --- | --- |
| TOPOGRAPHY | | | | | |
| MAPS | MANY AVAILABLE | NAA/SID | NONE | NAA/SID MAP | NONE |
| SURFACE TERRAIN | | | | | |
| MOUNTAINS, PLAINS, SEAS, VALLEYS | ALL EXIST - VARIABLE SMOOTHNESS | ROUGH, MOUNTAINOUS, CRATERS, PITS, RIDGES | DRY, DUSTY & MOUNTAINOUS | RELATIVELY SMOOTH, ELEVATED AREAS & PLATEAUX, NO MOUNTAINS OVER 9000 FT, DESERTS | ROUGH & IRREGULAR, PARCHED |
| SURFACE COMPOSITION RIGIDITY OR STRESS | ROCK, WATER, DUST, ETC. | DUST (2-3 CM) ROCKY 250 psi to 10000 PSI CRUSHING STRESS | UNKNOWN | SIMILAR TO LIMONITE (IRON HYDROXIDE) VEGETATION POSSIBLY | CRUSTY LAVA & ROCK |
| SURFACE TEMPERATURE | 350 °R to 600 °R | 210 °R to 720 °R | POSSIBLY 1060 °R | 366 °R to 546 °R | TWILIGHT ZONE 260 °R to 960 °R |
| VOLCANOS | YES | POSSIBLE | UNLIKELY | UNLIKELY | ---- |
| FLOODS | YES | NO | VERY UNLIKELY | --- | NO |
| EARTHQUAKES | YES | POSSIBLE | UNLIKELY | --- | --- |

*ARDC MODEL ATMOSPHERE NO. 86, 1956

FORM R 18-G-18

TABLE 3

MOON LITERATURE REVIEW

| | REF. 1 | REF. 2 | REF. 3 | REF. 4 | REF. 5 | REF. 6 | COMMENTS | CONSENSUS |
|---|---|---|---|---|---|---|---|---|
| ATMOSPHERE | | | | | | | | |
| Surface Pressure | $2116 \times 10^{-12}$ lb/ft$^2$ | | | | | | Most authors suggest a vacuum for the atmosphere | $2116 \times 10^{-12}$ lb/ft$^2$ |
| Surface Density | $2.337 \times 10^{-12}$ Slugs/Ft$^3$ | | $10^{-4}$ to $10^{-13}$<br>$2.337 \times 10^{-13}$ Slugs/Ft$^3$ | | $10^{-4}$ to $10^{-13}$<br>$2.337 \times 10^{-13}$ Slugs/FT$^3$ | | Values higher than $10^{-9}$ are omitted because they are inconsistent with other findings | $2.337 \times 10^{-15}$ Slugs/Ft$^3$ |
| Composition | $SO_2$, $O_3$, A, $K_i$, $X_e$ (Suggested but not Verified) | | | | $CO_2$, $H_2S$, $SO_2$ Suggested but not Verified | | There is general agreement that the atmosphere may contain some of the heavy gases in unknown proportions | A, Kr, $X_e$, $SO_2$ $CO_2$, $H_2S$, $O_3$ |
| Surface Temperature | Variation from 672 °R Sub-solar pt. to 220 °R Dark Side | | | | Lunar Day 720 to 540 °R<br>Lunar Night 220 °R<br>Temp. falls very rapidly | Mid-day at equator 675 °R, Midnight 210 °R, Max. Temp. much lower at poles | Review of all references used indicates a max. daily temp. of 720 °R & a min. night time temp. of 210 °R | 720° to 210 °R |
| Eclipse Effect on Temp. | | | Approx. 340 R° Change in Temp. per Hour | | | | During eclipse, there is a very rapid change of approx. 340 R° | |
| TOPOGRAPHY | | | | | | | | |
| General Description | Surface extremely rough, many small pits, depressions & elevations. Radio active dust, varying in depth from several ft. to large areas free of dust. | Highlands more rugged than maria in gross topography. Large amts. of rubble present on highland surface & surrounding late craters on maria. Maria are lava plains covered by burst vesicles with max. dia. of 3 ft & 1 or 2 ft deep. Surface covered by dust. estimates of depth 0.2 to 3 cm. Possibility of dust being sintered. | Micro structure of surface very rough, many small pits intermixed with loose stones, all of this being covered with thin layer of silica dust of ½ millimeter grain size. Mountain surfaces are not steep but may have frequent pockets of dust & areas of exposed granite or balsaltic rock. Mean dust layer in mountain of approx. 1 millimeter. Composition & depth of maria unknown. | Surface composed of pumice type rock and dust in varying proportions. Suggested values for crushing strength<br>Low Strength S = 250 psi<br>Ave. Strength S = 2000 psi<br>Hi. Strength S = 10,000 psi | | Surface wholly or partly covered with layer of ash or dust, presumably volcanic or meteoric at a depth of 1 or 2 in. | Surface very rough, larger rocks probably in the highlands surrounding craters. Highlands or continents more rugged than maria. Maria may be covered with many small pits & burst vesicles ranging in size from the very large visible craters down to 2 or 3 ft in depth & dia. The surface is probably covered with a layer of dust that may be compared to pumice. The depth of the dust layer is generally thought to be 2 or 3 cm. There may be dust free areas in the highlands of exposed rock | Highlands<br>more rugged, larger rocks, more rigid surface, dust free areas, larger craters, greater slopes,<br>Maria<br>2 to 3 CM dust layer, many small pits, low walled craters & ridges, smoother over-all topography. |
| Continents | Cover 60% of surface | More rugged than maria | Higher frequency of larger craters. | | | | | |
| Seas or Maria | Cover 40% of surface plains dotted with craters and have very long low ridges | | Composition & depth of surface unknown. Low walled craters. | | | | | |
| Walled Plains | Ave. Dia. 508000 ft<br>Ave. Depth 12,450 ft<br>Ave. Rim height 6,600 ft | | | | | | | |
| Craters | Ave. Dia. 180,000 ft<br>Ave. depth 8,530 ft<br>Ave. Rim height 4,200 ft | Dia. 164,000 ft. have mean inner slope of 28° | | | | | | |
| Mountains | Highest peaks 26,000 ft above maria | | | | | | | |

TABLE 5

PLANET MARS LITERATURE REVIEW

| ITEM | REF. 10 | REF. 11 | REF. 12 | REF. 13 | REF. 14 | COMMENTS | CONSENSUS |
|---|---|---|---|---|---|---|---|
| **ATMOSPHERE** | | | | | | | |
| Surface Pressure | 216.6 lb/ft$^2$ | 178 lb/ft$^2$ decreasing by 1/10 for 128,000 ft change in altitude | 188 lb/ft$^2$ decreasing by 1/10 for 156,000 ft increase in altitude | | | Possibly 650,000 ft. thick | Surface Press. 178 lb/ft$^2$ decreasing by 1/10 for a 128,000 ft increase in altitude. |
| Surface Density | Mass of Atmos. over unit area = 1/8 to 1/3 that on earth | Mass of Atmos. over unit area = 1/5 that on earth | | | | | Mass of atmos. over unit area 1/5 that on earth |
| Composition | gas / % Volume<br>$N_2$ / 97.5<br>$O_2$ / .1<br>A / 1.2<br>$CO_2$ / 1.25 | gas / % vol.<br>$N_2$ / 95<br>A / 5<br>$CO_2$ / 1<br>$H_2O$<br>Ne<br>Kr<br>Xe<br>very small amounts | $CO_2$ positively ident. 2 % as much as on earth<br>98% by Vol. $N_2$<br>No evidence of $O_2$ | | N, Small amts. A & $CO_2$, possibly a trace of O | | 95% $N_2$<br>5% A<br>by Volume |
| Surface Temperature | Sub solar point<br>546 °R - perihelion<br>499 °R - aphelion<br>312 °R to 384 °R in winter hemisphere | Mean 450 °R, Diurnal variation at equator 366 °R to 546 °R temp<br>Alt. vs. Temp<br>5-82,000 ft Lapse Rate = 1.925 x $10^{-3}$ R°/ft<br>82,000 ft-444,000 ft -325 °R ± 90 R° -probably increases to 4.5 x $10^6$ ft | Mean 450 °R<br>Tropical regions 510°R to 384°R | 366 °R to 528 °R light areas<br>366 °R to 550 °R dark areas<br>overall daily range 100 to 180 R° | Diurnal Temp. variations of 50 R° at equator. Greater temp. extremes in southern hemisphere | 546 °R to 366 °R Range | 546 °R max.<br>366 °R min. |
| Cloud Cover | | | All Clouds below 98,000 ft | | Transparent Clouds | | |
| White Clouds | White clouds<br>Tiny ice crystals elevation 65,600 to 82,000 ft. | Ice crystals larger than 1 micron diameter | Ice crystals larger than 1 micron | | Extend to 60,000 or 70,000 ft | White clouds are composed of ice crystals & at altitude of 65,600 ft to 82,000 ft. | |
| Yellow Clouds | Dust, elevation up to 16,400 ft more frequent at perihelion | Low alt. - large areas dust storms from surface winds | Due to dust storms from winds over desert areas | | Layer of ice crystals of 35,000 to 50,000 ft. yellow clouds may be dust | Yellow clouds are composed of dust due to surface winds over desert areas. Alt. up to 16,400 ft. | |
| Blue Clouds | Blue clouds & violet haze layer. Alt. 98,500 to 115,000 ft possibly $H_2O$ or $CO_2$ | Same height as haze layer, 3 to 10 times the density | Condensation of moisture on smaller particles of the violet haze | | Whitish haze could be hoar-frost or ice fog. | Blue clouds are probably water droplets or ice crystals at altitude of 98,500 ft. | |
| Violet Haze | | Layer several 1000 ft. thick, 32810 ft-65,600 ft. alt. - Ice crystals 1 micron diameter | Finely divided dust or water droplets 0.1 to 1.0 micron diameter | | | Violet haze - less dense layer of blue cloud formation | |
| Rain | | No | | | | | |
| Snow | | Doubtful | | | | | |
| Frost | | Yes | | | | | |
| Winds | | Up to 20 m.p.h. | | | | | |
| **TOPOGRAPHY** | | | | | | | |
| General Description | No mountains can exist over 6000 to 9000 ft. Desert areas of albedo similar to earth deserts. Possible limonite or igneous rock of silicate of aluminum. There is strong evidence of some areas being covered with vegetation or growth. | Light areas cover more than ½ of surface. Dust covered deserts composed of limonite or felsitic rhyolite. Dark areas unknown probable that surface conditions are same as light areas. | Surface appears exceptionally smooth free from mountains & depressions<br>Ice caps - frozen $H_2O$<br>Canals - nature unknown. | Surface very dusty fine grains. Desert surfaces have properties similar to terrestrial limonite. Dark surface area probably vegetation or volcanic ash. Canals-Nature unknown. | Broad reddish tracts or "deserts" cover 3/4 of surface. Color may be due to oxidized minerals. Darker areas probably covered with lowly vegetation. Well defined polar ice caps undergo seasonal changes. | | Surface is relatively smooth with no mts. higher than 9000 ft. but elevated areas or plateaux do exist. This is suggested by the polar ice caps. Lighter areas are considered desert with a surface composition similar to limonite (iron hydroxide). Darker areas that change color seasonally are probably regions of very thick vegetation. |

TABLE 4

PLANET VENUS LITERATURE REVIEW

| ITEM | REF. 15 | REF. 20 | REF. 10 | REF. 16 | REF. 17 | REF. 14 | REF. 18 | COMMENTS | CONSENSUS |
|---|---|---|---|---|---|---|---|---|---|
| ATMOSPHERE | | At least 98,500 ft.deep | | | | | | At least 328,000 ft. thick. | approx.500,000 ft. |
| Pressure | Alt.(ft) / Press. ($lb/ft^2$)<br>0 / $10.6x10^6$<br>131,500 / 2116.0<br>230,000 / 21.16<br>328,100 / .2116 | Same as Ref. 15 | Surface Press. 1692 to 21160 $lb/ft^2$ | | Cloud Top Press. 189 $lb/ft^2$ | | | | |
| Density | | | | | | | See Curve. | | |
| Composition | $CO_2$ above cloud layer & possibly $N_2$ & Argon. Below cloud layer unknown. | $CO_2$ above clouds. Clouds possibly carbon suboxide, dust or $H_2O$ vapor. | 90% by wt. $CO_2$. Most of balance $N_2$. | $CO_2$ positively identified. | $CO_2$ 15% by volume. | $CO_2$, 250 times as much per unit vol. as earth. Perhaps 2% as much O or $H_2O$ vapor. N may be present. | Constituent % Wt.<br>$N_2$ 8 to 10<br>$CO_2$ 90 to 92<br>A Trace. | $CO_2$ seems to predominate. | 90% $CO_2$ By Wt.<br>10% $N_2$<br>Clouds are dust or $H_2O$ vapor. |
| Temperature | 1082°R surface temp. to 540°R above cloud layer. 328,000 above cloud layer temp. of 2700°R may exist. | Same as Ref. 15. | 424°R above cloud layer 521 to 540°R within clouds. 1032°R ± 180° surface of Planet. | "visible" surface temp. 427°R. Small temp. difference between day & night side. | Cloud Top Temp. 427°R. | | | | |
| Winds | Strong convective winds probable. | | | Stratified atmos. in which convection & turbulent air motions are supressed. | | | | Winds seem to prevail. | Assume windy conditions. |
| Lightning | Possible. | Possible. | | | | | | | |
| Cloud Cover | Possibly $H_2O$ or Dust. | 131,500 ft. cloud top. | Very opaque clouds. | | | | | Dust or $H_2O$ vapor 98,000 to 131,000 ft. top of clouds. | 98,000 to 131,000 ft. cloud top. |
| TOPOGRAPHY | | | | | | | | | |
| General Description | Probably very dry, aver.temp. 1032°R, variations with seasons. Surface winds may produce dust storms. | Same as Ref. 15. | Very dry surface. | Infers a universal ocean, but at least the upper portion of this ocean is a liquid other than water (possibly hydrocarbons) & below top layer may be water. This ocean is covered by a thin smog layer & the top of this smog is the visible surface. It is believed that the temp. will not change greatly within or below this layer, Therefore surface temp. will be slightly higher than visible surface temp. | | The surface remains entirely hidden below the Atmosphere. It has been pictured as a huge dust bowl, a continuous ocean, or rugged mountainous terrain. | | It is the general opinion that if the surface temp. of 1082°R is accepted, then there can be no oceans of water or hydrocarbons. This leaves the dry dusty surface conditions as the most likely. | Dry, crusty surface similar to Moon. |

# TABLE 6

## PLANET MERCURY LITERATURE REVIEW

| ITEM | REF. 10 | REF. 12 | REF. 14 | COMMENTS | |
|---|---|---|---|---|---|
| ATMOSPHERE | No detectable Atmosphere | None or very thin (.003 that of earth) | May be slight & thin | Even if thin (i.e. .0003 of earth alt.) would give 30-45 ft of atmos. | Consider none or similar to moon |
| Pressure | | $1.56 \times 10^{-5}$ lb/ft$^2$ | | Not known | 0 or about $2116 \times 10^{-12}$ lb/ft$^2$ |
| Density | | | | Not known | None or same as moon $2.337 \times 10^{-15}$ slubs/ft$^3$ |
| Composition | | No $N_2$, $O_2$, or $H_2O$ Possibly $CO_2$ | | Possibly $CO_2$ but not verified | None |
| Surface Temperature | Subsolar Point 1284 °R Perihelion anti-solar point is few degrees R | @ Mean Distance from sun @ sub-solar point temp. is 1098 °R (1233 °R @ Perihelion) (1000 °R @ Aphelion) Unlighted region 0 °R | 1230 °R max. 260 °R min. | Sunside between 1010 °R & 1260 °R depending on orbit location. Cold side 0 °R twilight zone may be 260 °R to 960°R. Landings (if made) will probably be in twilight zone | Assume twilight zone 260 °R to 960 °R |
| TOPOGRAPHY | | | | | |
| GENERAL | | Some observed markings. Possibly like moon with very irregular rough surface | Permanent dark patches seen by telescope. Probably mountainous | Rough & irregular surface | Assume as rough as moon highlands for twilight zone |
| SURFACE COMPOSITION | | Thought to be rock composed of basalt and dark lava | Rocky terrain barren & parched on sunlit side | Appears to be rocky. Probably very crusty & brittle on sun side. Twilight zone may exhibit same type of surface. Should be more crusty than moon | Rock or lava and crusty |

The moon temperatures (-250 to 260 F.) and the Mercury temperatures (twilight zone estimate - 200 to 500 F.) may result in storage problems for all the propellants, and design protection appears necessary. Propellants may experience autoignition, chemical breakdown, thermal expansion, and high vapor pressures at the high temperatures. The low temperatures present freezing, thermal shrinkage and contraction problems.

Venus. The Venus atmosphere is comprised of $CO_2$ and $N_2$, with possible traces of A and O. The absence of oxygen negates propellant or exhaust product reactions and would be similar to the Moon and Mercury combustion conditions. If ice crystale (i.e. water vapor) are a constituent in the Venus clouds, this could provide a fire hazard to some propellants such as the fluorines.

The Venus surface composition is unknown, so no prediction of propellant compatibility can be made. The estimated surface temperature of 600 F. will require design protection of the propellants.

Mars. The Mars atmosphere is estimated to consist of 95 percent $N_2$ with the remainder $CO_2$ and A. Traces of $O_2$ and the rare gases are possibilities. Here again the absence of oxygen negates hazards of propellants and exhaust products.

The surface temperatures (-94 to 86 F.) should only be a problem at the cold extremes requiring some protection.

The surface composition may be limonite (iron hydroxide) which may react with some fuels such as hydrazine. However, no serious hazards appear to exist in the nonoxygen environment.

Visual Interference. Ground visibility is dependent upon the nature of the landing rocket exhaust pattern and on the properties of the exhaust gases. In order to determine the luminosity of a gas, it is necessary to have a temperature and pressure mapping in addition to absorption and emissivity coefficients as a function of temperature and pressure. A full and accurate mapping of the temperature and pressures would require an extended program, since the flow field is complex. However, approximate values along the shock front can be readily obtained. The absorption and emissivity coefficients for NTO/50-50 UDMH-$N_2H_2$, are not available in the visible spectrum but only in the infrared range. An extensive experimental program would be needed to determine these values.

A knowledge of the functional relationship between the emissivity of gases and the temperature and pressure shows that the emissivity is low if the temperature and/or pressure is low. This prompted an investigation into some representative values for the temperatures and pressures in the flow field.



FORM 608 B (LEDGER) REV. 1 58

It was first necessary to determine the free jet boundary of the flow fields. The engine parameters used were expansion ratio, ( $\epsilon$ ) of 40:1 and ratio of specific heats, ( $\gamma$ ) of 1.25. The ambient pressure of ($P_a$) is taken as 0. Using these values and assuming an 80-percent bell nozzle, and that the flow can be approximated at the exit lip of the nozzles by two-dimensional Prandtl-Meyer flow, the free jet boundary is predicted as follows: From a computed flow analysis of a 40:1 80-percent bell, the exit Mach no., $M_e$, is determined as 4.24; the exit contour angle, $\theta_e$, as 8.1 degrees; and the Prandtl-Meyer turning angle, $\omega_e$, is 85.5 degrees. For $\gamma = 1.25$, $\omega_{max} = 180$ degrees, the free jet boundary angle is then given as:

$$\omega_{max} = \omega_e + \theta_e = 180-85.5+8.1 = 102.6 \text{ degrees}$$

Using this as the approach flow angle of impingement for very large Mach numbers, an approximate shock pattern can be determined.

Since weak oblique shocks occur under the influence of small flow turning angles and strong, nearly normal shocks occur with large flow turning angles, it was necessary to investigate both cases. Computations were performed to determine the oblique shock properties at $\gamma = 1.25$ and for normal shocks at high Mach numbers. The results of these show that deflection angles above 53 degrees cause strong shocks and above Mach number 10.0, the pressure after shock is very small while the temperature is substantially equal to the combustion chamber temperature.

Using the jet spreading data from earlier studies, Mach number values can be found in front of the shocks as a function of distance from the nozzle exit after the shock front has been located. The shock front is located by using the shock polar or normal shock technique, whichever is applicable. Using these Mach numbers, the temperature and pressure ratios can be determined across the shock by normal shock relations. A straight line was used to approximate the shape of the shock front. This was based on assuming that the direction of the flow field was parallel to the free jet boundary. In reality, the flow becomes more axial as one goes downstream. This would cause the actual shock front to curve away from the vehicle somewhat. However, the straight line approximation gives values on the conservative side.

As the low pressures encountered, the emissivity in the visible range can be expected to be quite low. With a reasonable amount of background light, such as reflection of the sun from the Earth, this intensity is low enough to cause negligible visibility problems.



FORM 608 B (LEDGER) REV. 1 58

Lunar Surface Interactions. An investigation into the interaction of the main thrust chamber jet with the lunar surface has been attempted. A detailed theoretical analysis was not attempted at this time. In essence, a study of this nature would involve determining the momentum transport of the gases to the surface particles. The determination of the Mach disc which occurs before impingement of the jet on the surface would have to be a trial and error procedure. Either laborious hand calculations or an IBM program is needed to provide the desired result. In view of the lack of knowledge of the nature of the lunar surface and dust particles, such a task would be of questionable value.

Reference ( 23) shows the experimental results of a study conducted to determine the nature of a lunar surface-exhaust jet interaction. In one phase of this study, the lunar surface was represented by 0.010-inch diameter white sand particles. A vacuum system was used to simulate lunar ambient conditions. The nozzle total-to-ambient pressure ratio was maintained between 100,000:1 and 10,000:1 over a 2.7 second period while erosion patterns were recorded photographically. Descent heights were varied from 200 to 600 throat diameters and the erosion pattern varied from a concave hole of 200 to 250 throat diameters. The depth remained essentially constant at 60 throat diameters. Assuming a main thrust chamber throat diameter, $D_t = 6.6$ inches gives an average hole diameter of 225 $D_t$ or 124 ft. and 33.2 ft. as the hole depth. The erosion may not be quite as severe as this in an actual lunar landing. First, the jet will spread out more than that of this experimental simulation, allowing less gases to hit the surface. Second, some investigators believe the surface to be hard rather than soft.

Figure 3 shows the expected particle trajectory for a lunar landing. In all known cases of such an interaction, the particles are always forced away from the vehicle and never hit the vehicle. An average value of 50 degrees may be taken as the angle of the particles as they are blown away from the surface.



FORM 608 B (LEDGER) REV. 1 58

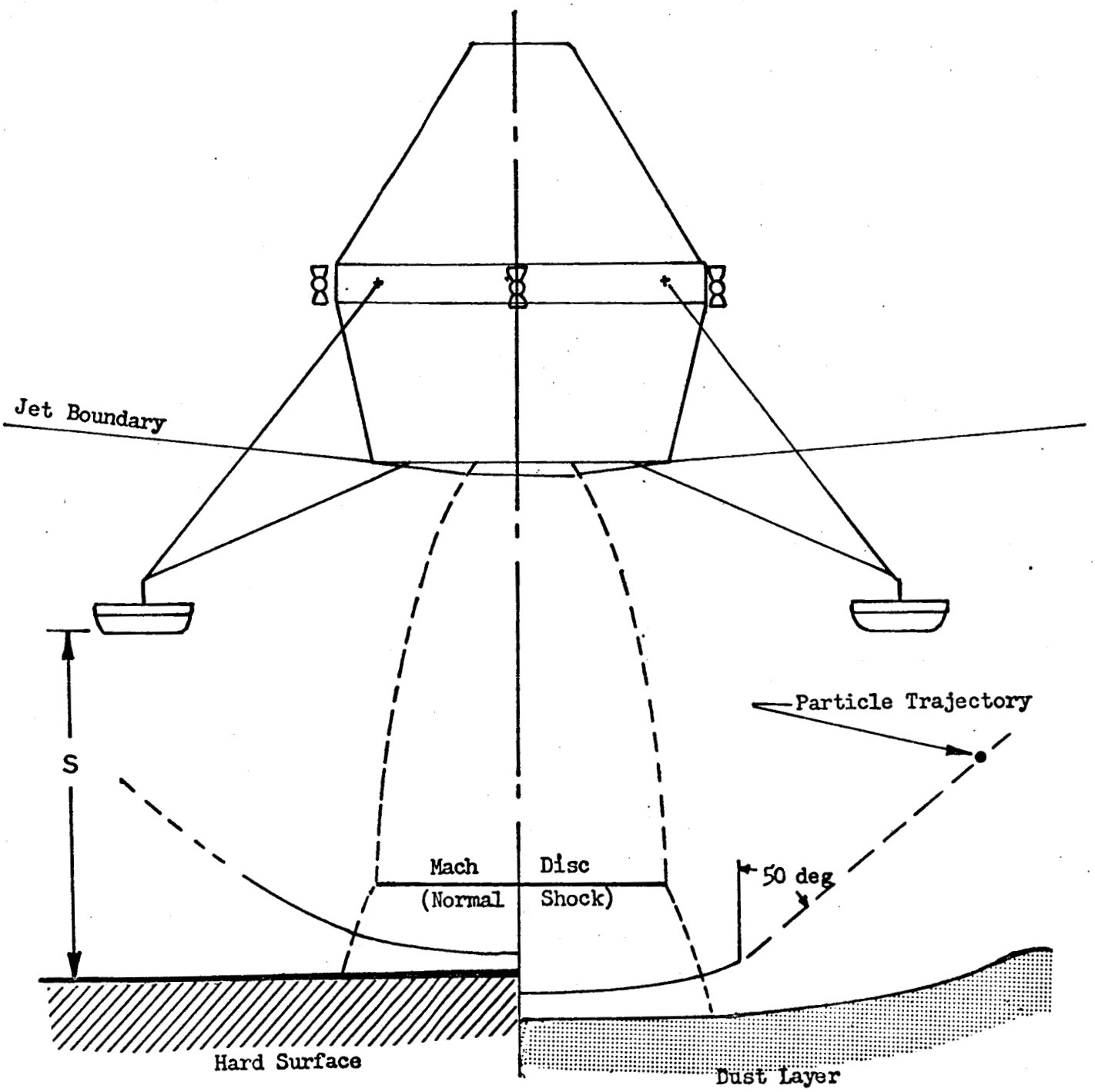


Figure 3. Jet Interaction with Lunar Surface

# APPENDIX B

## VEHICLE REQUIREMENTS FOR INTERPLANETARY MISSIONS

### Introduction

In the future, vehicles will be designed to land instrumented probes on the planetary surfaces and subsequently return them to the Earth. Though this type of mission is sufficiently far in the future that one cannot presently foresee what a typical planetary landing mission/vehicle combination will be, it is informative to look at various mission/vehicle combinations to gain insight into vehicle and engine size and operating requirements.

These requirements, in particular the feasibility of the launch vehicle size required, indicate the feasibility of the overall vehicle/mission combination. This study provides descriptions of a Mercury probe vehicle, a Mars landing and return vehicle, and a Venus landing and return vehicle, all of which use bipropellant liquid systems for all major propulsive maneuvers. These missions are of greatest interest for analysis of landing systems.

### Selected Missions

The three missions are described in Tables 7 and 8. Departure dates and trip times are indicated in Table 7, and the corresponding mission hyperbolic velocity requirements are presented in Table 8.

Though a specific date of departure is considered for each mission, similar trajectories will occur at other dates. Every Venusian synodic period (approximately 580 days) a Venusian mission of very similar hyperbolic velocities and related trip times will occur. Mars missions, primarily because of the higher eccentricity of the Mars orbit, do not repeat as well every Mars synodic period. Three Mars missions are presented in Table 9. The three missions are only somewhat similar; the missions in 1975 and 1973 require higher trip times or hyperbolic velocity requirements than the selected trip in 1971. The Mercury mission, because of the high eccentricity and inclination to the ecliptic of the Mercury orbit, has poor repetition. The next time that a mission similar to the selected 1973 mission is possible would be in 1986.

A payload of 2000 pounds was selected for the Mercury mission. For the Mars and Venus missions, a 50,000-pound payload, which is large enough for manned applications, was selected.



FORM 608-B (LEDGER) REV. 1-58

TABLE 7

SELECTED MISSIONS

| | |
|---|---|
| **Mercury Landing Probe Mission** | |
| Time Mission Departure | 10 May 1973 |
| Earth-Mercury Coast Time, days | 90 |
| Payload, pounds | 2000 |
| **Mars Landing and Return Mission** | |
| Time Mission Departure | 6 June 1971 |
| Earth-Mars Coast Time, days | 80 |
| Mars Stay Time, days | 12 |
| Mars-Earth Coast Time, days | 260 |
| Total Mission Time, days | 352 |
| Payload, pounds | 50,000 |
| **Venus Landing and Return Mission** | |
| Time Mission Departure | 30 November 1968 |
| Earth-Venus Coast Time, days | 125 |
| Venus Stay Time, days | 5 |
| Venus-Earth Coast Time, days | 145 |
| Total Mission Time, days | 275 |
| Payload, pounds | 50,000 |



FORM 608 B (LEDGER) REV. 1-58

TABLE 8

SELECTED MISSION HYPERBOLIC VELOCITY REQUIREMENTS

| Mission | Hyperbolic Velocities | | | |
|---|---|---|---|---|
| | Earth Departure Excess ft/sec | Planetary Arrival ft/sec | Planetary Departure Excess ft/sec | Earth Arrival ft/sec |
| Mercury Landing Probe | 31,000 | 30,000 | - | - |
| Mars Landing and Return Mission | 20,500 | 34,400 | 18,000 | 27,000 |
| Venus Landing and Return Mission | 21,000 | 31,000 | 29,000 | 20,000 |

TABLE 9

MARS MISSION HYPERBOLIC VELOCITY REQUIREMENTS

| Launch Date | Total Mission Time, days, | Hyperbolic Velocities | | | |
|---|---|---|---|---|---|
| | | Earth Departure Excess, ft/sec | Mars Arrival ft/sec | Mars Departure Excess ft/sec | Earth Arrival ft/sec |
| 6 June 1971 | 352 | 20,500 | 34,400 | 18,000 | 27,000 |
| 6 August 1973 | 355 | 23,400 | 34,400 | 19,800 | 32,100 |
| 15 September 1975 | 395 | 21,100 | 31,100 | 19,600 | 46,800 |



FORM 608-B (LEDGER) REV. 1-58

Mission and Vehicle Characteristics

In Tables 10 and 11, a summary of the three selected vehicle/mission combinations is shown. For each mission, the required maneuvers are listed along with the type of stage or system which is to perform the maneuver. The vehicle weight at the initiation of each maneuver is also presented.

Boost-to-Earth orbit vehicles of several types were considered in this study. The vehicle indicated as alternative A in Tables 10 and 11 was a two-stage vehicle with the exact orbital payload capability required by the mission. This vehicle has a first stage using $O_2$/RP-1 propellants, engines similar in performance to the Rocketdyne F-1 which develops 1,500,000 pounds thrust, and has a propellant fraction of 0.92. The second stage uses $O_2/H_2$ propellants, has engines with performance similar to the Rocketdyne J-2 which develops 200,000 pounds thrust, and a propellant fraction of 0.90.

Since the orbital payload requirements of the three missions are high, the boost-to-orbit maneuver may be performed by a group of vehicles whose payloads rendezvous in orbit to form the required space vehicle. As alternatives to the single vehicle, rendezvous of various smaller vehicles was considered. The three smaller vehicles considered are presented in Table 12 . For the Mercury mission, 3 C-5 vehicles can be rendezvoused to perform the mission, or one 12 F-1 Nova can perform the mission. For Mars, nine 12 F-1 Novas must be rendezvoused or 5 of the 24,000,000-pound takeoff thrust, two-stage, $O_2/H_2$ vehicles must be rendezvoused to obtain the required orbital payload. The Venus mission orbital payload is so large that the selected vehicle/mission combination seems highly unlikely. A total of 106 of the 24,000,000-pound takeoff thrust, $O_2/H_2$ vehicles would have to be rendezvoused to obtain the required orbital payload.

Stage tank and structure weights, insulation weights, and boiloff weights were estimated based on past studies. Stage trapped propellant weight was assumed to be 1 percent of stage propellant weight. A reserve propellant weight was included in each stage, capable of providing 5 percent additional ideal velocity over the nominal requirement in all cases except the midcourse-terminal correction systems. For these systems, since ideal velocity requirements are more difficult to predict accurately, a 20 percent allowance was provided. The thrust and ideal velocity requirements for the various maneuvers were determined from results presented in other sections of this study and in Reference 24.

Propulsive braking was used only when approaching the planet Mercury. At Mars, Venus, and Earth, atmospheric drag was used to decelerate the vehicle. The aerodynamic entry vehicles were ablatively cooled. For all vehicles,



FORM 608-B (LEDGER) REV. 1 58

TABLE 10

MERCURY LANDING MISSION

| Required Maneuvers | Type of System | Vehicle Weight at Maneuver Initiation, pounds |
|---|---|---|
| 1. Boost-to-Earth Orbit | Alternatives | |
| | A. Two-Stage Vehicle<br>First Stage - $O_2$/RP<br>Second Stage - $O_2/H_2$ | 12,910,000 |
| | B. 3 Rendezvoused C-5's | 18,000,000 |
| | C. 12 F-1 Nova | 14,400,000 |
| 2. Earth Orbit Departure | One $O_2/H_2$ Stage | 555,000 |
| 3. Space Transfer Propulsion | | 71,000 |
| Attitude Control | Cold Gas System | |
| Midcourse Corrections | $O_2/H_2$ System | |
| Terminal Correction | Performed by Midcourse System | |
| 4. Mercury Orbit Establishment | Two $O_2/H_2$ Stages | 63,840 |
| 5. Landing From Orbit | One $F_2/H_2$ Stage | 6,160 |
| 6. Hover Translation | Performed by Landing Stage | 2,880 |
| 7. Mercury Landing Terminal Deceleration Phase | Frangible Tube Landing Legs | 2,742 |
| | | (Payload = 2,000) |



FORM 608-B (LEDGER) REV. 1-58

ROCKETDYNE
A DIVISION OF NORTH AMERICAN AVIATION, INC

TABLE 11

PLANETARY LANDING AND RETURN MISSIONS

| Required Maneuvers | Mars | | Venus | |
|---|---|---|---|---|
| | Type of System | Vehicle Weight at Maneuver Initiation, pounds | Type of System | Vehicle Weight at Maneuver Initiation, pounds |
| 1. Boost-to-Earth Orbit | Alternatives<br>A. Two Stage Vehicle<br>First Stage - $O_2$/RP<br>Second Stage - $O_2/H_2$<br>B. 9 Rendezvoused<br>12 F-1 Novas<br>C. 5 Rendezvoused $O_2/H_2$ Vehicles<br>Takeoff Thrust = 24,000,000 pounds | <br>118,200,000<br><br>129,600,000<br><br>96,000,000 | Alternatives<br>A. Two Stage Vehicle<br>First Stage - $O_2$/RP<br>Second Stage - $O_2/H_2$<br>B. 106 Rendezvoused $O_2/H_2$ Vehicles<br>Takeoff Thrust = 24,000,000 pounds | <br>2,496,000,000<br><br>2,035,200,000 |
| 2. Earth Orbit Departure | One $O_2/H_2$ Stage | 5,090,000 | One $O_2/H_2$ Stage | 107,300,000 |
| 3. Space Transfer Phase Propulsion<br>Attitude Control<br>Midcourse Correction<br>Terminal Correction | <br>$F_2/H_2$ System<br>$F_2/H_2$ System<br>Performed by Midcourse System | 1,311,000 | <br>Cold Gas System<br>$F_2/H_2$ System<br>Performed by Midcourse System | 27,690,000 |
| 4. Braking for Planetary Landing | Aerodynamic Entry Vehicle with Ablative Heat Shield | 1,098,000 | Aerodynamic Entry Vehicle with Ablative Heat Shield | 23,560,000 |
| 5. Planetary Landing Terminal Deceleration Phase | Pararocket - Frangible Tube Landing Legs | 1,003,000 | Parachute - Frangible Tube Landing Legs | 19,790,000 |
| 6. Planetary Takeoff to Orbit | One $F_2/H_2$ Stage | 726,000 | Three $F_2/H_2$ Stages | 13,880,000 |
| 7. Planetary Orbit Departure | One $F_2/H_2$ Stage | 235,800 | One $F_2/H_2$ Stage | 418,000 |
| 8. Space Transfer Phase Propulsion<br>Attitude Control<br>Midcourse Corrections<br>Terminal Correction | <br>Cold Gas System<br>$N_2O_4$/50-50 System<br>Performed by Midcourse System | 85,800 | <br>Cold Gas System<br>$N_2/O_4$/50-50 System<br>Performed by Midcourse System | 79,500 |
| 9. Braking for Earth Landing | Aerodynamic Entry Vehicle with Ablative Heat Shield | 67,240 | Aerodynamic Entry Vehicle with Ablative Heat Shield | 62,310 |
| 10. Earth Landing Terminal | Parachute - Frangible Tube Landing Legs | 56,920<br>(Payload = 50,000) | Parachute - Frangible Tube Landing Legs | 55,240<br>(Payload = 50,000) |



FORM R 18-G-18

TABLE 12

BOOST TO ORBIT VEHICLES

| | | Saturn C-5 | 12 F-1 Nova | Future $O_2/H_2$ Vehicle |
|---|---|---|---|---|
| Propellants: | First Stage | $O_2$/RP | $O_2$/RP | $O_2/H_2$ |
| | Second Stage | $O_2/H_2$ | $O_2/H_2$ | $O_2/H_2$ |
| Propulsion: | First Stage | 5 F-1 | 12 F-1 | 24,000,000-pound $O_2/H_2$ Engine |
| | Second Stage | 5 J-2 | 3 M-1 | 4 M-1 |
| Takeoff Thrust, pounds | | 7,500,000 | 18,000,000 | 24,000,000 |
| Gross Weight, pounds | | 6,000,000 | 14,400,000 | 19,200,000 |
| Payload (300 n mi. Orbit) pounds | | 220,000 | 620,000 | 1,130,000 |



ROCKETDYNE
A DIVISION OF NORTH AMERICAN AVIATION, INC
FORM 608-B (LEDGER) REV. 1-58

the ablation shield weight was determined from the equation

$$L = e^{8.04 \times 10^{-5} V - 4.114}$$

Because detailed heat shield weights are not currently available this equation was used for entry at all three planets although the Venus entry would require higher heat shield weights and the Mars entry lower heat shield weights than those required at Earth. For the Mars and Venus landings, the heat shield must protect a takeoff and Earth-return vehicle. The heat shield will therefore probably require a separate support structure. The aerodynamic entry vehicle structure was assumed to be 25 percent of the weight of the entry vehicle payload. The ablative heat shield does not entirely ablate; part remains as an insulation layer. In this study, 2/3 of the heat shield weight was assumed to ablate while the other 1/3 remained as insulation layer.

The terminal deceleration phase for an atmospheric deceleration landing is performed by a system using parachutes, followed by a retrorocket (where desirable) and frangible-tube landing legs. For the Earth and Venus landings, the system did not include a retrorocket; however a system including a retrorocket was used for the Mars landing.

Attitude control system analysis, as presented in Reference 24, indicates that attitude control system propellant weights and thrust level requirements are small. Exact system weights are highly dependent upon the vehicle and attitude control system designs. Because of the low system weight requirements and the difficulty in determining exact weights, 1 percent of transfer vehicle gross weight was assumed to be the allowance for attitude control.

A separate system is provided for the midcourse and terminal corrections in all cases. These systems have redundant engines but not redundant propellant and tankage. For additional redundancy, the propulsion system which is to perform the next main propulsive maneuver could be used for the midcourse and terminal corrections. This would not impose a significant weight penalty if the midcourse-terminal system propellant can be transferred into the main propellant tansk (no propellant redundancy). This capability was considered for the Mercury mission but not the Mars and Venus missions which do not have a major terminal phase propulsion system.



FORM 608 (LEDGER) REV 1.58

## Selected Vehicle Description

The final vehicle descriptions for the three mission/vehicle combinations are presented at Tables 13 and 14. In these tables, the vehicle weight, a system description and a maneuver description are presented for each maneuver of the mission. For the boost-to-orbit maneuver, the system presented is Alternative A of Tables 10 and 11 (i.e., a single vehicle of the exact required size).



FORM 608-B (LEDGER) REV. 1-58

TABLE 13

PLANETARY LANDING AND RETURN MISSIONS

MANEUVER ONE, BOOST-TO-(EARTH) ORBIT

| Propulsion Systems | Mars | Venus |
|---|---|---|
| First Stage | | |
| $O_2$/RP Propellant | | |
| Pump Fed | | |
| Regeneratively Cooled Bell Nozzle | | |
| Chamber Pressure, psia | 1,000 | 1,000 |
| Expansion Area Ratio | 16:1 | 16:1 |
| Engine Mixture Ratio | 2.25:1 | 2.25:1 |
| Specific Impulse at Sea Level, seconds | 265 | 265 |
| at Vacuum, seconds | 305 | 305 |
| Thrust, pounds | 147,800,000 | 3,120,000,000 |
| Engine Weight, pounds | 2,110,000 | 44,600,000 |
| Number of Required Starts | 1 | 1 |
| Second Stage | | |
| $O_2/H_2$ Propellants | | |
| Pump Fed | | |
| Regeneratively Cooled Bell Nozzle | | |
| Chamber Pressure, psia | 630 | 630 |
| Expansion Area Ratio | 27.5:1 | 27.5:1 |
| Engine Mixture Ratio | 5:1 | 5:1 |
| Engine Specific Impulse, seconds | 426 | 426 |
| Thrust, pounds | 26,500,000 | 559,000,000 |
| Engine Weight, pounds | 282,000 | 5,950,000 |
| Number of Required Starts | 2 | 2 |
| Maneuver Description | | |
| Intermediate Coast Phase Trajectory to Low Altitude Parking Orbit (300 n mi) | | |
| Ideal Velocity Requirement | | |
| Stage One, ft/sec | 11,900 | 11,900 |
| Stage Two, ft/sec | 17,900 | 17,900 |
| Total | 29,800 | 29,800 |
| Thrust-to-Weight Ratio | | |
| Stage One | 1.25 | 1.25 |
| Stage Two | 1.00 | 1.00 |



FORM 608-B (LEDGER) REV. 1-58

TABLE 13

(Continued)

| Vehicle Weight | Mars | Venus |
|---|---|---|
| First Stage | | |
| Vehicle Takeoff Gross Weight | 118,200,000 | 2,496,000,000 |
| Nominal Consumed Propellant Weight, pounds | - 84,360,000 | -1,782,000,000 |
| Stage Jettisoned Weight, pounds | - 7,340,000 | - 155,000,000 |
| Final Vehicle Weight, pounds | 26,500,000 | 559,000,000 |
| Second Stage | | |
| Initial Vehicle Weight, pounds | 26,500,000 | 559,000,000 |
| Nominal Consumed Propellant Weight, pounds | -19,280,000 | -406,800,000 |
| Stage Jettisoned Weight, pounds | - 2,130,000 | - 44,900,000 |
| Final Vehicle Weight, pounds | 5,090,000 | 107,300,000 |

MANEUVER TWO, EARTH ORBIT DEPARTURE

| Propulsion System | Mars | Venus |
|---|---|---|
| $O_2/H_2$ Propellants | | |
| Pump Fed | | |
| Regneratively Cooled Bell Nozzle | | |
| Chamber Pressure, psia | 730 | 730 |
| Expansion Area Ratio | 50:1 | 50:1 |
| Thrust Chamber Mixture Ratio | 5.3:1 | 5.3:1 |
| Engine Specific Impulse, seconds | 432 | 432 |
| Thrust, pounds | 2,540,000 | 53,700,000 |
| Engine Weight, pounds | 40,700 | 860,000 |
| Number of Required Starts | 1 | 1 |



FORM 608-B (LEDGER) REV. 1-58

TABLE 13

(Continued)

| Maneuver Description | Mars | Venus |
|---|---|---|
| Earth Hyperbolic Excess Velocity, ft/sec | 20,500 | 21,000 |
| Thrust Parallel-to-Velocity Departure from 300 n mi Orbit | | |
| Thrust-to-Weight Ratio | 0.5 | 0.5 |
| Ideal Velocity Requirements, ft/sec | 16,400 | 16,600 |
| **Vehicle Weight** | | |
| Initial Vehicle Weight, pounds | 5,090,000 | 107,300,000 |
| Nominal Consumed Propellant Weight, pounds | -3,520,000 | - 74,730,000 |
| Stage Trapped Propellant Weight, pounds | - 36,000 | - 770,000 |
| Stage Reserve Propellant Weight, pounds | - 87,000 | - 1,740,000 |
| Stage Tank and Structure Weight, pounds | - 95,000 | - 1,510,000 |
| Stage Engine Weight, pounds | - 41,000 | - 860,000 |
| Final Vehicle Weight, pounds | 1,311,000 | 27,690,000 |

MANEUVER THREE, SPACE TRANSFER PHASE PROPULSION

| Propulsion System | Mars | Venus |
|---|---|---|
| Attitude Control | | |
| $F_2/H_2$ Propellants | | |
| Pressure Fed | | |
| Total 16 Ablative Thrust Chambers (8 Redundant) | | |
| Complete Redundancy of Components | | |
| Midcourse and Terminal | | |
| $F_2/H_2$ Propellants | | |
| Pressure Fed | | |
| Two Engines (One Engine out Capability) | | |
| Regeneratively Cooled Bell Nozzle | | |
| Chamber Pressure, psia | 112 | 112 |
| Expansion Area Ratio | 50:1 | 50:1 |
| Mixture Ratio | 16.4:1 | 16.4:1 |
| Specific Impulse, seconds | 448 | 448 |
| Thrust (One Engine), pounds | 26,200 | 552,000 |
| Engine Weight (one engine), pounds | 370 | 7,730 |
| Number of Required Starts | 4 | 4 |



FORM 608-B (LEDGER) REV. 1-58

TABLE 13

(Continued)

| Maneuver Description | Mars | Venus |
|---|---|---|
| Attitude Control | | |
| Acquisition of Vehicle Coast Phase Orientation | | |
| Rotation to Orientation for Propulsive Phase | | |
| Disturbed Limit-Cycle Position Stabilization | | |
| Midcourse Corrections | | |
| Number of Corrections | 3 | 3 |
| Time After Launch of Corrections, days, | 1,60,73 | 1,94,115 |
| Total Ideal Velocity Requirement, ft/sec | 600 | 600 |
| Thrust-to-Weight Ratio | 0.02 | 0.02 |
| Terminal Correction | | |
| Distance from Planet of Correction, n mi | 70,000 | 70,000 |
| Ideal Velocity Requirement, ft/sec | 1,000 | 1,000 |
| Thrust-to-Weight Ratio | 0.02 | 0.02 |
| Vehicle Weight | | |
| Initial Vehicle Weight | 1,311,000 | 27,690,000 |
| Propellant Boiloff | | |
| Takeoff Stage One, pounds | - 1,100 | - 27,200 |
| Takeoff Stage Two, pounds | | - 8,500 |
| Takeoff Stage Three, pounds | | - 2,000 |
| Orbit Departure Stage, pounds | - 500 | - 1,300 |
| Midcourse System, pounds | - 600 | - 8,000 |
| Nominal Consumed Propellant Weight, pounds | -135,600 | -2,851,000 |
| System Trapped Propellant Weight, pounds | - 1,600 | - 34,000 |
| System Reserve Propellant Weight, pounds | - 28,500 | - 575,000 |
| System Tank and Structure Weight, pounds | - 9,100 | - 162,000 |
| System Insulation Weight, pounds | - 300 | - 2,000 |
| System Engine Weight, pounds | - 700 | - 15,000 |
| Attitude Control System, pounds | - 13,100 | - 276,000 |
| Entry Vehicle Meteor Shield, pounds | - 21,900 | - 168,000 |
| Final Vehicle Weight, pounds | 1,098,000 | 23,560,000 |



FORM 608 B (LEDGER) REV. 1-58

TABLE 13

(Continued)

MANEUVER FOUR, BRAKING FOR LANDING

| Type Vehicle | Mars | Venus |
|---|---|---|
| Aerodynamic Lifting Body | | |
| Ablative Heat Shield | | |
| **Maneuver Description** | | |
| Planet Hyperbolic Arrival Velocity, ft/sec | 34,400 | 31,000 |
| Planet Atmosphere Entry Angle, degrees | 22.7 to 24.1 | 6.1 to 7.5 |
| Maximum Aerodynamic Deceleration, g | 6 | 6 |
| **Vehicle Weight** | | |
| Initial Vehicle Weight, pounds | 1,098,000 | 23,560,000 |
| Ablated Heat Shield *, pounds | - 95,000 | - 3,770,000 |
| Final Vehicle Weight, pounds | 1,003,000 | 19,790,000 |

*Of the total heat shield weight, 2/3 was assumed to ablate while the other 1/3 remains as an insulation layer.

| | | |
|---|---|---|
| Ablated Heat Shield, pounds | 95,000 | 3,770,000 |
| Heat Shield Insulation, pounds | +48,000 | +1,880,000 |
| Total Heat Shield Weight, pounds | 143,000 | 5,650,000 |



FORM 608-B (LEDGER) REV 1-58

TABLE 13

(Continued)

MANEUVER FIVE, LANDING TERMINAL DECELERATION PHASE

| | |
|---|---|
| Type of Deceleration System | |
| Mars | |
| Parachute Deceleration to, ft/sec | 120 |
| Retrorocket Deceleration from, ft/sec | 120 to 35 |
| Retrorocket Thrust-to-Weight Ratio | 0.8 |
| Retrorocket Specific Impulse, seconds | 240 |
| Frangible Tube Landing Legs | |
| Venus | |
| Parachute Deceleration to, ft/sec | 42 |
| Frangible Tube Landing Legs | |

| Vehicle Weight | Mars | Venus |
|---|---|---|
| Initial Vehicle Weight, pounds | 1,003,000 | 19,790,000 |
| Heat Shield Insulation, pounds | - 48,000 | - 1,880,000 |
| Pararocket System, pounds | - 38,000 | - 340,000 |
| Frangible Tube Landing Legs, pounds | - 9,000 | - 220,000 |
| Heat Shield Support Structure, pounds | - 182,000 | - 3,470,000 |
| Final Vehicle Weight, pounds | 726,000 | 13,880,000 |

MANEUVER SIX, TAKEOFF-TO-ORBIT

| Propulsion System | Mars | Venus |
|---|---|---|
| First Stage | | |
| $F_2/H_2$ Propellants | | |
| Pump Fed | | |
| Regeneratively Cooled Bell Nozzle | | |
| Chamber Pressure, psia | 1,280 | 1,000 |
| Expansion Area Ratio | 50:1 | 5:1 |
| Thrust Chamber Mixture Ratio | 16.4:1 | 12:1 |



FORM 608-B (LEDGER) REV. 1-58

TABLE 13

(Continued)

| | Mars | Venus |
|---|---|---|
| Engine Specific Impulse | | |
| Surface, seconds | 445 | 322 |
| Vacuum, seconds | 456 | 397 |
| Thrust (Vacuum), pounds | 593,000 | |
| Thrust (Surface), pounds | | 18,360,000 |
| Engine Weight, pounds | 7,350 | 266,000 |
| Number of Required Starts | 2 | 1 |
| Second Stage | | |
| $F_2/H_2$ Propellants | | |
| Pump Fed | | |
| Regeneratively Cooled Bell Nozzle | | |
| Chamber Pressure, psia | | 1,000 |
| Expansion Area Ratio | | 10:1 |
| Thrust Chamber Mixture Ratio | | 12:1 |
| Engine Specific Impulse | | |
| Surface, seconds | | 271 |
| Vacuum, seconds | | 421 |
| Thrust (Vacuum) | | 5,590,000 |
| Engine Weight, pounds | | 63,000 |
| Number of Required Starts | | 1 |
| Third Stage | | |
| $F_2/H_2$ Propellants | | |
| Pump Fed | | |
| Regeneratively Cooled Bell Nozzle | | |
| Chamber Pressure, psia | | 1,280 |
| Expansion Area Ratio | | 50:1 |
| Thrust Chamber Mixture Ratio | | 16.4:1 |
| Engine Specific Impulse (Vacuum), seconds | | 456 |
| Thrust (Vacuum), pounds | | 1,670,000 |
| Engine Weight, pounds | | 20,700 |
| Number of Required Starts | | 2 |



FORM 608-B (LEDGER) REV. 1-58

TABLE 13

(Continued)

| Maneuver Description | Mars | Venus |
|---|---|---|
| Intermediate Coast Phase Trajectory to Low Altitude Parking Orbit (300 n mi) | | |
| Ideal Velocity Requirement, ft/sec | | |
| Stage One | 14,200 | 12,200 |
| Stage Two | | 13,900 |
| Stage Three | | 13,900 |
| Total | | 40,000 |
| Thrust-to-Weight Ratio | | |
| Stage One | 0.8 | 1.33 |
| Stage Two | | 1.33 |
| Stage Three | | 1.33 |
| Vehicle Weight | | |
| First Stage | | |
| Initial Vehicle Weight, pounds | 726,000 | 13,880,000 |
| Nominal Consumed Propellant Weight, pounds | -450,600 | - 8,925,000 |
| Stage Trapped Propellant Weight, pounds | - 4,700 | - 92,000 |
| Stage Reserve Propellant Weight, pounds | - 13,000 | - 248,000 |
| Stage Tank and Structure Weight, pounds | - 14,100 | - 175,000 |
| Stage Insulation Weight, pounds | - 500 | - 8,000 |
| Stage Engine Weight, pounds | - 7,300 | - 266,000 |
| Final Vehicle Weight, pounds | 235,800 | 4,166,000 |
| Second Stage | | |
| Initial Vehicle Weight | | 4,166,000 |
| Nominal Consumed Propellant Weight, pounds | | - 2,676,000 |
| Stage Trapped Propellant Weight, pounds | | - 28,000 |
| Stage Reserve Propellant Weight, pounds | | - 73,000 |
| Stage Tank and Structure Weight, pounds | | - 63,400 |
| Stage Insulation Weight, pounds | | - 2,600 |
| Stage Engine Weight, pounds | | - 63,000 |
| Final Vehicle Weight | | 1,260,000 |



FORM 608-B (LEDGER) REV. 1-58

TABLE 13

(Continued)

| Third Stage | Mars | Venus |
|---|---|---|
| Initial Vehicle Weight, pounds | | 1,260,000 |
| Nominal Consumed Propellant Weight, pounds | | - 769,400 |
| Stage Trapped Propellant Weight, pounds | | - 8,000 |
| Stage Reserve Propellant Weight, pounds | | - 22,200 |
| Stage Tank and Structure Weight, pounds | | - 21,100 |
| Stage Insulation Weight, pounds | | - 600 |
| Stage Engine Weight, pounds | | - 20,700 |
| Final Vehicle Weight, pounds | | 418,000 |

MANEUVER SEVEN, ORBIT DEPARTURE

| Propulsion System | Mars | Venus |
|---|---|---|
| $F_2/H_2$ Propellants | | |
| Pump Fed | | |
| Bell Nozzle, Regenerative to 20:1 with Radiation Cooled Skirt | | |
| Chamber Pressure, psia | 1,840 | 1,840 |
| Expansion Area Ratio | 200:1 | 200:1 |
| Thrust Chamber Mixture Ratio | 17.0:1 | 17.0:1 |
| Engine Specific Impulse, seconds | 473 | 473 |
| Thrust, pounds | 38,000 | 146,000 |
| Engine Weight, pounds | 720 | 2,800 |
| Number of Required Starts | 1 | 1 |
| Maneuver Description | | |
| Planet Hyperbolic Excess Velocity, ft/sec | 18,000 | 29,000 |
| Thrust Parallel to Velocity Departure from 300 n mi Orbit | | |
| Thrust-to-Weight Ratio | 0.16 | 0.35 |
| Ideal Velocity Requirement, ft/sec | 13,400 | 21,300 |



FORM 608 B (LEDGER) REV. 1 58

TABLE 13

(Continued)

| Vehicle Weight | Mars | Venus |
|---|---|---|
| Initial Vehicle Weight, pounds | 235,800 | 418,000 |
| Nominal Consumed Propellant Weight, pounds | -137,700 | -314,100 |
| Stage Trapped Propellant Weight, pounds | - 1,400 | - 3,200 |
| Stage Reserve Propellant Weight, pounds | - 4,300 | - 7,100 |
| Stage Tank and Structure Weight, pounds | - 5,700 | - 10,900 |
| Stage Insulation Weight, pounds | - 200 | - 400 |
| Stage Engine Weight, pounds | - 700 | - 2,800 |
| Final Vehicle Weight, pounds | 85,800 | 79,500 |

MANEUVER EIGHT, SPACE TRANSFER PHASE PROPULSION

| Propulsion Systems | Mars | Venus |
|---|---|---|
| Attitude Control | | |
| Cold Gas System | | |
| Total 16 Chambers (8 Redundant) | | |
| Complete Redundancy of Components | | |
| Midcourse and Terminal | | |
| 50-50 ($N_2H_4$-UDMH)/$N_2O_4$ Propellants | | |
| Pressure Fed | | |
| Two Engines (One Engine Out Capability) | | |
| Regeneratively Cooled Bell Nozzle | | |
| Chamber Pressure, psia | 150 | 150 |
| Expansion Area Ratio | 50:1 | 50:1 |
| Thrust Chamber Mixture Ratio | 2.13:1 | 2.13:1 |
| Specific Impulse, seconds | 322.8 | 322.8 |
| Thrust, pounds (one engine) | 1,720 | 1,590 |
| Engine Weight, pounds (one engine) | 18.4 | 17 |
| Number of Required Starts | 6 | 5 |



FORM 608-B (LEDGER) REV. 1 58

TABLE 13

(Continued)

| Maneuver Description | Mars | Venus |
|---|---|---|
| Attitude Control | | |
| Acquisition of Vehicle Coast Phase Orientation | | |
| Rotation to Orientation for Propulsive Phase | | |
| Disturbed Limit-Cycle Position Stabilization | | |
| Midcourse Corrections | | |
| Number of Corrections | 5 | 4 |
| Time of Corrections, days | 1, 195, 238<br>253, 258 | 1, 109<br>133, 141 |
| Total Ideal Velocity Requirements, ft/sec | 600 | 600 |
| Thrust-to-Weight Ratio | 0.02 | 0.02 |
| Terminal Correction | | |
| Distance of Correction from Planet, n mi | 70,000 | 70,000 |
| Ideal Velocity Requirement, ft/sec | 1,000 | 1,000 |
| Thrust-to-Weight Ratio | 0.02 | 0.02 |
| Vehicle Weight | | |
| Initial Vehicle Weight, pounds | 85,800 | 79,500 |
| Attitude Control System, pounds | - 860 | - 800 |
| Nominal Consumed Propellant Weight, pounds | -12,220 | -11,330 |
| Stage Trapped Propellant Weight, pounds | - 150 | - 130 |
| Stage Reserve Propellant Weight, pounds | - 2,260 | - 2,090 |
| Stage Tank and Structure Weight, pounds | - 830 | - 770 |
| Stage Engine Weight, pounds | - 40 | - 30 |
| Payload Meteor Shield, pounds | - 2,200 | - 2,040 |
| Final Vehicle Weight, pounds | 67,240 | 62,310 |



FORM 608-B (LEDGER) REV. 1-58

TABLE 13

(Continued)

MANEUVER NINE, BRAKING FOR EARTH LANDING

| Type Vehicle | Mars | Venus |
|---|---|---|
| Aerodynamic Lifting Body | | |
| Ablative Heat Shield | | |
| **Maneuver Description** | | |
| Earth Hyperbolic Arrival Velocity, ft/sec | 27,000 | 20,000 |
| Earth Atmosphere Entry Angle, degrees | 5.6 to 7.3 | 5.4 to 7.4 |
| Maximum Aerodynamic Deceleration, g | 6 | 6 |
| **Vehicle Weight** | | |
| Initial Vehicle Weight, pounds | 67,240 | 62,310 |
| Ablated Heat Shield*, pounds | - 10,320 | - 7,070 |
| Final Vehicle Weight, pounds | 56,920 | 55,240 |

*Of the total heat shield weight 2/3 was assumed to ablate while the other 1/3 reamins as an insulation layer

| | | |
|---|---|---|
| Ablated Heat Shield, pounds | 10,320 | 7,070 |
| Heat Shield Insulation, pounds | + 5,150 | + 3,530 |
| Total Heat Shield Weight, pounds | 15,470 | 10,600 |

MANEUVER TEN, EARTH LANDING TERMINAL DECELERATION PHASE

| Type of Deceleration System | Mars | Venus |
|---|---|---|
| Main Chute Deployment, ft/sec | 400 | 400 |
| Parachute Deceleration, ft/sec | to 55 | to 55 |
| Frangible Tube Landing Legs | | |



FORM 608-B (LEDGER) REV. 1-58

TABLE 13

(Continued)

| Vehicle Weight | Mars | Venus |
|---|---|---|
| Initial Vehicle Weight, pounds | 56,920 | 55,240 |
| Heat Shield Insulation, pounds | - 5,150 | - 3,530 |
| Parachute System, pounds | - 820 | - 800 |
| Frangible Tube Landing Legs, pounds | - 950 | - 910 |
| Final Mission Payload, pounds | 50,000 | 50,000 |



FORM 608-B (LEDGER) REV. 1-58

TABLE 14

MERCURY LANDING AND RETURN MISSION

MANEUVER ONE, BOOST-TO-(EARTH) ORBIT

| Propulsion Systems | Mercury |
|---|---|
| First Stage | |
| $O_2$/RP Propellant | |
| Pump Fed | |
| Regeneratively Cooled Bell Nozzle | |
| Chamber Pressure, psia | 1000 |
| Expansion Area Ratio | 16:1 |
| Engine Mixture Ratio | 2.25:1 |
| Engine Specific Impulse at Sea Level, Seconds | 265 |
| at Vacuum, seconds | 305 |
| Thrust, pounds | 16,130,000 |
| Engine Weight, pounds | 231,000 |
| Number of Required Starts | 1 |
| Second Stage | |
| $O_2/H_2$ Propellants | |
| Pump Fed | |
| Regeneratively Cooled Bell Nozzle | |
| Chamber Pressure, psia | 630 |
| Expansion Area Ratio | 27.5:1 |
| Engine Mixture Ratio | 5:1 |
| Engine Specific Impulse, seconds | 426 |
| Thrust, pounds | 2,890,000 |
| Engine Weight, pounds | 30,800 |
| Number of Required Starts | 2 |
| Maneuver Description | |
| Intermediate Coast Phase Trajectory to Low Altitude Parking Orbit (300 n mi) | |
| Ideal Velocity Requirement | |
| Stage One, ft/sec | 11,900 |
| Stage Two, ft/sec | 17,900 |
| Total | 29,800 |
| Thrust-to-Weight Ratio | |
| Stage One | 1.25 |
| Stage Two | 1.00 |

TABLE 14

(Continued)

| Vehicle Weight | Mercury |
|---|---|
| First Stage | |
| Vehicle Takeoff Gross Weight, pounds | 12,910,000 |
| Nominal Consumed Propellant Weight, pounds | -9,220,000 |
| Stage Jettisoned Weight, pounds | - 800,000 |
| Final Vehicle Weight, pounds | 2,890,000 |
| Second Stage | |
| Initial Vehicle Weight, pounds | 2,890,000 |
| Nominal Consumed Propellant Weight, pounds | -2,103,000 |
| Stage Jettisoned Weight, pounds | - 232,000 |
| Final Vehicle Weight, pounds | 555,000 |

MANEUVER TWO, EARTH ORBIT DEPARTURE

| Propulsion System | Mercury |
|---|---|
| $O_2/H_2$ Propellants | |
| Pump Fed | |
| Regeneratively Cooled Bell Nozzle | |
| Chamber Pressure, psia | 730 |
| Expansion Area Ratio | 50:1 |
| Thrust Chamber Mixture Ratio | 5.3:1 |
| Engine Specific Impulse, seconds | 432 |
| Thrust, pounds | 278,000 |
| Engine Weight, pounds | 4,450 |
| Number of Required Starts | 1 |
| Maneuver Description | |
| Earth Hyperbolic Excess Velocity, ft/sec | 31,000 |
| Thrust Parallel-to-Velocity Departure from 300 n mi Orbit | |
| Thrust-to-Weight Ratio | 0.5 |
| Ideal Velocity Requirements, ft/sec | 23,300 |



FORM 608-B (LEDGER) REV. 1 58

TABLE 14

(Continued)

| Vehicle Weight | Mercury |
|---|---|
| Initial Vehicle Weight, pounds | 555,000 |
| Nominal Consumed Propellant Weight, pounds | -450,000 |
| Stage Trapped Propellant Weight, pounds | - 4,600 |
| Stage Reserve Propellant Weight, pounds | - 8,500 |
| Stage Tank and Structure Weight, pounds | - 16,400 |
| Stage Engine Weight, pounds | - 4,500 |
| Final Vehicle Weight, pounds | 71,000 |

MANEUVER THREE, SPACE TRANSFER PHASE PROPULSION

| Propulsion Systems | Mercury |
|---|---|
| **Attitude Control** | |
| Cold Gas System | |
| Total 16 Chambers (8 Redundant) | |
| Complete Redundancy of Components | |
| **Midcourse and Terminal** | |
| $O_2$/ $H_2$ Propellants | |
| Pressure Fed | |
| Two Engines (One Engine out Capability) | |
| Regeneratively Cooled Bell Nozzle | |
| Chamber Pressure, psia | 75 |
| Expansion Area Ratio | 50:1 |
| Mixture Ratio | 5.5:1 |
| Specific Impulse, seconds | 430 |
| Thrust (One Engine), pounds | 1,400 |
| Engine Weight (one engine), pounds | 28 |
| Number of Required Starts | 4 |

Maneuver Description

**Attitude Control**

Acquisition of Vehicle Coast Phase Orientation
Rotation to Orientation for Propulsive Phase
Disturbed Limit-Cycle Position Stabilization



FORM 608-B (LEDGER) REV. 1 58

TABLE 14

(Continued)

| | Mercury |
|---|---|
| Midcourse Corrections | |
| Number of Corrections | 3 |
| Time After Launch of Corrections, days | 1, 68, 83 |
| Total Ideal Velocity Requirement, ft/sec | 600 |
| Thrust-to-Weight Ratio | 0.02 |
| Terminal Correction | |
| Distance from Planet of Correction, n mi | 60,000 |
| Ideal Velocity Requirement, ft/sec | 700 |
| Thrust-to-Weight Ratio | 0.02 |
| Vehicle Weight | |
| Initial Vehicle Weight | 71,000 |
| Propellant Boiloff: | |
| First Stage Orbit Establishment | - 520 |
| Second Stage Orbit Establishment | - 140 |
| Landing Stage | - 210 |
| Nominal Consumed Propellant Weight | - 6,290 |
| Final Vehicle Weight | 63,840 |

MANEUVER FOUR, MERCURY ORBIT ESTABLISHMENT

| Propulsion System | Mercury |
|---|---|
| First Stage | |
| $O_2/H_2$ Propellants | |
| Pump Fed | |
| Bell Nozzle, Regenerative to 20:1 with Radiation Cooled Skirt | |
| Chamber Pressure, psia | 1150 |
| Expansion Area Ratio | 200:1 |
| Thrust Chamber Mixture Ratio | 6.75:1 |
| Engine Specific Impulse, seconds | 446 |
| Thrust, pounds | 35,000 |
| Engine Weight, pounds | 840 |
| Number of Required Starts | 5 |



FORM 608 B (LEDGER) REV 1-58

TABLE 14

(Continued)

| | |
|---|---|
| Second Stage | Mercury |
| $O_2/H_2$ Propellants | |
| Pump Fed | |
| Bell Nozzle, Regenerative to 20:1 with Radiation Cooled Skirt | |
| Chamber Pressure, psia | 1150 |
| Expansion Area Ratio | 200:1 |
| Thrust Chamber Mixture Ratio | 6.75:1 |
| Engine Specific Impulse, seconds | 446 |
| Thrust, pounds | 9600 |
| Engine Weight, pounds | 230 |
| Number of Required Starts | 1 |
| **Maneuver Description** | |
| Mercury Hyperbolic Arrival Velocity, ft/sec | 30,000 |
| Thrust Parallel to Velocity 300 n mi Orbit Establishment | |
| Two Stage Vehicle | |
| Thrust-to-Weight Ratio Both Stages | 0.5 |
| Ideal Velocity Requirement, ft/ sec | 24,040 |
| **Vehicle Weight** | |
| First Stage | |
| Initial Vehicle Weight, pounds | 63,840 |
| Attitude Control System , pounds | - 710 |
| Nominal Consumed Propellant Weight, pounds | - 35,710 |
| Stage Trapped Propellant Weight , pounds | - 440 |
| Stage Reserve Propellant Weight, pounds | - 1,520 |
| Stage Tank and Structure Weight, pounds | - 3,210 |
| Stage Insulation Weight, pounds | - 310 |
| Stage Engine Weight, pounds | - 840 |
| Midcourse System Trapped Propellant Weight, pounds | - 80 |
| Midcourse System Reserve Propellant Weight, pounds | - 1,030 |
| Midcourse System Tank and Structure Weight, pounds | - 760 |
| Midcourse System Insulation Weight, pounds | - 60 |
| Midcourse System Engine Weight, pounds | - 60 |
| Final Vehicle Weight, pounds | 19,110 |



FORM 608 B (LEDGER) REV 1 58

TABLE 14

(Continued)

| Second Stage | Mercury |
|---|---|
| Initial Vehicle Weight, pounds | 19,110 |
| Nominal Consumed Propellant Weight, pounds | -10,830 |
| Stage Trapped Propellant Weight, pounds | - 110 |
| Stage Reserve Propellant Weight, pounds | - 360 |
| Stage Tank and Structure Weight, pounds | - 1,330 |
| Stage Insulation Weight, pounds | - 90 |
| Stage Engine Weight, pounds | - 230 |
| Final Vehicle Weight, pounds | 6,160 |

MANEUVER FIVE, LANDING FROM ORBIT

| Propulsion System | Mercury |
|---|---|
| $F_2/H_2$ Propellants | |
| Pump Fed | |
| Regeneratively Cooled Bell Nozzle | |
| Chamber Pressure, psia | 1,010 |
| Expansion Area Ratio | 50:1 |
| Thrust Chamber Mixture Ratio | 16.6:1 |
| Engine Specific Impulse, seconds | 456 |
| Thrust, pounds | 6,160 |
| Engine Weight, pounds | 78 |
| Number of Required Starts | 2 |
| Fixed Area Throttling:Throttling Ratio | 12:1 |
| Maneuver Description | |
| Landing from 300 n mi Orbit | |
| Constant Altitude Braking at 300 n mi | |
| Coast on Ellipse: Apoapsis = 300 n mi | |
| Periapsis= 10.7 n mi | |
| Thrust Parallel to Velocity Braking Beginning at Periapsis | |
| Maneuver Terminated when Vehicle Velocity Equals Zero | |
| Total Maneuver Ideal Velocity Requirement, ft/sec | 11,200 |
| Thrust-to-Weight Ratio | 1.0 |



FORM 608-B (LEDGER) REV. 1-58

TABLE 14

(Continued)

| Vehicle Weight | Mercury |
|---|---|
| Initial Vehicle Weight, pounds | 6,160 |
| Nominal Consumed Propellant Weight, pounds | -3,280 |
| Final Vehicle Weight, pounds | 2,880 |

MANEUVER SIX, HOVER TRANSLATION

| Propulsion System | Mercury |
|---|---|
| Maneuver is Performed by Landing Stage | |
| Maneuver Description | |
| Low Altitude Hover, Horizontal Translation and Slow Descent to Near the Mercury Surface | |
| Thrust-to-Mercury Weight Ratio Approximately One | |
| Hover-Translation Time, seconds | 60 |
| Ideal Velocity Requirement, ft/sec | 750 |
| Vehicle Weight | |
| Initial Vehicle Weight, pounds | 2,880 |
| Nominal Consumed Propellant Weight, pounds | - 138 |
| Final Vehicle Weight, pounds | 2,742 |

MANEUVER SEVEN, MERCURY LANDING
TERMINAL DECELERATION PHASE

| Type of Deceleration System | Mercury |
|---|---|
| Frangible Tube Landing Legs | |
| Maximum Input Velocity, ft/sec | 50 |



FORM 608 B (LEDGER) REV 1 59

TABLE 14

(Continued)

| Vehicle Weight | Mercury |
|---|---|
| Initial Vehicle Weight, pounds | 2,742 |
| Landing Stage Tank and Structure Weight, pounds | - 434 |
| Landing Stage Insulation Weight, pounds | - 41 |
| Landing Stage Engine Weight, pounds | - 78 |
| Landing Stage Trapped Propellant Weight, pounds | - 42 |
| Landing Stage, Reserve Propellant Weight, pounds | - 106 |
| Frangible Tube Landing Legs, pounds | - 41 |
| Final Mission Payload, pounds | 2,000 |



FORM 608 B (LEDGER) REV. 1-58

# APPENDIX C

## ENGINE START TECHNIQUES FOR EXTRATERRESTRIAL LANDING ENGINES

### Summary

A design study was conducted to determine the methods available for starting and restarting liquid rocket engines of the type used for extraterrestrial landing propulsion systems. Engine start was divided into four distinct phases. These were:

1. Supply propellants
2. Ready engine
3. Supply turbine power
4. Ignite Propellant

Evaluation of different methods of accomplishing each of the above phases was conducted. Results indicate that the simplest and most reliable means of starting landing propulsion systems in a zero g, vacuum environment is to incorporate the following features:

For pressure-fed engines,

1. a. Nonpositive expulsion tanks
   b. Main thrust chamber propellant settling

2. Hypergolic propellants (either naturally hypergolic or hypergolic because of chemical additives)

For pump-fed engines,

1. a. Nonpositive expulsion tanks
   b. Main thrust chamber propellant settling

2. Tapoff turbine drive

3. Hypergolic propellants

### Discussion

Extraterrestrial landing propulsion systems must have the capability of starting (at least once, and several times in most cases) in the zero gravity, vacuum environment of space. A broad range of rocket engines,



FORM 608 B (LEDGER) REV. 1-58

described below, was considered in a design study to define the simplest and most reliable techniques for accomplishing engine start.

Engine Characteristics

| | |
|---|---|
| Thrust Level | 20,000 to 100,000 pounds |
| Number of starts | 2 - 6 |
| Propellant feed | Pump or pressure-fed |
| Propellants | Cryogenic or noncryogenic |

The conditions required for starting or restarting a liquid propellant rocket engine in a space environment are:

1. Supply propellants in usable form
2. Ready engines, which may include
   a. Prefire purge
   b. Chill down
   c. Engine controls checkout
3. Supply turbine power
4. Ignite thrust chamber propellants

The purpose of this study was to investigate all possible types of engine systems with respect to the stated requirements and then to define and evaluate the applicable systems.

The major variable affecting the engine system operation is the vehicle-propellant tank configuration, specifically whether they are positive expulsion type or not. Engine system comparisons were made for both positive expulsion tanks and for tanks where no positive expulsion device is employed. The possible avenues of approach for engine starting are shown in Table 15.

Propellant Supply. It is necessary to supply liquid propellants within the design temperature and pressure range to the engine inlets. This may be accomplished in two ways. First, liquid propellants may be assured by a positive expulsion device such as diaphragms or force fields as discussed in Reference 25. Care must be taken either to prevent vaporization on the liquid side of the diaphragm or to enable the expulsion device to separate the gas phase and control its position. If a positive expulsion device is used, no engine modification is required for a zero 'g' environment.



FORM 608 B (LEDGER) REV. 1 58

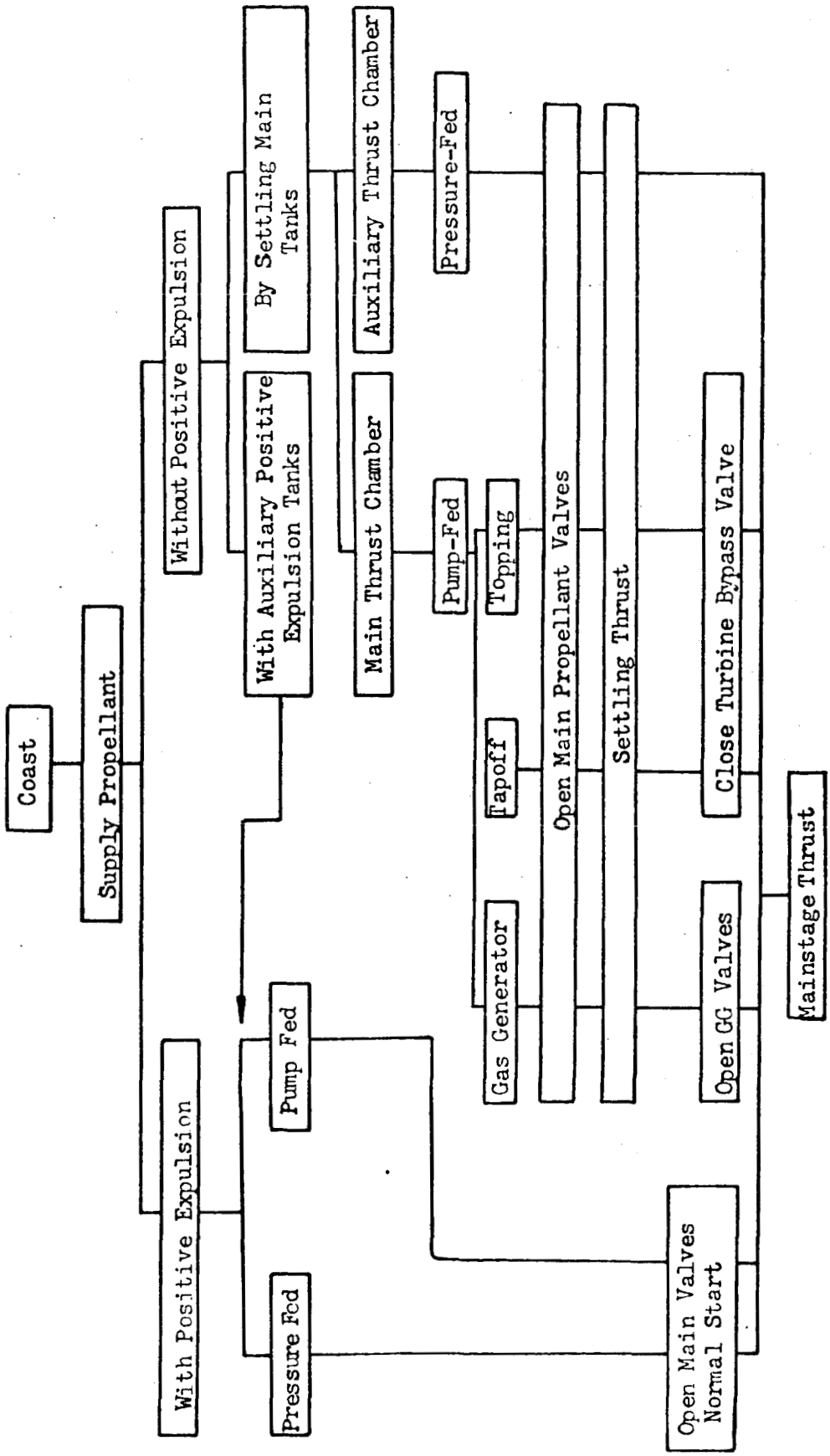


Table 15. Engine Start Methods



Form 608-B (Vellum) Rev. 1-58

Second, if no positive expulsion device is used, the liquid phase propellants may be supplied to the engine inlets by applying a settling thrust, that is, a thrust and consequently an acceleration to the vehicle in such a direction that the liquids will settle to the bottom of the propellant tank and the gases to the top of the tank. This propulsive settling thrust may be obtained by either the main thrust chamber or an auxiliary thrust chamber. Auxiliary positive expulsion start tanks, Figure 4a, may be supplied to provide liquid propellants to the pump- or pressure-fed engine, to allow mainstage operation prior to main propellant tank settling. These start tanks must be sized for as many starts as required. The start characteristics then become identical to the case of positive expulsion tanks. The settling time for different gross weight vehicles and different propellant combinations is shown in Figures 5 and 6. Certain system modifications must be made to some engine systems before the main thrust chamber can be used for settling. These modifications are discussed below for each type engine system.

Pressure-Fed (Figure 4b). Settling thrust may be obtained in a pressure-fed system by opening the main propellant valves. This permits propellants to flow to the combustion chamber where they can be ignited to provide settling thrust. The effect of any pressurant gas flowing into the engine is discussed later. If a nonregeneratively cooled thrust chamber is used, no modification is required. If a regeneratively cooled chamber is used, heat transfer studies must be made to assure acceptable tube wall temperatures over the expected range of engine operation during start.

Pump-Fed Systems. As in the case of the pressure-fed system, if a regeneratively cooled thrust chamber is used, its cooling capabilities must be investigated. The major consideration when using the pump-fed engine is to insure liquid propellants are in the turbopumps prior to applying turbine power. This condition is necessary to prevent pump overspeed and bearing failure.

Gas Generator System (Figure 4c). In a conventional gas generator system, settling thrust may be obtained by opening the main valves while keeping the gas generator valves closed and igniting the main chamber propellants.

Tapoff Turbine Drive System (Figure 4d). The main combustion chamber may be used for settling thrust only if a gas shutoff valve is provided in the turbine inlet line.

Topping Turbine Drive System. Three types of turbine drive systems are possible which would be termed topping cycle turbine drives. They are the bipropellant gas generator, Figure 4e, the monopropellant gas generator,



FORM 604 B (LEDGER) REV. 1 58

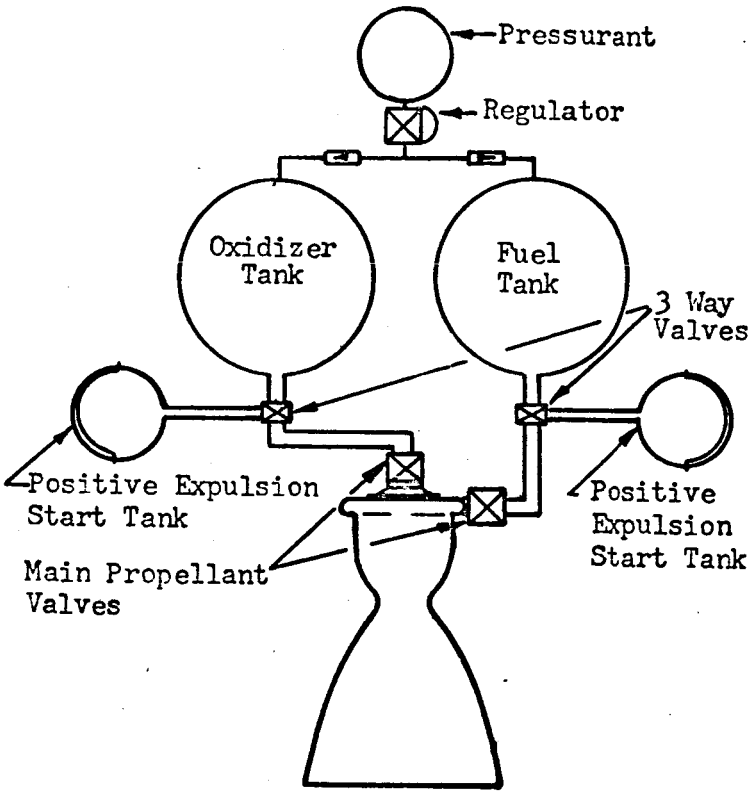


4a. Pressure Fed System with Auxiliary Positive Expulsion Start Tanks

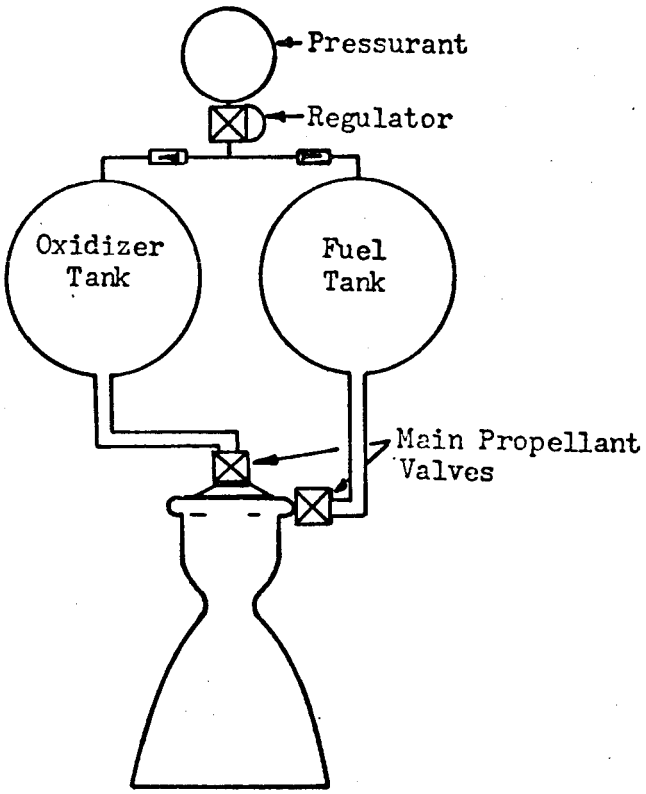


4b. Pressure Fed System

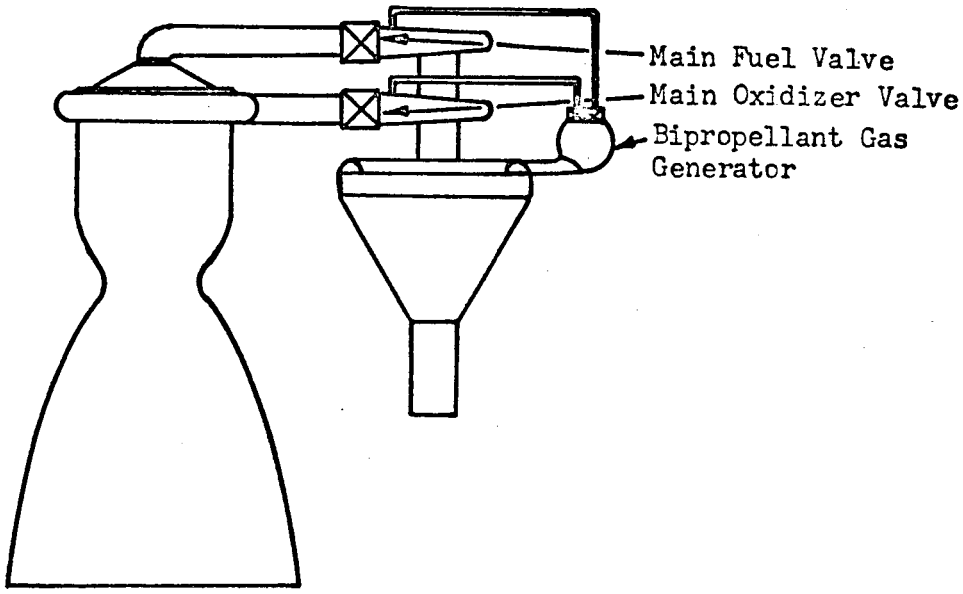


4c. Bipropellant Gas Generator



Form 608-B (Vellum) Rev. 1-58

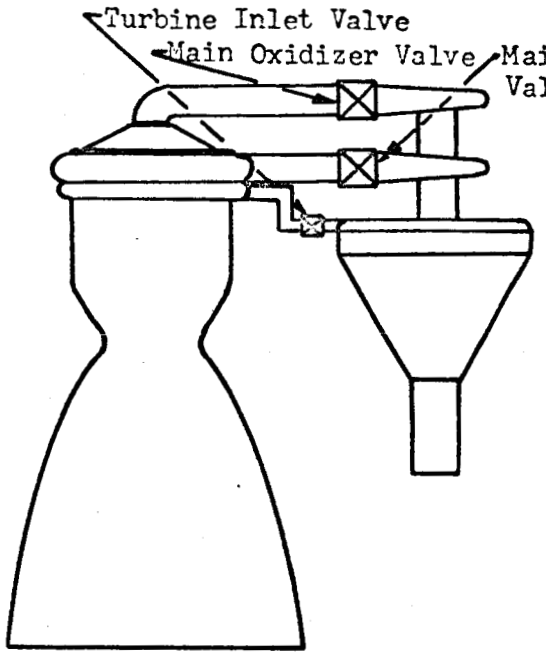


4d. Main Combustion Chamber Tapoff

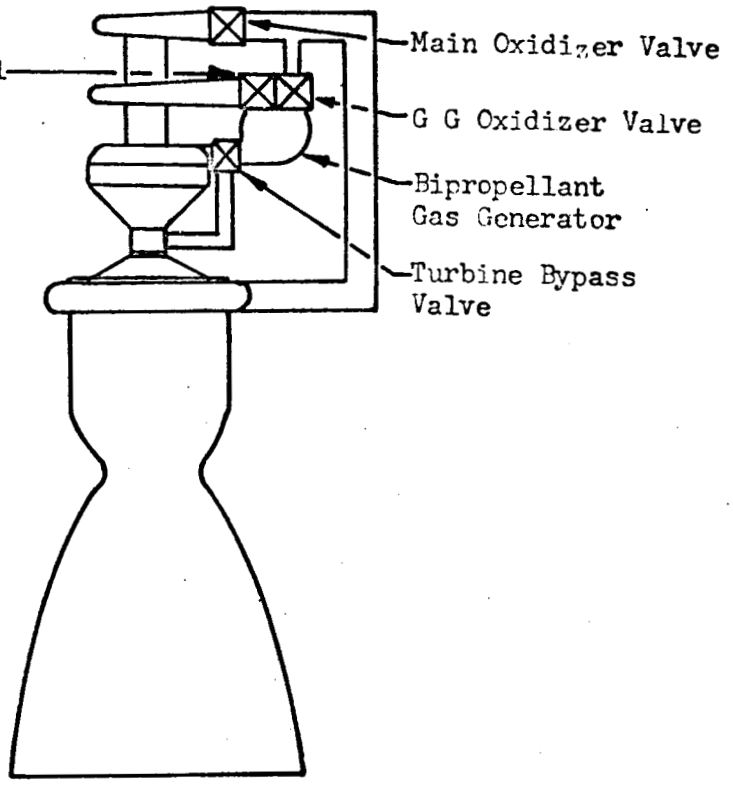


4e. Topping Cycle Bipropellant GG

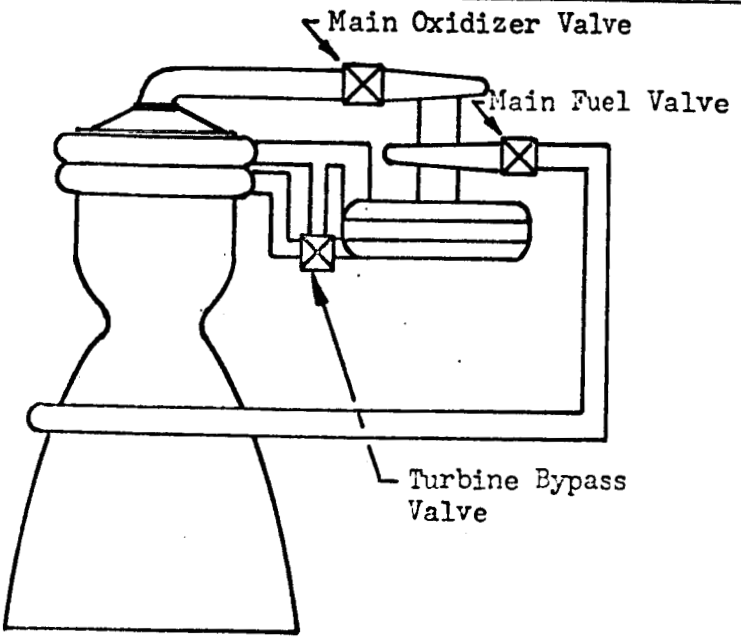


4f. Regenerative Topping Cycle

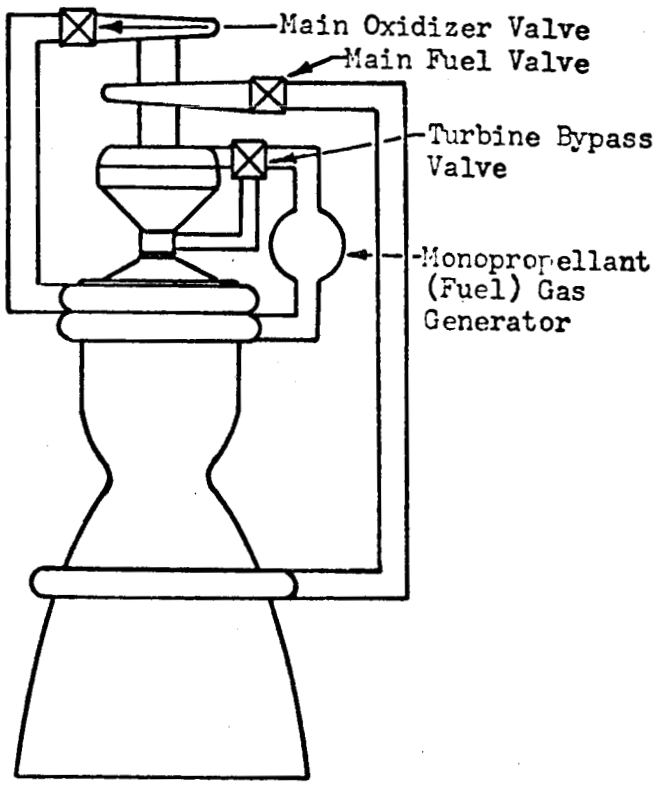


4g. Topping Cycle - Monopropellant GG



Form 608-B (Vellum) Rev. 1-58

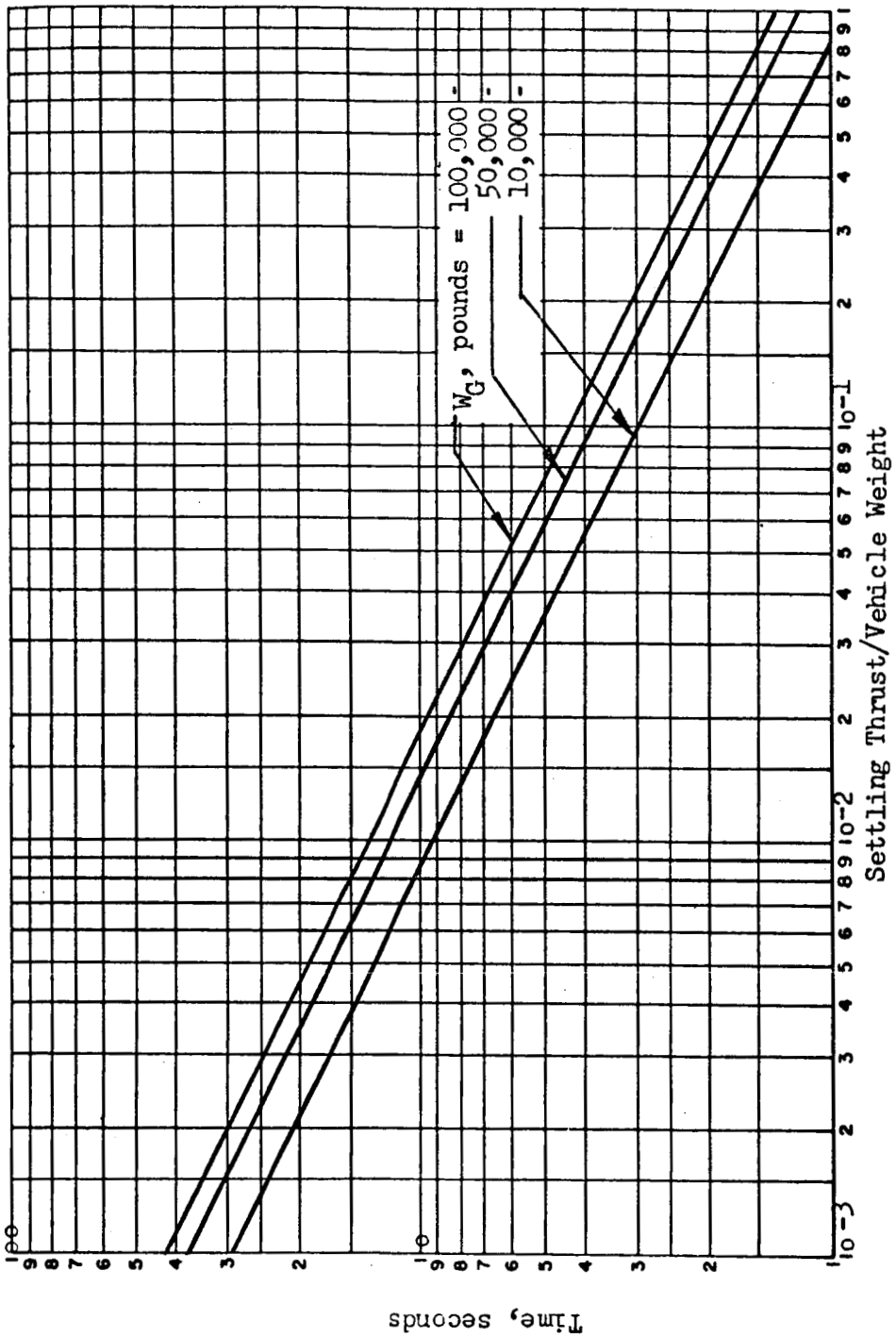


Figure 5. Propellant Settling Time vs Thrust $O_2/H_2$

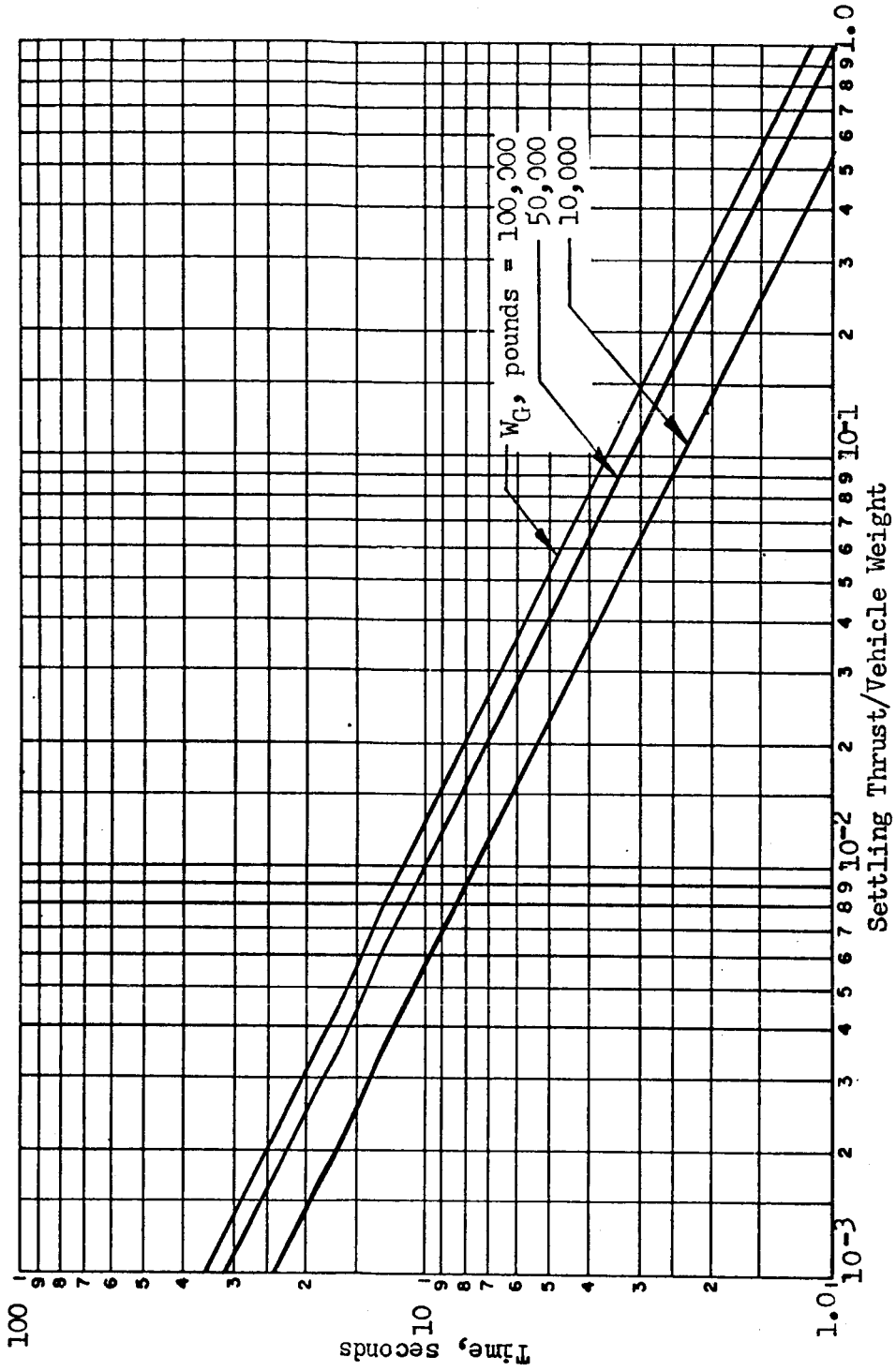


Figure 6. Propellant Settling Time vs Thrust NTO/MMH

Figure 4g, and the regenerative, Figure 4f, topping cycles. In order to use the main combustion chamber for propellant settling, the turbine inlet must be closed with a valve and a bypass around the turbine with a valve is required.

For the tapoff and topping cycles, the valves which are required for obtaining settling thrust may also be required for throttling in which case the effect on engine reliability is not great.

Auxiliary Engine. If the coolant jacket in a regeneratively cooled engine is found to be inadequate for the requirements of the settling thrust operation, an auxiliary thrust chamber may be used to provide the required thrust. If the system complexity required for main chamber settling thrust is great and excessively penalizes system reliability, an auxiliary thrust chamber may be advantageous. The landing propulsion system may include a suitable thrust chamber whose main function is midcourse correction, or attitude control, which can be used for settling thrust without sacrificing system reliability. The operating characteristics of this engine with two phase propellant flow will be similar to the pressure-fed engine as described later.

Prefire Engine Preparation. Prior to engine start, the following operations are sometimes required to provide a safe repeatable start.

1. Controls checkout
2. Prefire purge
3. Chilldown

The controls checkout in some form will be accomplished, but is not pertinent to the present discussion. The purpose of the prefire purge is to eliminate foreign fluids in the injector, dome and feed lines prior to the admission of main propellants. In a space environment, the presence of any fluids in these areas is prevented by the low pressure environment. A purge in one propellant feed line may be utilized to prevent recirculation of the other propellant during the start sequence and to allow safe ground testing.

Chilldown is required in certain cases. First, where turbopumps are used, a chilldown is required to insure that the propellant at the inducer blades is at design temperatures. This is necessary to prevent cavitation of the inducers when power is applied to the pumps. Also, where a regeneratively cooled thrust chamber is used, and if there is a phase change of the propellant in the tube bundle, a chilldown is sometimes required to provide a repeatable flow buildup in the coolant jacket and provide adequate cooling during engine start.



FORM 608-B (LEDGER) REV. 1 58

Turbine Power (Pump-Fed Systems Only). Turbine power may be applied only after liquid propellants under design conditions of temperature and pressure are in the turbopumps. As described earlier, turbine power may be obtained by a gas generator, either monopropellant or bipropellant, by a tapoff of the main combustion chamber, or by a topping cycle. Initial starting of the turbine may be accomplished by any of the following start methods:

1. Tank head
2. Start tanks
3. Gas spin
4. Solid propellant spinner
5. Auxiliary gas generator, either bipropellant or monopropellant

The associated weights and reliabilities of the above system applied to a typical extraterrestrial landing propulsion engine are shown in Table 16. As seen from the table, the lightest and most reliable system for each type turbine drive is obtained by a tank head start. Sufficient cause must exist before another type of start system is selected. Among possible reasons for inadequacy of a tank head start, which is characterized by a relatively slow thrust buildup (on order of two seconds):

1. Emergency fast start requirement after propellants are settled. May be required if engine-out capability is accomplished by a standby engine and required response is determined to be less than available from tank head.
2. Thrust buildup impulse tolerance is beyond capabilities of relatively slow start.
3. Combustion stability is inadequate for relatively slow buildup. However, since landing engines require a variable thrust range, a stable combustion regime is required over a wide range of thrust so that stability is assured during most of thrust buildup.

Where no positive expulsion tanks are used, the possibility exists that both liquid and gaseous propellants will be admitted to the engine. This will occur when starting the pressure-fed thrust chamber or when operating a main or auxiliary thrust chamber of a pump-fed system to provide a settling thrust.

The effect of this gas phase on the ignition and operating characteristics of the engine must be evaluated. Generally speaking, the presence of a gas phase propellant will not in itself prevent ignition where it would normally occur. In fact, all tests and theory indicate that the ignition delay is decreased with higher gas partial pressure, Reference 26. In other words, the presence of a gas phase will improve the ignition characteristics of a given propellant combination. Superimposed is the effect of shifting mixture ratio due to the propellant density change. The mixture ratio shift will cause wide variance in ignition characteristics, combustion temperature, molecular weight, weight flow rate, thrust, and specific impulse.

TABLE 16

| | Estimated Reliability | Start System Weight, pounds |
|---|---|---|
| Bipropellant GG | | |
| Tank Head | | |
| Start Tanks | 0.9773 | |
| $O_2/H_2$ | | |
| Rechargeable 1 start | 0.9767 | 6.0 |
| 4 starts | 0.9767 | 18.5 |
| Nonrechargeable 6 starts | 0.9768 | 27.8 |
| $O_2/H_2$* | 0.9768 | 32.0 |
| $O_2/H_2$* | | |
| Rechargeable 1 start | 0.9767 | 15 |
| 4 starts | 0.9767 | 50 |
| Nonrechargeable 6 starts | 0.9768 | 75 |
| Gas Spin | | |
| Rechargeable 1 start | 0.9763 | 69.9 |
| 4 starts | 0.9763 | 265.0 |
| Nonrechargeable 6 starts | 0.9764 | 394.5 |
| Monopropellant GG start | 0.9748 | 36.6 |
| Solid Spinner | 0.9650 | 131.0 |
| Main Chamber Tapoff | | |
| Tank Head | | |
| Gas Spin Start | 0.9838 | |
| Rechargeable 1 start | 0.9820 | 74.9 |
| 4 starts | 0.9820 | 270.0 |
| Nonrechargeable 6 starts | 0.9821 | 399.5 |
| Solid Cartridges | 0.9721 | 180.0 |
| Monopropellant GG | 0.9822 | 53.2 |

* Gaseous



FORM NOH 8 (LEDGER) NOV 1 60

The variations in thrust chamber operation for two-phase $O_2/H_2$ in a pressure-fed engine is shown in Figure 7. The assumptions made in deriving the data for these curves are: nominal engine operation is with liquid propellants which are supplied by tanks with equal pressures; fluid discharge coefficients are constant and independent of flowrate; flow area for two-phase flow is the sum of flow area of the gas plus the flow area for the fluid. Also, the gas phase propellants are assumed to be ideal gases.

The nominal engine parameters chosen for this study are:

| | |
|---|---|
| Propellants | Oxygen/Hydrogen |
| Mixture Ratio | Oxidizer/Fuel 5.0 |
| Chamber Pressure | 100 psia |
| Tank Pressure | 165 psia |

As seen from Figure 7 for the $O_2/H_2$ combination, the hydrogen quality does not greatly affect engine thrust, and the thrust is nearly linear with oxygen quality. Thrust is essentially directly related to chamber pressure; the discrepancy due to the variation in the gas specific heat ratio amounts to less than 5 percent.

Consideration of noncryogenic propellants, in this case NTO/MMH, for a pressure fed engine leads to a somewhat different result than obtained with cryogenic combinations. Gas phase propellants will not occur in non-cryogenic systems as the temperatures required for vaporization are prohibited by safety considerations. However, if no positive expulsion tanks are used, there exists the possibility that entrained pressurant gases will pass through the injector. Since these gases are generally inert, the effect on chamber performance is different than for vaporized propellants. Complete definition of the stable combustion parameters over the entire range of possible conditions is not easily attained and is not covered here. However, general parameters can be defined.

For the case of liquid fuel combined in the chamber with only oxidizer tank pressurant gas admitted through the oxidizer feed line, the chamber temperature ideally will drop below the freezing temperature of the fuel. Preliminary investigation indicates that the chamber pressure will be approximately 2 psia, although the influence of several variables cannot be precisely determined. Among them are the time transients required to transform the phase of the fuel, and to transfer heat from the surroundings to the combustion chamber gases. Similar results are obtained in analyzing liquid oxidizer with fuel tank pressurant gases supplied through the fuel feed line. However, even with only 2-psia chamber pressure, the time required for settling the propellants is less than 10 seconds.



FORM 608 B (LEDGER) REV. 1-59

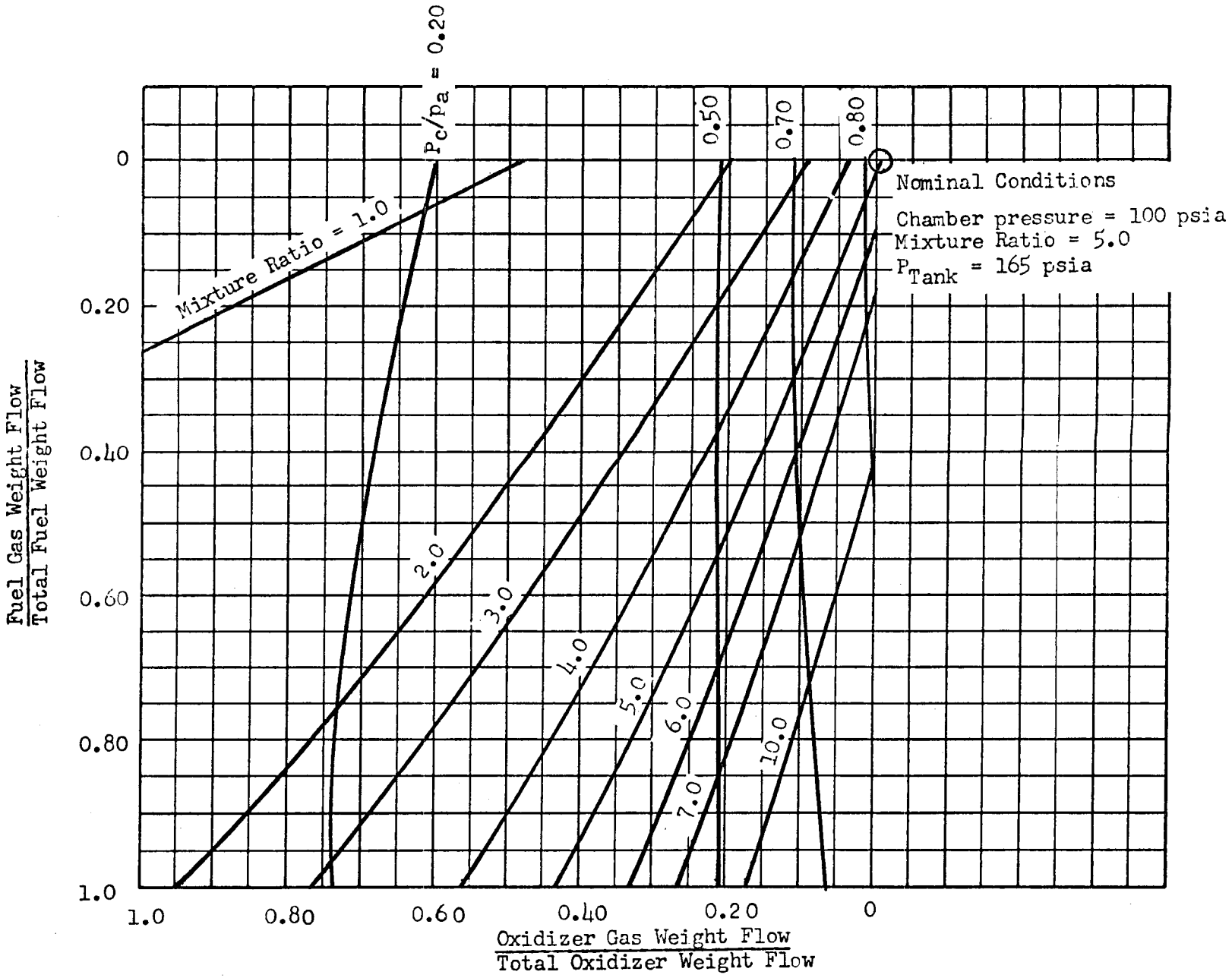


Figure 7. Engine Operation With Two-Phase Propellants



ROCKETDYNE
A DIVISION OF NORTH AMERICAN AVIATION, INC.

The data presented in Figure 8 show the effect of inert pressurant gas ingestion over a limited range of conditions. The propellants used are NTO/MMH and the pressurant was assumed to be inert. The nominal engine parameters chosen were:

| | |
|---|---|
| Mixture ratio | 1.5 |
| Chamber pressure | 100 psia |
| Tank pressure | 165 psia |
| Fluid temperatures | 60 F |

Ignition. The method of igniting propellants affects the reliability of the propulsion system. An extraterrestrial landing engine is required to start as many as seven times so that the ignition method must be able to be reused an equal number of times with high reliability. The following ignition methods include all systems currently in use in liquid propellant rocket engines and all those known to have been considered by Rocketdyne. A brief description of each type, as applied to a space mission with many restarts, is included. Primary emphasis is placed on thrust chambers in the 20,000 to 300,000 pounds thrust range.

Hypergolic Propellants: (Figure 9A). When the chemical properties of a propellant combination are such that under normal ambient conditions the combination will chemically react without the addition of external energy or the presence of any particular foreign material, the combination is said to be hypergolic. When a hypergolic propellant combination is used, no ignition system is required. NTO/MMH is an example of a hypergolic propellant combination.

Propellant Additives Which Cause Hypergolicity: Figure 9A) Chemical compounds may sometimes be added to one propellant of a combination to cause the combination to be hypergolic. A propellant combination in which an additive has been used will be termed artificially hypergolic. An example of this is the addition of Ozone Fluoride to oxygen causing the combination of liquid oxygen/ liquid hydrogen to be hypergolic (Reference 25 ).

Auxiliary Start Tank of Hypergol Propellant: (Figure 9B). This system uses an auxiliary supply of a liquid propellant which is hypergolic with the oxidizer or fuel. The auxiliary hypergol is admitted into the thrust chamber just prior to one propellant and creates a heat source which causes ignition of the fuel and oxidizer. An example of this type system is shown in Figure wherein the addition of Fluorine prior to hydrogen in an $O_2/H_2$ system reacts with the oxidizer to provide the ignition source (Reference 27).

Hypergol Cartridge: (Figure 9C). This system in principle is identical to the auxiliary hypergol start tank. The cartiridge, however is a positive displacement tank holding only sufficient hypergol for a single start. For multiple starts either multiple cartridges must be used, or a refill operation must be included for each start. The cartridge type system is currently being used on the Atlas and Saturn engines for single starts.



FORM 608 B (LEDGER) REV. 1-59

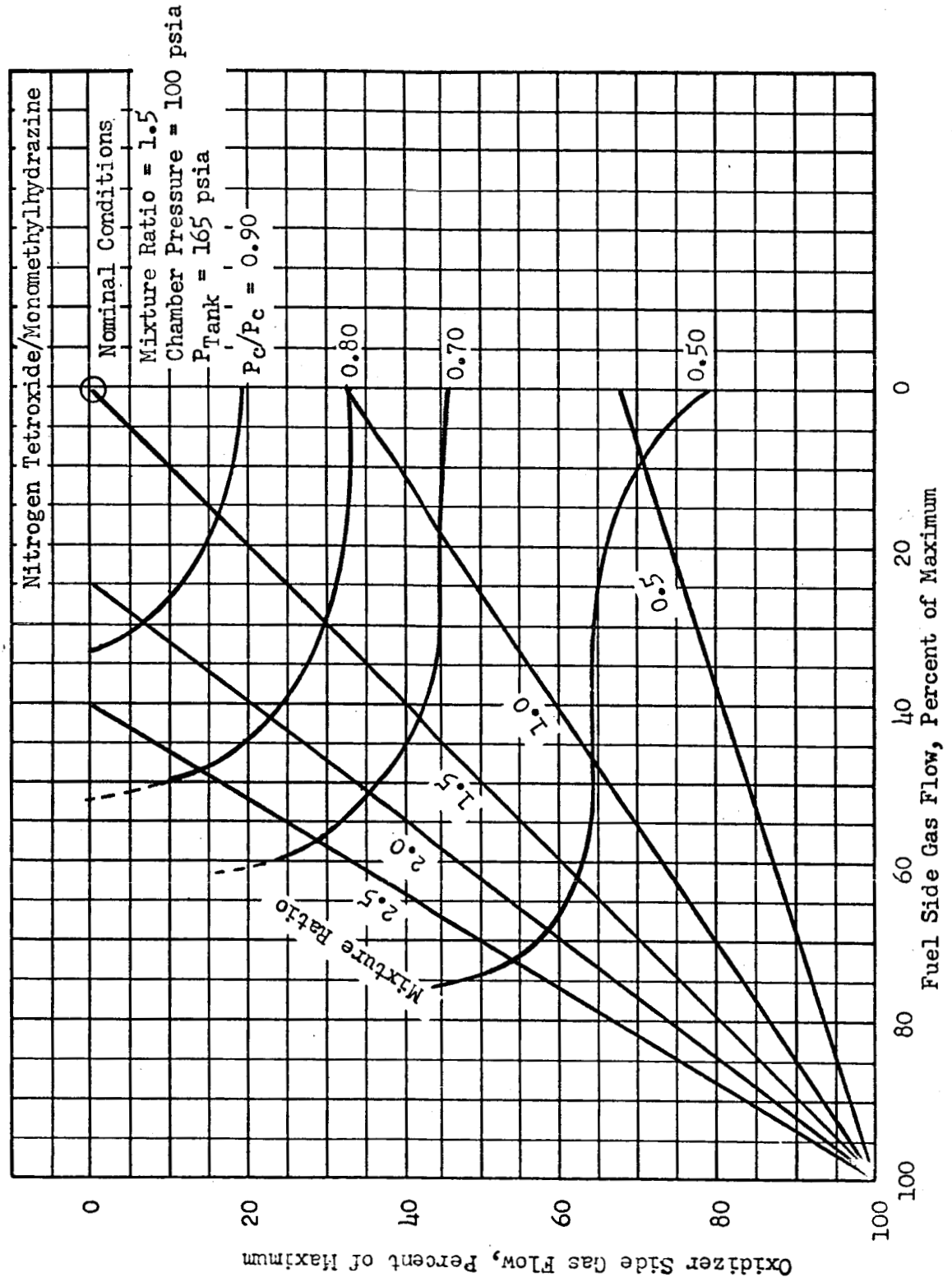


Figure 8. Effect of Pressurant Gas Entrainment on Thrust Chamber Performance

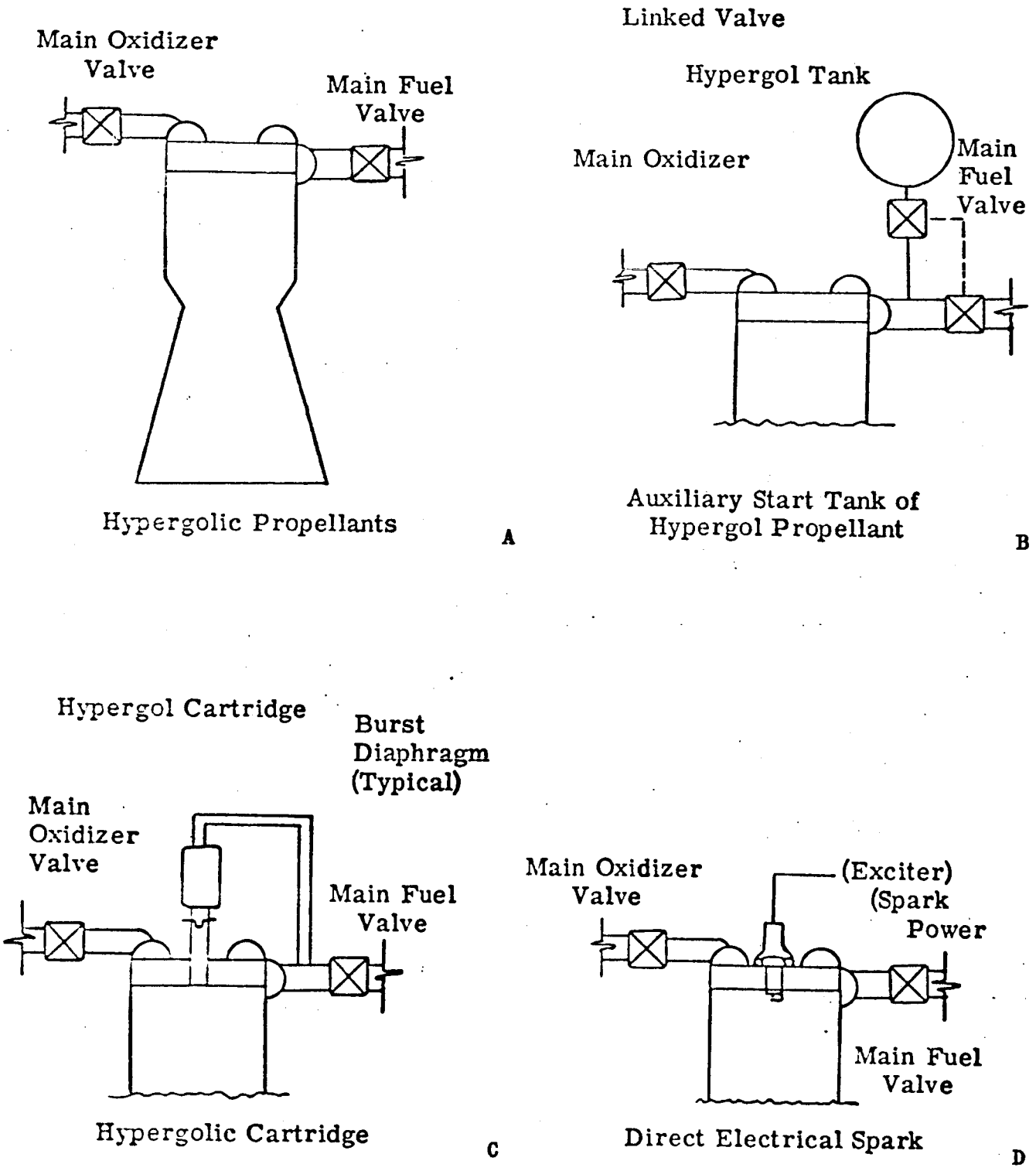


Figure 9. Propellant Ignition Methods

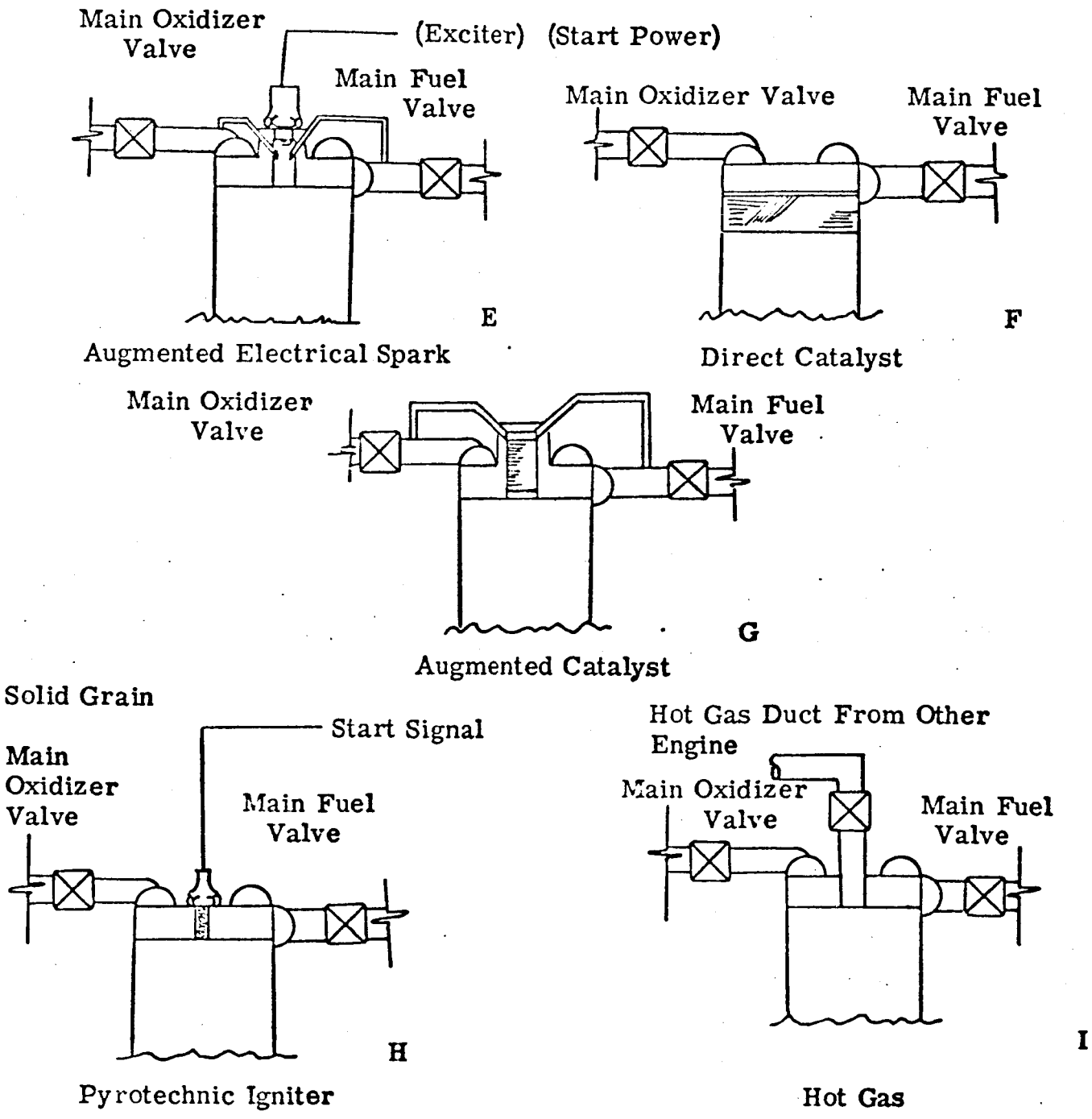


Figure 9. Propellant Ignition Methods



FORM 600 B (LEDGER) REV 1 58

Direct Electrical Spark: (Figure 9D). This igniter provides an electrical spark which supplies energy to the mixed propellants causing their ignition. The direct spark ignition system does not require any additional plumbing or particular propellant feed sequencing (Reference 28). It is necessary to provide a combustible mixture in the vicinity of the spark discharge. The spark igniter may be located on the side of the chamber or in the injector or sometimes recessed in the injector in order to obtain this mixture consistently. Direct spark ignition is currently being used on the F-1 and J-2 gas generators and the Pratt and Whitney RL-10 engine which have nominal flowrates in the range of a few pounds to several hundred pounds per second.

Augmented Electrical Spark Igniter: (Figure 9E). This system ignites a small combustor which is generally recessed in the injector face. This small combustor then ignites the main combustion chamber propellants. Separate propellant valves are used to supply propellant to the auxiliary chamber prior to main thrust chamber propellant flow. An augmented spark igniter is used on Rocketdyne's J-2 engine which operates at a thrust of 200,000 pounds.

Direct Catalyst: (Figure 9F). The direct catalyst bed is located directly in or adjacent to the main combustor. The direct catalyst ignites the propellants as they are supplied by the main propellant valves. Currently, Rocketdyne is testing Palladium coated alumina pellets for ignition of oxygen/hydrogen (Reference 29).

Augmented Catalyst: (Figure 9G). Analogous to the augmented electrical spark discharge, the augmented catalyst igniter requires separate propellant feed lines and valves. The augmented catalyst igniter propellant flows to the main combustion chamber where, once the igniter flame is established, main propellants are admitted and main chamber ignition takes place.

Pyrotechnics: (Figure 9H). These small solid propellant grains are ignited generally by an electrical bridge wire and as they burn, provide heat to ignite the main propellant flow. Separate grains must be used for each engine start. Pyrotechnic igniters have been used on the Thor, Jupiter and Atlas engines for single starts.

Hot Gases From Other Sources (Figure 9I). Ignition of any combustible mixture of propellants can be initiated by means of a suitable energy source. Sufficient heat is sometimes available from an auxiliary piece of equipment, either an alternate engine or perhaps the gas generator of an auxiliary power unit. This heat source must be available prior to the time the thrust chamber is to be ignited to allow for thermal lag in the hot gas feed lines.



FORM 608 B (LEDGER) REV 1 58

When considering the ignition methods applicable to a space system requiring many restarts, such as would be typical of extraterrestrial landing engines, the use of pyrotechnic or hypergolic cartridge igniters can be eliminated due to the large number of components required and the resultant low reliability. The duty cycle of the engine would not be the same as any other engine so that a hot gas source would not always be available for ignition when required. Of the remaining ignition methods, the choice must be based on reliability, weight, availability, and ease of development. The best engine system of those considered is obtained with hypergolic propellants, either normally or artificially hypergolic. Additives which cause hypergolicity, however, are not currently in use and must be developed before being recommended. A comparison of Figures 9D and 9E shows that the augmented spark system has no advantage over a direct spark method (so long as the direct spark supplies sufficient energy for ignition) and will not be considered further. Similarly, the augmented catalytic igniter (Figure 9G) shows little advantage over the direct catalytic igniter (Figure 9F) and need not be considered further. The advantages that the augmented methods offer are realized in large engine systems where the igniter power for a direct spark system would be prohibitive and the difficulty of developing a large effective direct catalyst configuration is not warranted. The auxiliary start tank of hypergolic propellants which must be fed into the combustion chamber in the correct sequence is shown in Figure 9B. The complexity of this system is greater than that of the direct catalytic ignition method so that the reliability of the catalytic method would be significantly higher. Also, the weight of the stored hypergol propellant system would be greater than the weight of the catalytic system.

The above brief comparison may be represented on a rating chart. The preferred ignition systems for advanced and current engine systems respectively are indicated in Table 17 by the subtotal and total points scored.

For an advanced engine, the preferred ignition systems as indicated by the subtotal scores are:

1. Hypergolic propellants - Figure 9A
2. Catalytic Igniter - Figure 9F
3. Direct spark igniter - Figure 9D

For a current engine program, the preferred ignition systems as indicated by the total score in Table 17 are:

1. Direct electrical spark
2. Auxiliary tank of hypergol
3. Direct catalyst



FORM 608 B (LEDGER) REV. 1 58

TABLE 17

| Ignition System Type | Reliability | Cost | Ease of Development | Weight | Subtotal | Current Feasibility | Total |
|---|---|---|---|---|---|---|---|
| Maximum Rating | 10 | 5 | 5 | 5 | 25 | 20 | 45 |
| 1. Hypergolic Propellants | 10 | 5 | 5 | 5 | 25 | 5 | 30 |
| 2. Auxiliary Start Tank of Hypergol | 7 | 3 | 3 | 2 | 15 | 20 | 35 |
| 3. Hypergol Cartridge | 0<br>0 | 0 | 2 | 0 | 2 | 10 | 12 |
| 4. Direct Electrical Spark | 8 | 3 | 2 | 4 | 17 | 20 | 37 |
| 5. Augmented Electrical Spark | 6 | 2 | 2 | 3 | 13 | 20 | 33 |
| 6. Direct Catalyst | 8 | 4 | 3 | 4 | 19 | 15 | 34 |
| 7. Augumented Catalyst | 6 | 3 | 3 | 3 | 15 | 15 | 30 |
| 8. Pyrotechnics | 0 | 2 | 2 | 0 | 4 | 0 | 4 |
| 9. Hot Gases | 8 | 5 | 3 | 5 | -- | 10 | -- |

ROCKETDYNE
A DIVISION OF NORTH AMERICAN AVIATION, INC



FORM 608 B (LEDGER) REV. 1 58

Review of Advanced Engine Ignition Methods. The principal concern of the present study was advanced engines. The following discussion reviews the three ignition methods selected as best suited to advanced extraterrestrial landing engines.

Hypergolic Propellants. The principal advantage of a hypergolic propellant combination is that it enjoys a reliability advantage over other systems since no components or system operations need be added to obtain ignition. The effect of a vacuum environment is not detrimental to the ignition process as discussed in Reference 26. Propellant heating due to heat soak from the chamber to the feed lines increases the propellant vapor pressure and thereby improves the ignition process as indicated by a reduction in the ignition delay time, (Reference 26). A consideration which could adversely affect the ignition process with hypergolic propellants is the ingestion of inert pressurant gas. Information regarding the significance of this effect is not presently available. The combination of NTO/MMH is normally hypergolic and follows the criteria defined above.

Artificially hypergolic propellants are currently being studied at Rocketdyne and elsewhere. Primary consideration is being given to the $O_2/H_2$ combination since this combination has a distinct performance advantage over noncryogenic propellants for most missions. Current testing has indicated that 0.1 weight percent ozone fluoride ($O_3F_2$) when added to liquid oxygen till cause the combination of $O_2/H_2$ to be hypergolic (Reference 25). Further work is required to define minimum requirements of $O_3F_2$ percentage and to define storability limitations. Although not yet substantiated, this artificially hypergolic propellant can be expected to behave in a manner similar to the normally hypergolic combinations; that is, heat and vacuum will not adversely affect the ignition process.

Direct Spark Ignition. The application of energy by a direct spark igniter will ignite a nonhypergolic propellant combination. In general, a vacuum environment will not affect the ignition of $O_2/H_2$ since the atmosphere surrounding the spark discharge will be created and defined by the propellants fed into the combustion chamber and will not be affected by external ambient conditions of pressure and temperature. Development of the direct spark ignition system is required for each injector configuration to obtain a combustible gas phase mixture in the vicinity of the spark discharge. Supporting components are required to convert the engine start signal, generally 24 volts dc, to energy useful in creating a spark (Reference 28 ). These components, namely a spark exciter and monitor, detract from system reliability and require environment controls which add complexity to the engine system. The direct spark igniter system has been used on the J-2



FORM 608 B (LEDGER) REV. 1 58

gas generator and on the Pratt and Whitney RL-10 thrust chamber. The igniter of the RL-10 is recessed in the injector face, but no added plumbing is used and therefore it is classified as a direct spark system.

Catalytic Ignition. Reaction of nonhypergolic propellants may be induced by the presence of a catalyst. In this discussion, catalyst will be used in a broad sense including both materials which may be consumed by the ignition and combustion process and those materials which are not consumed. Work on a catalyst for $O_2/H_2$, Figure 10, is in progress at Rocketdyne (Reference 29). Here again, the effect of ambient pressure and increased temperature should not adversely affect the ignition process. A candidate material which acts as a catalyst for $O_2/H_2$ is Palladium coated alumina pellets. Further work is required before this system can be considered available for use. Considerations which need to be investigated include effect of contaminants and the magnitude of ignition response time.

Comparing the last two of the above methods and assuming the electrical power to be free, that is, no weight penalty incurred due to the power requirements, the complexity of the spark igniter system which includes spark device, wiring, spark exciter, monitor and power supply, precludes its choice over the catalytic igniter for an advanced engine.

In summary, the best ignition method for an advanced space engine with a large number of starts is, in order of decreasing desirability:

1. Hypergolic propellants which are either normally hypergolic or with additives which cause artificial hypergolicity.

2. Direct catalytic igniter

3. Augmented catalytic or direct spark



FORM 608 B (LEDGER) REV. 1 58

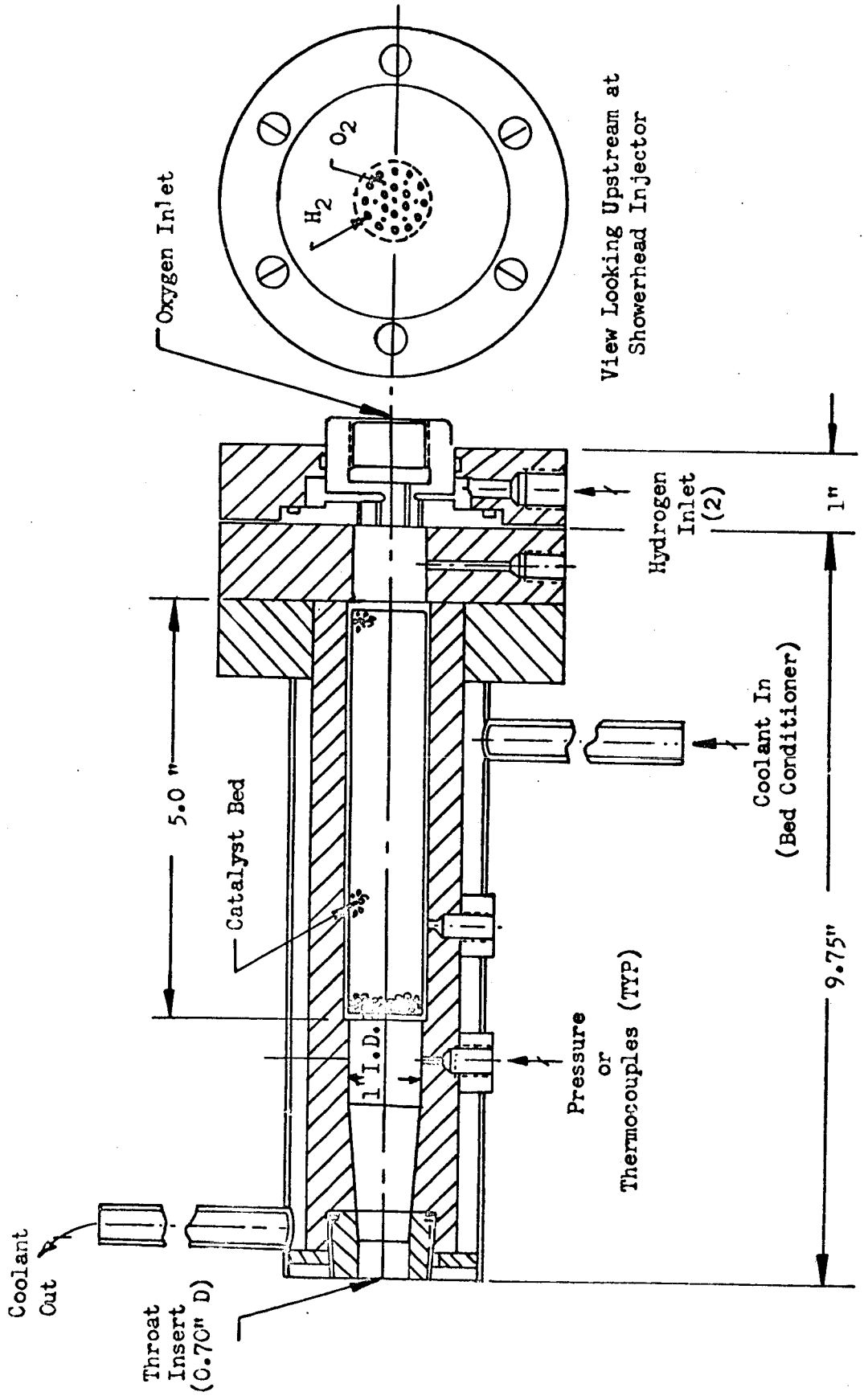


Figure 10. Schematic of 1-inch Diameter Combustor Showing 5.0-inch Bed and Showerhead Injector



Form 603-B (Vellum) Rev. 1-58

# APPENDIX D

## LANDING GEAR SYSTEMS FOR EXTRATERRESTRIAL LANDING VEHICLES

### Summary

A design study of landing gear systems for extraterrestrial landing vehicles was performed to define the requirements of touchdown devices, to determine the weights of various landing gear configurations and to select the system best suited to the lunar landing mission. The vehicle under consideration had a high center of gravity in comparison to its base diameter, representative of a vehicle which includes an expended propulsion system; this geometry causes a pronounced tipping instability to exist upon impact. To counteract the tipping instability, it was necessary to place the landing feet at large radial distances from the vehicle, thus making the structural weight of the landing gear much heavier than that of the energy absorber. An important conclusion of this investigation is that the energy absorbed per unit mass is not the most important factor in selecting the energy absorber, and other considerations such as packaging and reuseability can be considered to be equally or more important.

The total weight of the landing gear system ranged between 3 and 9 percent of the gross weight of the vehicle. Increasing or decreasing the impact velocity caused corresponding changes in the landing gear weight. Three different energy absorbers, the hydraulic cylinder, frangible tube, and crushable metal honeycomb were considered so that the effect of varying the energy absorber on total landing gear weight could be assessed. For long stroke landings (i.e., at high impact velocities and low deceleration rates) the frangible tube is superior to the hydraulic cylinder. For shorter stroke applications, the two are approximately equal, the hydraulic cylinder having the advantage of repeated landing capability.

### Discussion

General Design Considerations. In recent years, considerable interest has been shown in investigating and developing energy absorbing devices suitable for use in landing gear systems. In contrast to such conventional devices as hydraulic cylinders and dry friction brakes, more



FORM 608 B (LEDGER) REV 1 58

novel and unusual mechanisms have been developed such as crushable metal or fibrous honeycomb, crushing balsa wood, cold-working or straining a metal, frangible tubes, and air bags. The primary interest of investigations in this area has usually been directed towards increasing the energy absorption per unit mass of the energy absorber. The overall design and packaging of the landing gear and the stability of the vehicle-landing gear system upon impact was usually secondary in importance. In those studies which did consider landing stability upon impact, the vehicle was assumed to have low center of gravity (cg) in comparison to its base diameter, a ratio of 0.2 being typical (Reference 30, 31, 32, and 33).

For extraterrestrial landing vehicles which make a retrorocket-powered descent, a low cg configuration is unlikely since at impact, the lower section of the vehicle will consist primarily of empty tankage. A center of gravity height-to-base diameter ratio for such a craft might be approximately 2, an order of magnitude larger than the ratio previously mentioned. A severe instability problem will exist upon impact which can only be counteracted by placing the landing feet at large radial distances from the vehicle.

For such a configuration, it would be expected that the structural weight of the landing gear system would become large in comparison to that of the energy absorber. Therefore, the present study was concerned primarily with the placement and utilization of the different energy absorbers. Included were such considerations as the tipping stability of the vehicle upon impact, the effect of this factor upon landing gear weight, and the value of using very high performance energy absorbers as opposed to more conventional devices.

The approach utilized was to choose a particular landing vehicle and formulate a series of landing gear designs, varying such parameters as the deceleration rate, the type of energy absorber, and the impact velocity. Although the vehicle geometry and landing environment are also variables which strongly influence the weight and performance of the landing gear, they were not changed; it was felt that the vehicle and landing mission chosen were typical of extraterrestrial landings in which the vehicle makes a retrorocket powered descent. The designs were not fully optimized with respect to weight reduction; only a few values for each parameter were chosen. However, sufficient results were obtained to demonstrate trends and to permit general conclusions to be drawn.

To obtain an indication of the performance capabilities of a frictional energy absorber, the temperature rise was computed for different energy abosrbing materials having a mass equal to one percent of the gross weight



FORM 608-B (LEDGER) REV. 1 58

of the vehicle. An impact velocity of 20 ft/sec was chosen as typical. The resultant temperature increase for various materials is shown in Table 18. The average temperature increase is very small, indicating that the material is being used at well below its ultimate energy-absorbing capacity. Weight reductions of perhaps two orders of magnitude could be made while still imparting the same energy to the various materials.

TABLE 18

| Material | Temperature Rise, F |
|---|---|
| Oil | 2.04 |
| Aluminum | 3.91 |
| Stainless Steel | 6.85 |
| Asbestos | 4.25 |

Although frictional energy absorption makes very efficient use of the energy absorbing material, it is probably not much more than an order of magnitude better in this respect than more conventional, lower performance systems. Thus, for moderate impact velocities (in the neighborhood of 20 ft/sec) it is evident that the weight of most energy absorbers need not be a large fraction of the landing gear weight. Considerations such as packaging and deceleration characteristics can be used for their selection.

Landing Mission. The landing mission chosen for this study was a space craft landing on the moon. The important characteristics of the vehicle, terrain, and landing are given in Table 19.

TABLE 19

Vehicle Characteristics

| | |
|---|---|
| Weight | 30,000 pound mass |
| Height | 30 feet |
| Height of the c.g. | 20 feet |
| Base Diameter | 12 feet |
| Moment of Inertia about the cg | $0.5 \times 10^7$ lbm-ft$^2$ |

Terrain Characteristics

| | |
|---|---|
| Ground Roughness | ± 4 inches |
| Slope | 6 degrees maximum |
| Local Gravitational Constant | 5.35 ft/sec$^2$ |



FORM 608-B (LEDGER) REV. 1-58

TABLE 19 - Continued

Landing Parameters

| | |
|---|---|
| Vertical Impact Velocity | 10 to 50 ft/sec |
| Horizontal Impact Velocity | 2 ft/sec |
| Maximum Deceleration | 5 to 10 g |
| Maximum Onset Rate of Deceleration | 1500 g/sec |

The various parameters of the landing mission, although selected somewhat arbitrarily, are considered to be typical of most extraterrestrial landings.

Design and Packaging of the Landing Gear. The basic configuration chosen for the landing gear consists of a tripod, the feet of which are tied together by a steel guy wire. Each leg consists of two struts which contain the energy absorbing elements and which become compressed upon impact of the vehicle with the terrain. The structure is nonredundant and should be able to withstand sizeable sideward loads during impact without buckling.

An improvement upon the tripod configuration shown in Figure 11 is shown in Figure 12. The latter design is merely two tripods superimposed on each other, making a six foot landing pattern. This latter design is much more resistant to tipping than the previous model. A detailed veiw of a hydraulic energy absorber mounted in place in the landing gear is shown in Figure . For either model, packaging during flight can be accomplished by using the guy wires to draw the legs in close to the booster which supports the landing vehicle.

Since one of the objects of the study was to evaluate the importance of using a high performance energy absorber, two different energy absorbers, the hydraulic cylinder and frangible tubes, were considered. The frangible tube, shown schematically in Figure 14 and described in References 31 and has a very high energy absorption per unit mass and provides a good contrast to the hydraulic cylinder, a more conventional device.

When designing the hydraulic cylinder, the oil was pressurized to a nominal value of 300 psi and a maximum stress of 30,000 psi was imposed on the material used in the cylinder. In the design of the frangible tube, an attempt was made to make the compressive stress on the tube approximately 40 percent of the yield stress (Reference 31), although it was not always possible to do this. For both the frangible tube and the hydraulic cylinder, local and overall buckling constraints were imposed on the members under compression.



FORM 608-B (LEDGER) REV. 1-58

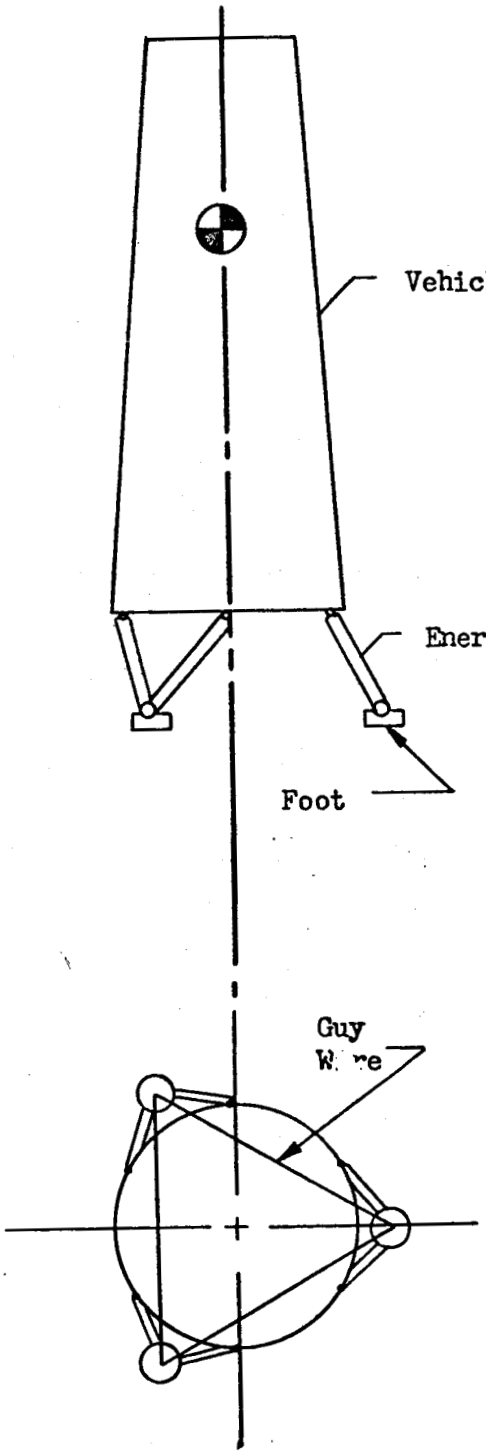


Figure 11. Schematic Representation of Landing Vehicle With Tripod Landing Gear

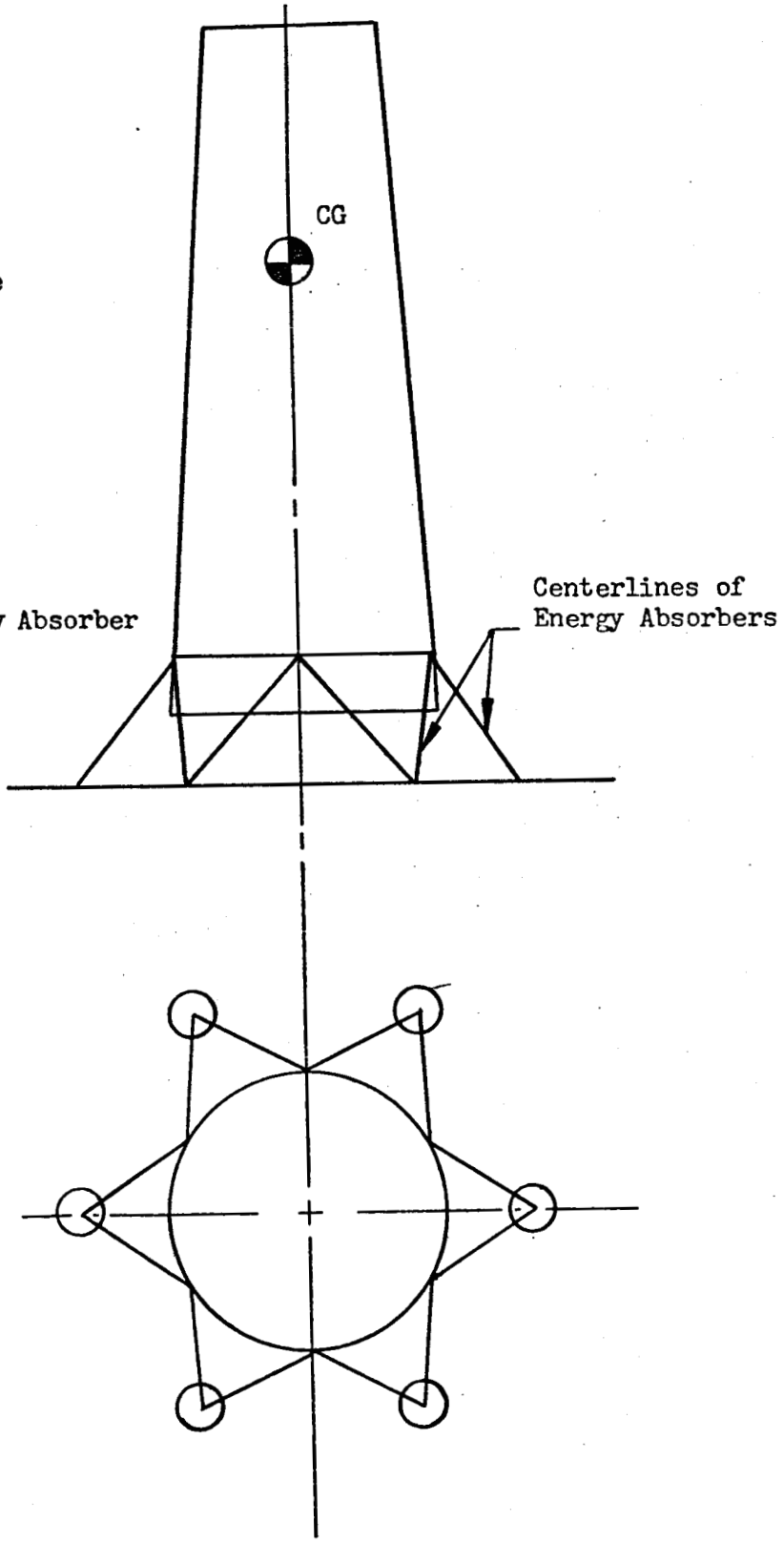


Figure 12. Schematic Representation of Landing Vehicle with Dual Tripod Landing Gear



FORM 608-B (LEDGER) REV. 1 58

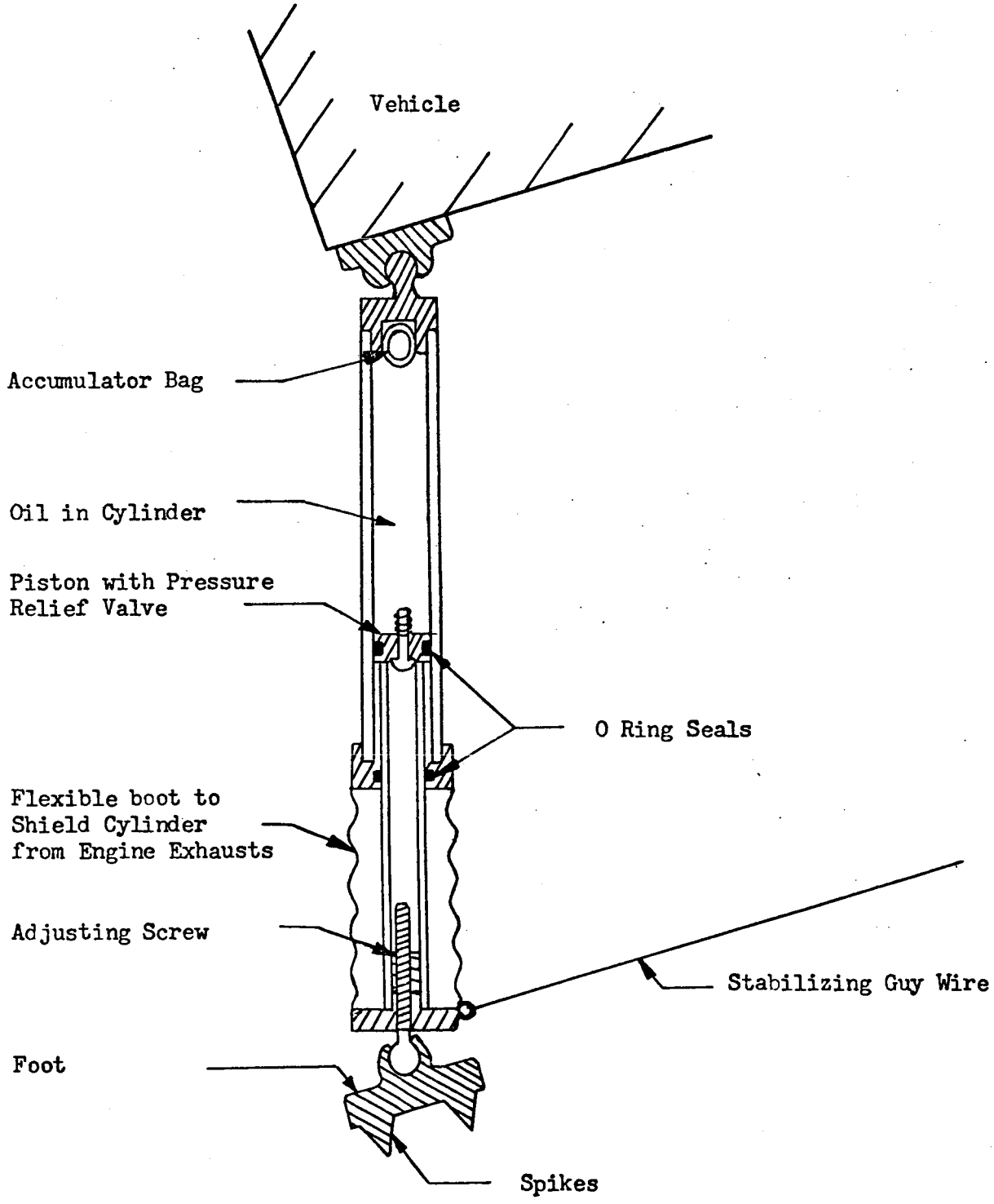


Figure 13. Detail of Hydraulic Damping Cylinder
Scale 1 inch equals 20 inches



FORM 608-B (LEDGER) REV. 1 58

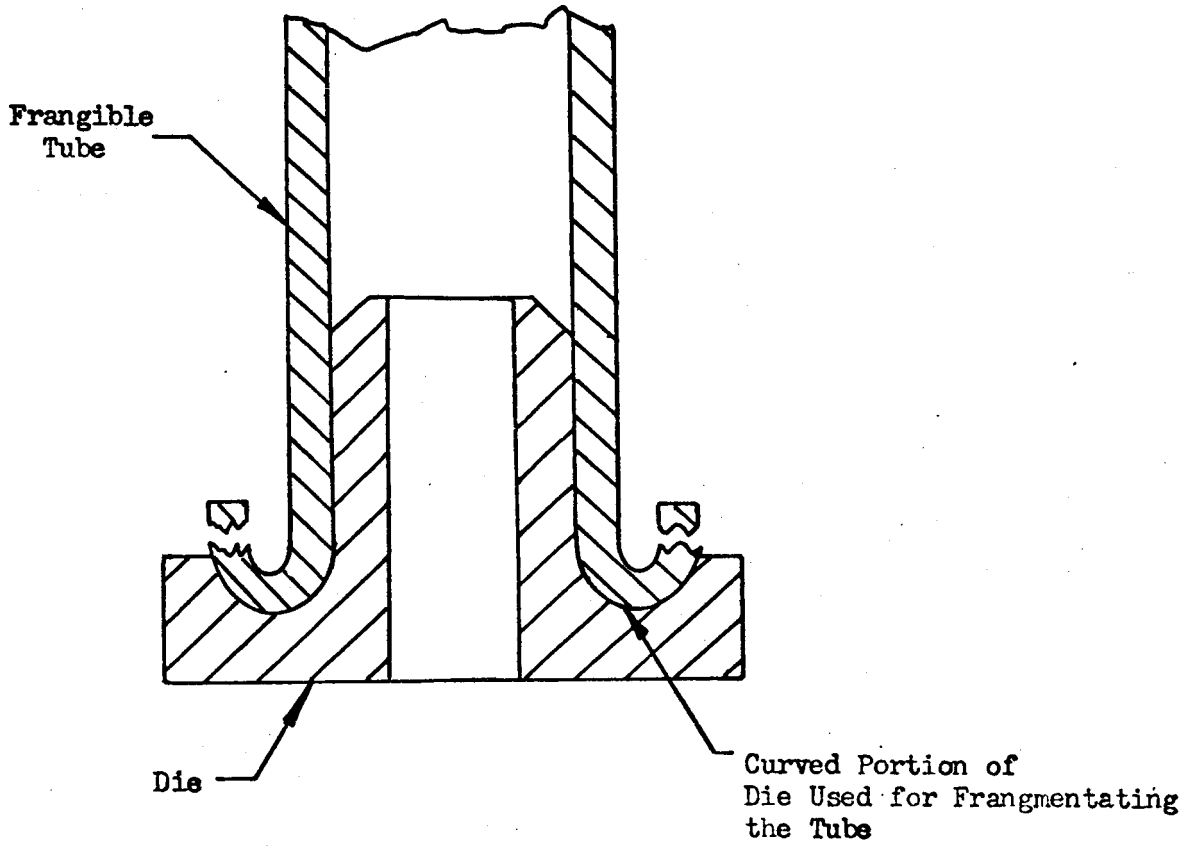


Figure 14. Schematic Diagram of the Frangible-Tube Energy Absorber



Form 608-B (Vellum) Rev. 1-58

## Results of the Design Study

The results of the design study are presented in Table 20 and the follow-in graphs. The first four models of the landing gear (A through D) are of fixed geometry, the deceleration rate and energy absorber being varied. Models E-1, E-2 and E-3 have a tripod configuration with very long legs, the feet at the ends of the legs being placed at a large radial distance from the vehicle to counteract the tipping instability. Model F is a dual tripod configuration such as shown in Figure 12 and G series models are dual tripod models showing the effect of varying the impact velocity while the deceleration rate and the final landing geometry are held fixed. In Table 20 ,only the G model for a 20 ft/sec impact velocity is shown. The variation of landing gear weight as a function of impact velocity for G models is shown in Figure 15 , and the variation of tube weight and component weight respectively are shown in Figures 16 and 17 .

The benefit of using a very high performance energy absorber depends primarily upon its packaging and the landing gear geometry. For landing gear configurations whose legs are not much longer than the deceleration length of the vehicle, the energy absorber will constitute a large percentage of the total weight. Models A through D have such a geometry and a substantial weight reduction, when frangible tube energy absorbers are substituted for hydraulic cylinders, is shown.

When the legs of the landing gear are made long to assure stability upon impact, the additional structural weight of the legs becomes large and makes weight reductions of the energy absorber less important. Models E-1 and E-2 which have very long legs show an increase instead of decrease of weight attending the use of a frangible tube energy absorber. This increase is largely contributed by the die which fragments the tube. Although the weight of the die can probably be reduced considerably by skillful design (perhaps the use of coated, aluminum die), the final total weight of the landing gear system would not be much less than the system using a hydraulic energy absorber.

Crushable, cellular structures such as metal honeycomb have a unique packaging advantage since they can be placed on the bottom of the landing feet and utilized directly. Model E-3, which uses metal honeycomb pads fastened to the bottom of the landing feet has a weight only 70 percent of the model using hydraulic cylinders. This weight reduction is probably optimistic, since it will be necessary for the honeycomb to withstand shearing forces upon impact. To keep the deceleration characteristics



FORM 608-B (LEDGER) REV. 1-58

TABLE 20

SUMMARY OF THE LANDING GEAR DESIGNS

| Model | Support | Energy Absorber | Diameter of Circle Circumscribing the Landing Feet, feet | Rest Height of Vehicle Above the Terrain, feet | Vehicle Deceleration, g | Max Horiz Velocity at 20 ft/sec Impact Velocity (Uphill impact on 6-degree sloping terrain), ft/sec |
|---|---|---|---|---|---|---|
| A | Tripod | Hydraulic Cylinder | 16 | 4.25 | 10 | -4.26 |
| B | Tripod | Hydraulic Cylinder | 18.4 | 3.66 | 5 | -4.95 |
| C | Tripod | Frangible Tube | 16 | 4.25 | 10 | -4.26 |
| D | Tripod | Frangible Tube | 18.4 | 3.66 | 5 | -4.95 |
| E-1 | Tripod with long legs | Frangible Tube | 32 | 1.66 | 5 | -5.55 |
| E-2 | | Hydraulic Cylinder | 32 | 1.66 | 5 | -5.55 |
| E-3 | | Metal Honeycomb | 32 | 1.66 | 5 | -5.55 |
| F | Dual Tripod | Frangible Tube | 20 | 1.66 | 5 | -0.80 |
| *G | Dual Tripod | Frangible Tube | 20 | 3.66 | 5 | -1.09 |

*Model G and Model F are similar configurations, but Model G is more conservative with respect to several dimensions.



ROCKETDYNE
A DIVISION OF NORTH AMERICAN AVIATION, INC

TABLE 20 - Continued

| Model | Maximum Horizontal Velocity - Level Landing, ft/sec | Maximum Vertical Impact Velocity, Impact on Uphill Leg, ft/sec | Total Weight of Landing Gear, lbm | Percent of Vehicle Weight |
|---|---|---|---|---|
| A | + 2.34 | 7.10 | 1240 | 4.14 |
| B | 2.83 | 9.80 | 1235 | 4.1 |
| C | 2.34 | 7.10 | 935 | 3.12 |
| D | 2.83 | 9.80 | 840 | 2.8 |
| E-1 | 9.25 | 12.5 | 2500 | 9.34 |
| E-2 | 9.25 | 12.5 | 1770 | 5.92 |
| E-3 | 9.25 | 12.5 | 1184 | 3.95 |
| F | 8.45 | 18.3 | 1110 | 4.18 |
| G | 7.35 | 17.4 | 1510 | 5.05 |



FORM 608-B (LEDGER) REV. 1-58

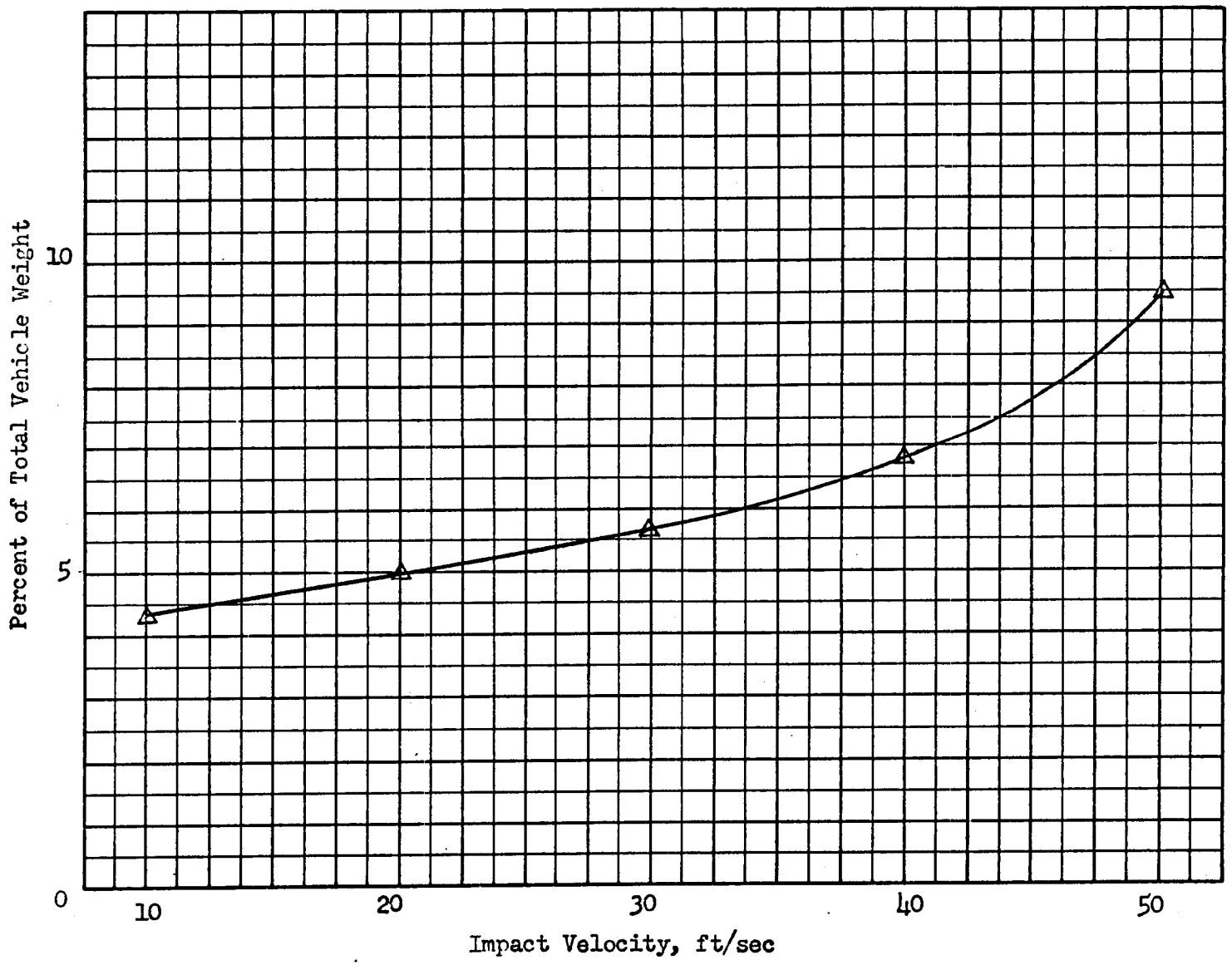


Figure 15. Variation of Landing Gear Weight vs Landing Impact Velocity ($M_{vehicle}$ = 30,000 lbm, 5 g Deceleration)

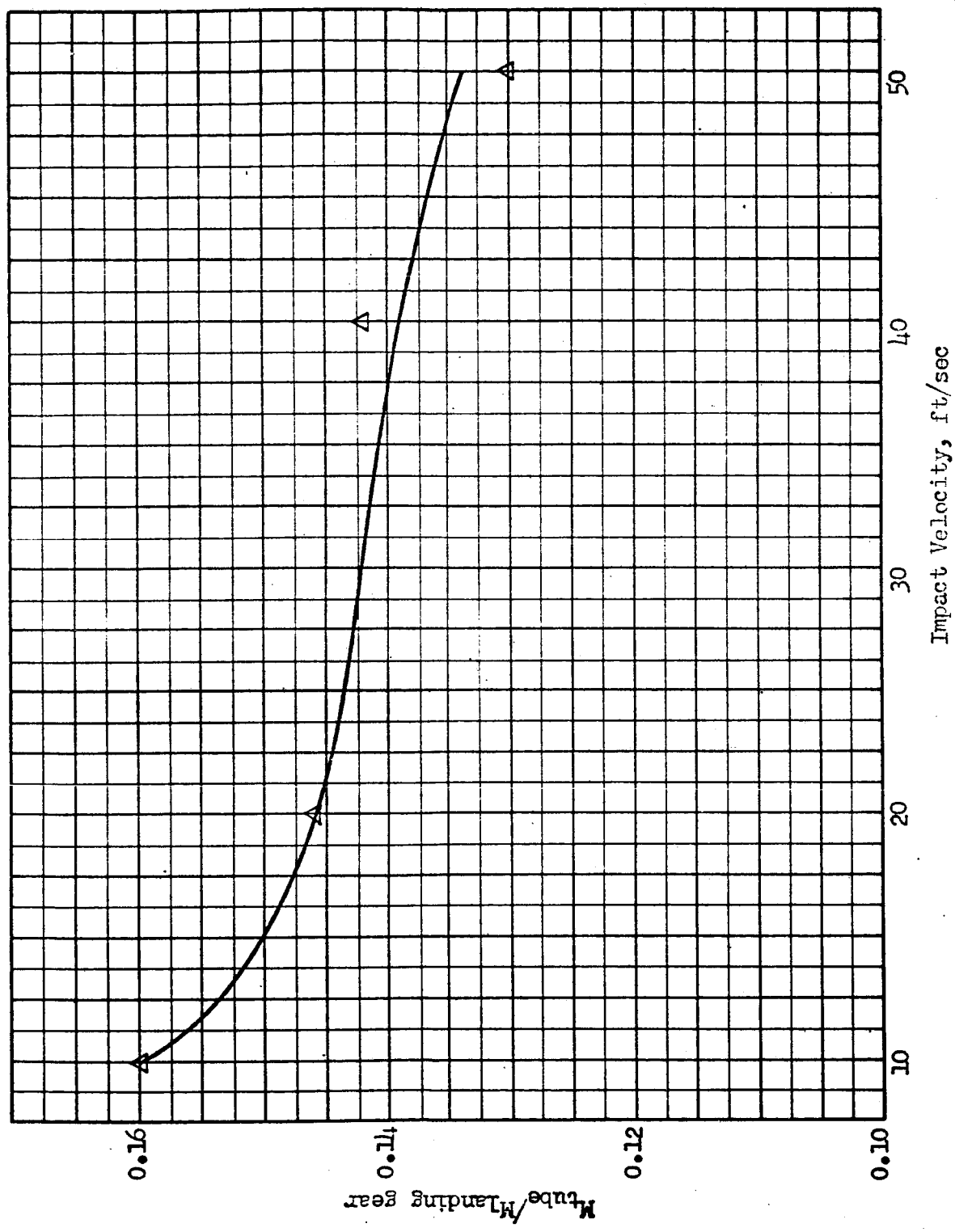


**Figure 16.** Ratio of Weight of Frangible Tube to Total Landing Gear Weights vs Impact Velocity

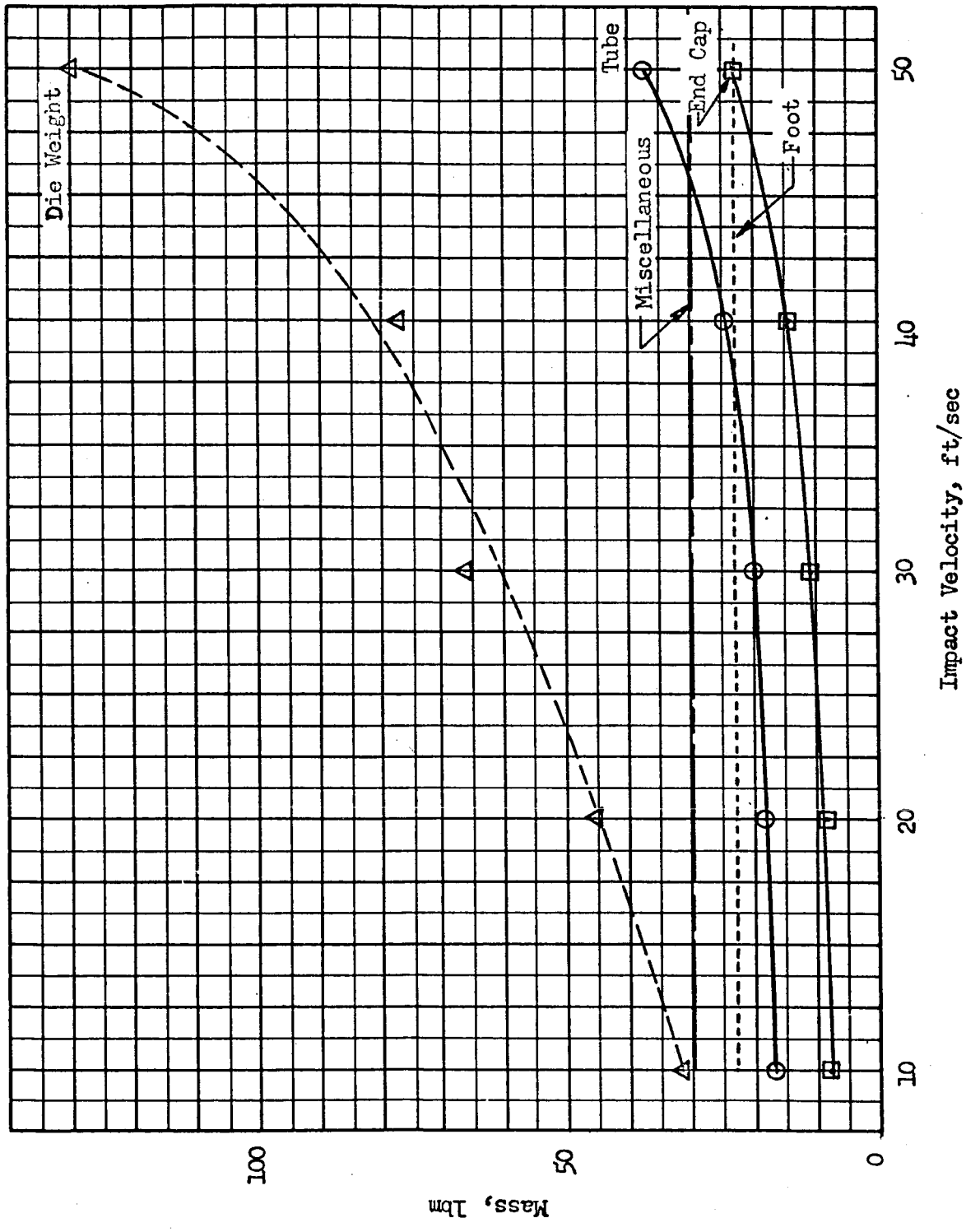


Figure 17. Variation of Component Weights vs Impact Velocity

uniform and to prevent the honeycomb from buckling or shearing, extra bracing and linkages are needed which will decrease the weight savings. This will be especially true if the deceleration length is long in comparison to the cross-sectional area of the honeycomb.

It is concluded that, although landing gear weight reductions can be accomplished by use of high performance energy absorbing materials, the percentage reduction is usually rather small for practical landing gear configurations. Thus considerations such as packaging, reuseability, and deceleration characteristics may be used for the selection of the energy absorber. Although this conclusion is drawn specifically for the vehicle-landing mission configuration under consideration, it is expected to apply to most missions in which the landing vehicle makes a retrorocket powered descent and where the local gravitational constant is low.

When comparing Models A through D, it is seen that the deceleration rate does not have a marked effect upon the landing gear weight when the legs of the landing gear are not much longer than the deceleration distance. This is due to the fact that the weight of the energy absorber, which constitutes a large portion of the leg weight, remains relatively insensitive to the deceleration rate. For landing gear systems with legs much longer than the deceleration length of the vehicle, this conclusion is not expected to hold. For such cases, an appreciable reduction in the weight of the legs results from using lower deceleration rates.

A further advantage of reducing the deceleration rate is that the deceleration length becomes longer in comparison to fluctuations in the terrain height, thus increasing the stability of the vehicle upon impact. It would thus be concluded that landing gear systems should be designed for relatively low deceleration rates.

The advantage, both in terms of stability and weight reduction, of using a six foot landing pattern as opposed to a tripod is readily seen by comparing Models E-1 and F.

The impact velocity scaling study performed on Models G showed a moderate increase in the total landing gear weight as the impact velocity was increased (Figure 15 ). Examination of Figure 17 shows that the die is responsible for most of the weight increase; the weight of the frangible tube remains a relatively small fraction of the total. It is expected that the weight of a hydraulic cylinder would behave in similar fashion, the weight of the die in Models G representing the weight of the hydraulic cylinder and the frangible tube corresponding to the extra-structural tube used to support the hydraulic cylinder.

As can be seen from Table 20 , a pronounced tipping instability exists upon impact. For hindleg impact on a sloping terrain, all of the configurations are unstable at impact velocities of 20 ft/sec (i.e., they require horizontal velocities directed uphill to maintain stability) and the maximum vertical velocity that can be tolerated by the most stable models is only 17 ft/sec. For landings on level surfaces, all can withstand moderate horizontal drift velocities.

The tipping instability is increased both by the very high center of gravity of the landing vehicle in comparison to its base diameter and by the low local gravitational constant. For any given extraterrestrial landing, the stability of the landing vehicle can only be increased by placing the feet of the landing gear as far as possible from the vehicle and by decreasing the deceleration rate so that the deceleration length is long in comparison to the terrain fluctuations.

The weight penalty resulting from making the legs long in comparison to the deceleration length is quite severe, as can be seen by comparing Models E-1 and E-2 with Models A through D. Decreasing the deceleration rate will increase the deceleration distance, and hence reduce the weight of landing gear models which have long legs. Decreasing the deceleration rate of the vehicle also increases its landing stability, and is therefore a very desirable method of reducing the landing gear weight.

## CONCLUSIONS AND RECOMMENDATIONS

For landing vehicles of the configuration and mission requirements considered in this study, further development and investigations of very high performance energy absorbers does not appear to be justified from the standpoint of weight reduction. The nonenergy absorbing structural weight of the landing gear is usually much larger than that of the energy absorbing material in the energy absorber. Thus, decreasing the weight of the energy absorbing material by using a more efficient energy absorber has little effect on the total weight of the landing gear.

In the design of a landing gear for a mission such as that considered, particular attention should be paid to packaging of the energy absorber. For example, by placing aluminum honeycomb on the bottom of the feet of the landing gear of Model E, substantial weight reduction was achieved. This weight reduction was primarily a result of placing the energy absorber where it could be used directly without the aid of additional peripheral hardware.



FORM 608-B (LEDGER) REV 1.58

Of the many landing gear designs possible, the dual tripod configuration shown in Figure 12 is recommended. The configuration has a relatively large effective base diameter, is easily stored during flight, and can take substantial shear loads during landing. In addition, since the landing gear struts are under pure compression, they will require no external bracing to enable them to take bending loads. Thus, this design will have lower weight than many other designs which have extensive bracing and support to the load carrying members.

In the design of a landing gear system, particular attention should be paid to the tipping stability of the landing vehicle upon impact. Failure to do this in the early stages of design can result in the selection of configurations in which a heavy weight penalty is paid for adapting them to meet stability requirements.

In the landing gear systems in which the energy absorber was varied, neither the hydraulic cylinder nor the frangible tube seemed markedly superior with respect to weight or performance. Selection of either would depend upon the mission under consideration, the hydraulic cylinder being better for repeated, short stroke landings and the frangible tube being superior when the deceleration length is a large portion of that of the landing gear strut.

Care must be used when selecting the frangible tube. It is indicated by the data from Reference 33 that the instantaneous force delivered by the frangible tube fluctuates widely about the mean value, thirty or forty percent being typical. These fluctuations would send undesirable pulses of force throughout the vehicle body. Another consideration of importance is that when the wall of the frangible tube becomes sufficiently thin in comparison to its diameter, it will begin to roll instead of fragmentating. The effect of the roll of metal upon the force-deflection characteristics of the tube at the end of a long stroke is not known.

An interesting method of decelerating the vehicle is to use the separation skirt between the vehicle and its booster as a crushable landing structure. Since the separation skirt would have to be carried most of the way to the landing point, it would not be assigned a very large effective weight for the landing mission. In addition, the problem of attachment, which has not been treated in the preceeding study, is already solved. The use of this technique, however, should be investigated further before it is seriously considered.



FORM 608-B (LEDGER) REV. 1-58

# APPENDIX E

## LUNAR SURFACE STORAGE OF LIQUID PROPELLANTS

### Selected Vehicle Configuration

A preliminary investigation of the storability characteristics of oxygen/hydrogen ($O_2/H_2$) and fluorine/hydrogen ($F_2/H_2$) propellant systems on a lunar equatorial site has been conducted to determine potential storage problems and indicate storage system weight requirements.

During lunar surface residence, heat transfer to the propellants from the Sun, the moon, and from components of the rocket vehicle will result in a propellant pressure and temperature rise for a nonvented system, or propellant boiloff for a vented system.

Investigation of a pump-fed propulsion system using nonvented tanks, because of their greater simplicity, was made. For the nonvented storage system, the propellant tanks are sealed and the absorbed heat causes an increase in pressure and temperature of the propellants, and thus, thermal protection of the cryogenic propellants from the adverse heating environment of the moon is required. If the thermal protection requirements are extensive, the potential advantage normally associated with the use of high energy cryogenic propellants is not obtained. Propellant tank design pressures (dictated by tank weight allowances) must not be exceeded, and the propellant must be maintained at a temperature (and vapor pressure) low enough for engine operation.

The interval over which a liquid propellant can be stored on the lunar surface is dependent upon the allowable propellant pressure and temperature rise (thus, the net total heat flux received during the storage period). The method developed herein for the analysis of propellant storability permits the calculation of heat transfer rates, storage times, and storage penalty weights (additional vehicle weight incurred in maintaining the propellants during the storage period) for thermally protected cryogenic liquid propellant tanks subjected to solar, lunar, and intravehicle heat sources. Due to the lack of any appreciable atmosphere on the moon, these thermal design conditions are determined principally by the laws and mechanisms of radiant and conductive heat transfer. The thermal protection system employed by the propellant tanks (see Figure 18) uses a cylindrical shell of superinsulation, a vehicle skin (outermost surface of insulation - exposed to external radiation) coating for control of solar absorptivity, and closely spaced reflective surfaces (foils) to reduce intravehicle heating.



FORM 608-B (LEDGER) REV. 1-58

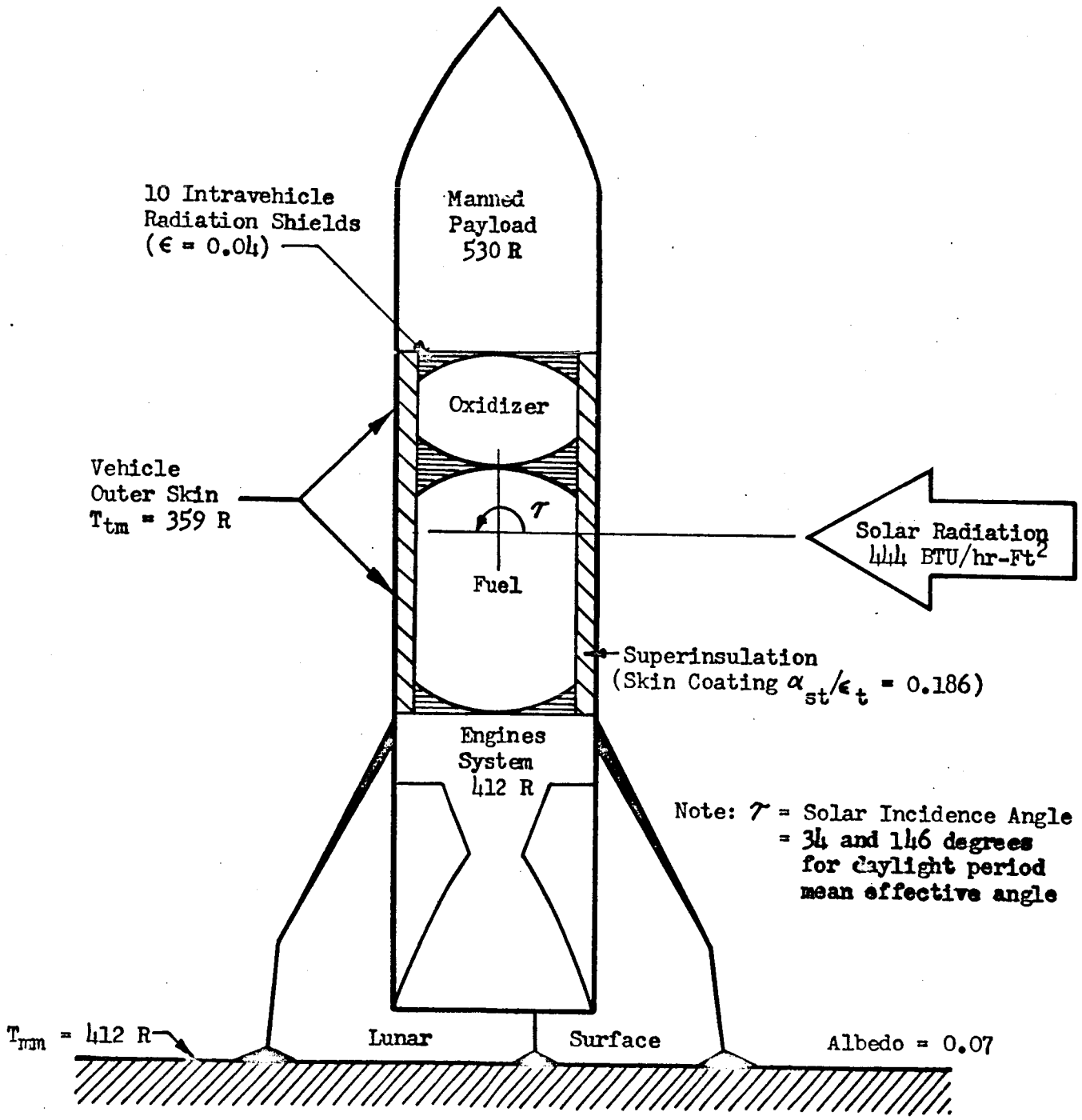


Figure 18 . Arrangement of Major Vehicle Components



Form 608-B (Vellum) Rev. 1-58

As the moon rotates about its own axis in its 27.3-day Earth orbit cycle, the solar heating effect varies as the sun passes overhead and vanishes during the dark phase of the cycle. The vehicle skin temperature thus varies as the Sun passes overhead; the temperature increases as the Sun's rays become less nearly perpendicular to the surface of the tank. For the purpose of simplifying the thermal analysis, a mean effective vehicle skin temperature for one complete lunar cycle was defined for use in estimating the heat transferred from the vehicle skin to the contained propellant by conduction through the insulation.

A lunar vehicle having a gross weight of 122,000 pounds, a total propellant weight of 61,800 pounds, and payload weight of 50,000 pounds was considered. These weights would provide an ideal velocity increment of approximately 10,000 ft/sec (for a lunar takeoff mission), based on a propellant fraction of 0.86, and a propellant specific impulse of 440 seconds. For the vehicle system investigated, the fuel and oxidizer are considered to be contained in separate cylindrical tanks of equal diameter with 2:1 ellipsoidal bulkheads, a combined length to diameter ratio of 1.75, and located below and in line with the payload as shown in Figure 18. (From the standpoint of heat transfer, the spherical tank is an optimum configuration because of its low surface area to volume ratio; however, a spherical tank offers little design flexibility as compared to a cylindrical tank of equal volume.) The vehicle was assumed to be sitting upright on the lunar equator, and no shadow shielding except that provided by the payload capsule was considered; therefore, the conditions assumed are severe with respect to storability problems.

## Propellant Storage Analysis

The objectives of this study were to evaluate the problem of cryogenic propellant storage in a lunar environment. The influence of various design parameters such as allowable propellant pressure rise ($\Delta p$) and propellant tank insulation thickness on the storage time, heat inputs, and storage penalty weights were investigated for vehicle systems using $O_2/H_2$ at a mixture ratio of 6:1, and $F_2/H_2$ at a mixture ratio of 15:1.

To simplify the analysis, the following basic assumptions were made: (1) the ecliptic plane and the lunar equatorial plane are coplanar, (2) the lunar landed vehicle is located on an infinitely flat plane at an equatorial site, (3) the insulation is considered to have the property of infinite lateral thermal conductivity so that its skin temperature is uniform throughout, (4) the tanks are initially perfectly insulated for determination of the vehicle skin temperature which is used in calculating the heat transferred through the insulation to the propellant, (5) the propellant is at a uniform temperature, and the propellant tank assumes the same temperature.



FORM 608-B (LEDGER) REV. 1-58

Heat Sources. The external sources of heat are the Sun and the moon. Heat is transferred between these sources and the cryogenic storage system by thermal radiation. Direct solar energy with an assumed average intensity of 444 Btu/hr-ft$^2$ irradiates the storage tanks during the lunar daytime period (time between lunar sunrise and sunset).

Solar energy which is reflected from the lunar surface (albedo) is assumed to have an average intensity of 7 percent (0.07) of the direct solar energy. Radiation emitted from the lunar surface (infrared) penetrates the storage tanks during the entire lunar cycle and is directly proportional to the fourth power of the absolute temperature of the lunar surface.

The intravehicle sources of heat to a propellant are the components adjacent to the tank such as the other propellant tank, the payload capsule (manned-assumed 530 degrees R in this analysis), or the rocket engines (assumed the same temperature as the lunar surface mean temperature, 412 degrees R). The heat transfer due to adjacent components is caused by thermal radiation and by conduction through structural members. The rate of heating by radiation is approximately proportional to the difference between the fourth powers of the absolute temperatures of the adjacent component and the propellant. The rate of heat transfer by conduction is directly proportional to the product of temperature difference between adjacent components and thermal conductivity and cross-sectional area of the supporting member, and inversely proportional to the length of the support.

Heat Conducted Through Insulation. The surface of the vehicle is considered to be the outermost surface of the insulation which surrounds the propellant tank and which is exposed to external radiation. For a given propellant temperature, type of insulation, and insulation thickness, the Fourier heat conduction equation shows that the instantaneous heat flux to the propellant is dependent upon the vehicle skin temperature. Because the insulation thickness is small compared to the tank diameter, the heat flux through the insulation has been calculated as for a flat plate

$$Q_{ins} = \frac{12 \pi D \ell k_{ins} (T_t - T_p)}{X} \qquad (1)$$

Since the vehicle skin temperature varies during the lunar cycle, it is generally necessary to compute the heat flux for small time increments and then sum up these heat fluxes to approximate the net total heat flux through the insulation for the entire storage period. In this analysis however,



FORM 608-B (LEDGER) REV. 1-58

for simplification, a mean effective vehicle skin temperature representative of the complete lunar cycle was determined for use in Equation 1 to estimate the heat flux conducted through the insulation for the entire storage period.

For determination of the approximate vehicle skin temperature as a function of the solar radiation incidence angle (designated time angle, $\tau$), the tank insulation was initially assumed to be 100 percent effective. This assumption is justified by the fact that the amount of heat transferred through the insulation is much smaller than the total amount impinging upon the insulation outer surface. In determining the vehicle skin temperature necessary for the heat emitted from the vehicle skin to balance the heat absorbed, a heat balance on the vehicle skin was performed:

$$\text{Emitted Heat} = \text{Direct Solar Heat} + \text{Albedo Heat} + \text{Infrared Heat} \qquad (2)$$

The actual form of this equation is presented as Equation 19 in the analysis appended to this section. The resulting vehicle skin temperature during the lunar daylight period is of the form

$$T_{td} = 100\ (153 \cos \tau + 1220 \sin \tau)^{0.25} \qquad 0 < \tau < \pi \qquad (3)$$

(See Equation 20)

During the lunar night period (interval of darkness between sunset and sunrise), the skin temperature of the vehicle is considered to be constant;

$$T_{tn} = 185 \text{ degrees R} \qquad \pi \leq \tau \leq 2\pi \qquad (4)$$

(See Equation 21)

A graphical representation of the two equations above for the entire lunar cycle based on cylindrical storage tanks (with $\alpha_{st}/\epsilon_t = 0.186$) located on the lunar surface at the equator is presented in Figure 19. A vehicle skin mean temperature of 359 R was determined for the complete cycle as indicated by the dashed line.

A graphical representation of the lunar surface temperature as a function of its location with respect to the Sun in terms of $\tau$ for the complete lunar cycle is presented in Figure 20. During the lunar night period, the lunar surface temperature is assumed to be constant at 220 R. The surface mean temperature for the complete cycle was calculated to be 412 R and is represented by the dashed line.



FORM 608 B (LEDGER) REV. 1-58

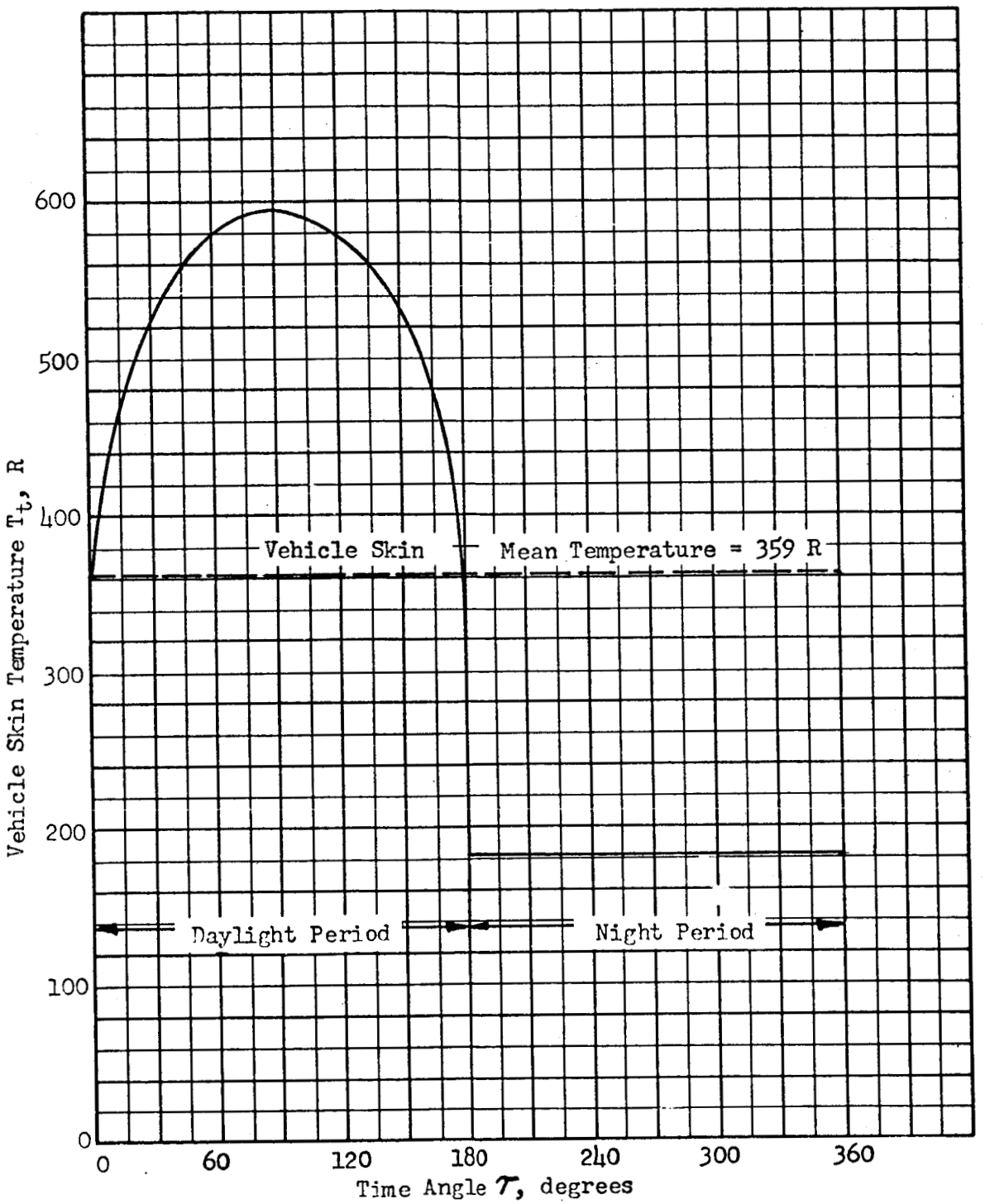


Figure 19. Variation of Vehicle Skin Temperature with Time Angle for One Complete Lunar Cycle (27.3 Earth Days).

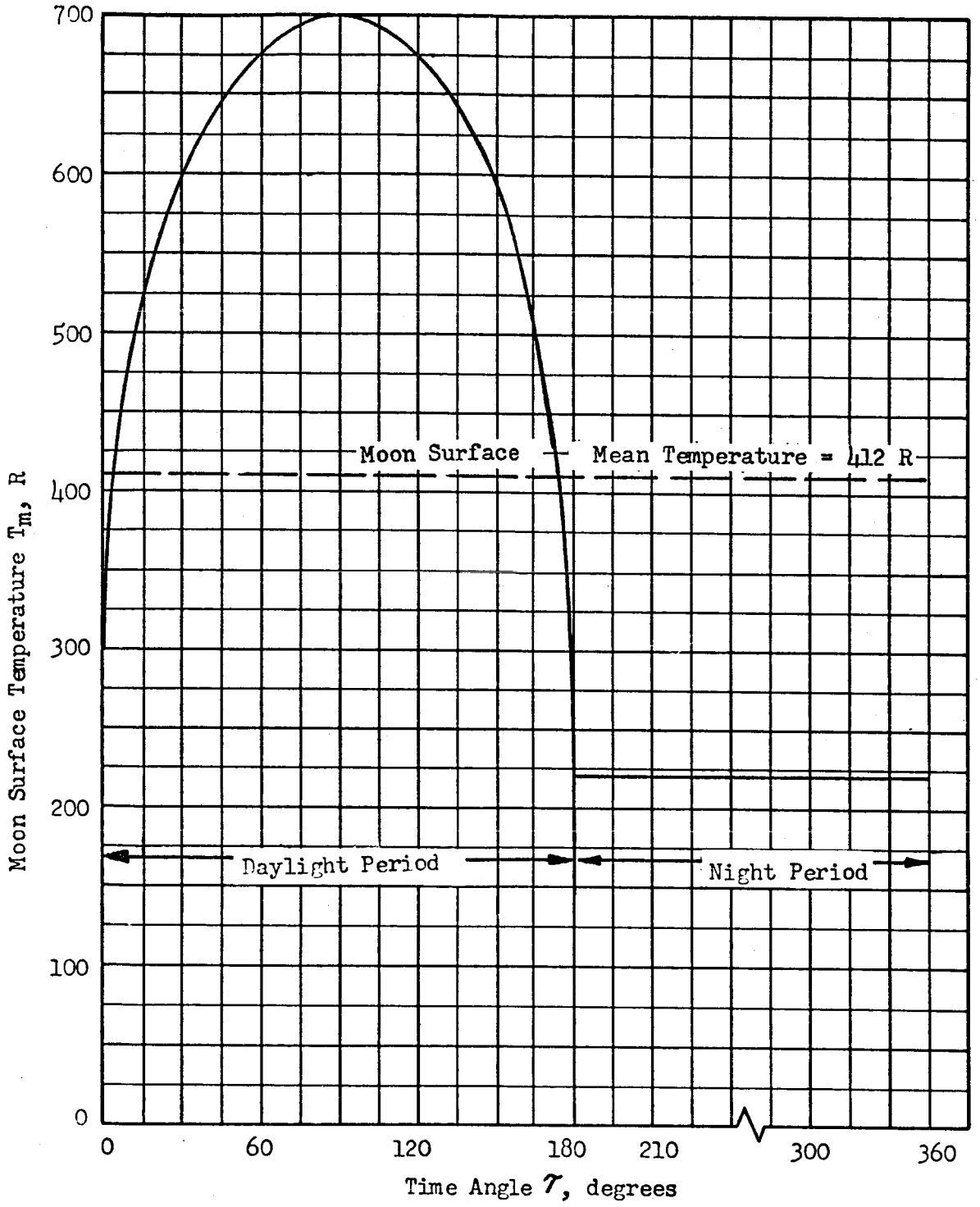


Figure 20 . Variation of Moon Surface Temperature with Time Angle for One Complete Lunar Cycle (27.3 Earth Days)

Insulation. The storability characteristics of a given propellant are greatly influenced by the type of insulation chosen to cover the tanks. In this investigation, Linde SI-4 insulation (layers of thin metal foils - requiring vacuum between layers) with an extremely low mean thermal conductivity of 0.000025 Btu/hr-ft-R (160-530 R temperature range) and a density of 4.7 lb/ft$^3$ is assumed to cover the longitudinal section of the tanks.

Tank Skin Coating. The rate of heat absorption by a surface in space subjected to solar radiation is strongly dependent upon the solar absorptivity and emissivity of the surface. The surface properties should have a minimum absorptivity to emissivity ratio ($\alpha_{st}/\epsilon_t$) to reflect the majority of incoming solar ratiation and emit the greatest amount of infrared radiation. Some control of these properties is possible through the use of coatings (paints, oxides, etc.). For the vehicle considered, a white paint coating with an $\alpha_{st}/\epsilon_t$ of 0.186 was assumed.

Heat Conducted Through Structural Supports. The heat transferred through structural supports between the propellant tanks and adjacent components (other propellant tank, payload, or engine system) is of considerable importance in estimating the net total heat input to the propellants. For a given support,

$$Q_{sup} = \frac{k_{sup} A_{sup} (T_{ac} - T_p)}{\Delta x_{sup}} \tag{5}$$

It was assumed that the cross-sectional area of tank supports would equal the cross-sectional area of a single bar required to support the necessary weight in tension during the maximum acceleration of the vehicle (assumed at 8 g in the boost from Earth). The structural support lengths assumed are D/2 for the supports between the two propellant tanks, and D/4 for the supports between the payload and the oxidizer tank, and between the engines system and the fuel tank.

The strength and thermal conductivity of the structural supports were determined assuming the use of 304 stainless steel. The ultimate tensile strength of 150,000 psi was reduced to a working allowable tensile stress of 100,000 psi. The thermal conductivities of the supports were taken from Reference 34 at the mean temperature between the propellant and the adjacent component in consideration.

Intravehicle Radiation. Another unavoidable heat flux to the propellants is intravehicle radiation which may be approximated by the difference between the fourth powers of the absolute temperatures of the propellant and the adjacent component. This radiative heat transfer can be greatly reduced by



FORM 608 B (LEDGER) REV. 1 58

inserting parallel, thermally isolated reflective shields between components as shown in the sketch below.

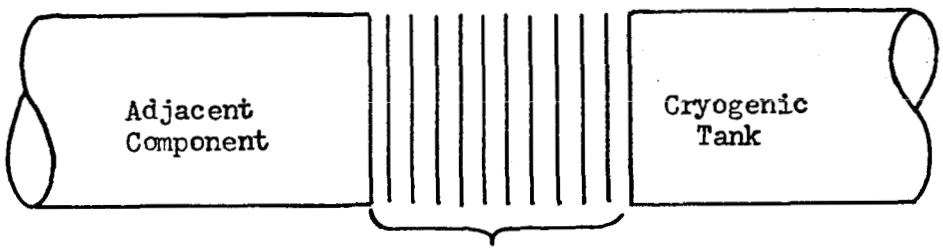


Reflective Shields

Thus, from Reference 35,

$$Q_{iv\text{-}rad} = \frac{\pi D^2 \sigma \left(T_{ac}^4 - T_p^4\right)}{4\left(\frac{2}{\epsilon_{rs}} - 1\right)(N + 1)} \tag{6}$$

In this analysis, intravehicle radiation shielding of the propellants was provided (between tanks, between oxidizer tank and payload, and between fuel tank and engines system) by 10 thin aluminum foils with an emissivity of 0.04. This shielding scheme weighs approximately 50 pounds total (30 shields) considering the supporting members and an aluminum foil thickness of 0.005 inches. Being such a relatively insignificant amount, this shielding was not included in storage penalty weight calculations.

Net Total Heat Input To Propellant. The net total heat input to the cryogenic liquid determines the time period (storage time, t) the propellant can be stored on the moon without excessive pressure and temperature rise:

$$Q_{net} = Q_{ins} + Q_{sup} + Q_{iv\text{-}rad} \tag{7}$$

and

$$Q_{net} = \frac{W_p C_p (T_{pf} - T_{pi})}{t} \tag{8}$$

In calculating the net total heat input to the propellants (Equation 8), the propellant specific heat ($C_p$) was determined at the mean temperature for the range between the initial and final fluid temperature.



FORM 608 B (LEDGER) REV. 1 58

Vehicle Weight Analysis. For the determination of vehicle weight penalties (insulation and increased tank weight), both the fuel and the oxidizer are assumed initially (lunar surface zero storage time) at a vapor pressure of 25 psia; this allows a 10.3 psi pressure rise enroute to the moon (propellant assumed tanked at its normal boiling point and one atmosphere of pressure). Along with having equal initial pressures, the fuel and its oxidizer are assumed (for insulation thickness calculations) to have equal pressure rises during the lunar storage period. For the purpose of determining necessary tank weights, the maximum allowable tank pressure (occurs at end of storage period) is the sum of the allowable propellant vapor pressure ($25 + \Delta p$, psia) and the required NPSH (20 psi).

The optimum (maximum payload) storage system is achieved by minimizing the combined weights of insulation and increased tankage. In this investigation, the total tank weights are determined from propellant weight-dependent tank-weight factors and ullage requirements developed for various cryogenic propellants.

Storage-penalty weights used as the criterion for relative storability consist of insulation and extra tank weight necessary to contain the increased pressure of the propellant due to the external heat addition. The defining equations are

$$W_{ins} = \pi DL \times d_{ins} \tag{9}$$

and

$$W_{TE} = W_p \left[ K_{Tf} (1 + U_f) - K_{Ti} (1 + U_i) \right] \tag{10}$$

The expression for the storage penalty weight is

$$W_{pen} = W_{ins} + W_{TE} \tag{11}$$

Because of the rather complex relations between propellant temperature (hence, propellant pressure and tank weight) and vehicle skin temperature (the propellant temperature is a function of the instantaneous tank skin temperature), a simplifying method of attack is employed in the analysis presented herein. A storage time is first determined to allow a specified $\Delta p$ in the fuel tank for a specified fuel tank insulation thickness. Enough insulation is then assumed to be added to the oxidizer tank so that the same $\Delta p$ as in the fuel tank exists at the end of the determined storage period.

Storage times corresponding to various fuel tank insulation thicknesses are presented for a range of $\Delta p$'s for both the $O_2/H_2$ and $F_2/H_2$ propellant combinations in Figures 21 and 22. The oxidizer tank insulation thicknesses sized to allow a specified $\Delta p$, are presented versus storage time in Figures

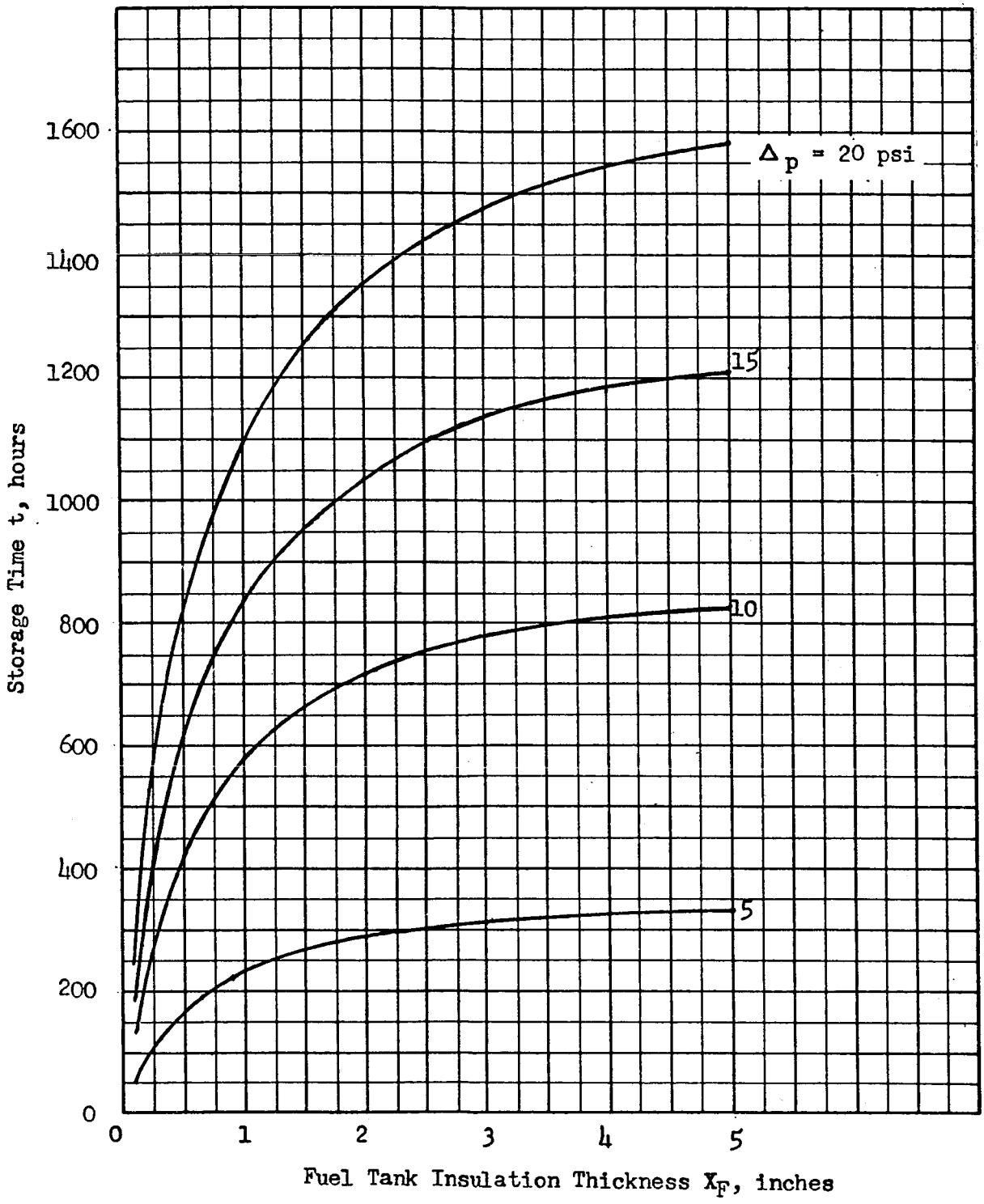


Figure 21 $O_2/H_2$ - Fuel Tank Insulation Thickness versus Storage Time for a 20-psi Range of Allowable Propellant Pressure Rises.



FORM 608 B (LEDGER) REV. 1-58

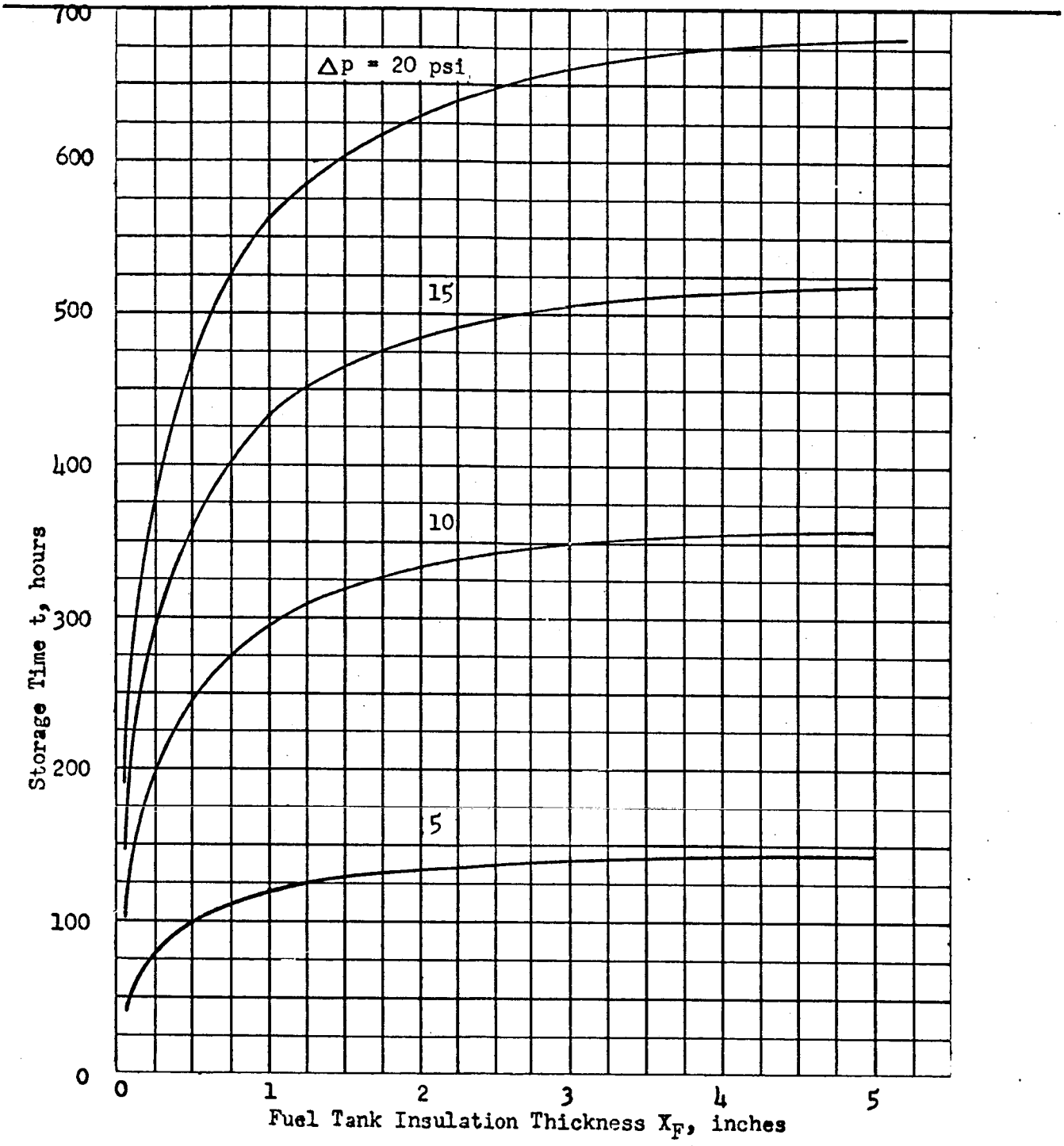


Figure 22 $F_2/H_2$ - Storage Time vs. Fuel Tank Insulation Thickness for a 20-psi range of allowable propellant pressure rises.



FORM 608-B (LEDGER) REV. 1-58

23 and 24. (The minute insulation thicknesses obtained are impractical; however, the results are presented to illustrate the effects of storage time and $\Delta p$.)

The resultant heat inputs to the fuel and its oxidizer are presented versus storage time in Figures 25, 26, 27, and 28 for an arbitrarily selected $\Delta p$ of 10 psi. As would generally be expected, for small insulation thicknesses (thus, short storage times), the majority of the heat input to the propellants is seen to be from external sources (conducted through the insulation).

Vehicle Weight Storage Penalty; Example. Considering the $O_2/H_2$ propellant combination with an assumed $\Delta p$ of 10 psi and having a fuel tank insulation thickness of 2 inches, from Figure 21, the allowable storage time is 720 hours (or 30 Earth days). From Figure 23, the corresponding necessary (for minimum storage penalty weight) oxidizer tank insulation thickness is 0.013 inches ($\Delta p$ = 10 psi), and from Figure 29, the corresponding system storage penalty weight is 970 pounds. Heat inputs (external through the insulation, through structural supports, intravehicle radiation, and net total) to both the fuel ($H_2$) and its oxidizer ($O_2$) may be determined from the curves of Figures 25 and 26.

In the same manner, allowable storage times, storage penalty weights, and heat inputs can be determined for the $F_2/H_2$ propellant combination from the curves presented. If however, a desired mission time (storage time) is specified, an optimum $\Delta p$, corresponding to minimum penalty weight, can be determined from the curves of Figures 29 and 30.

## Conclusions

Storage (1 or 2 lunar cycles) of a cryogenic liquid-propellant vehicle system on the lunar surface appears feasible for a nonvented storage system using superinsulations, surface coatings, and radiation shields. The main factor, other than insulation properties, is the allowable propellant pressure rise. Storage weight penalties up to approximately 2300 pounds ($\Delta p$ = 20 psi) for a 122,000-pound gross weight (50,000-pound payload) vehicle result as shown in Figures 29 and 30.

If engine operation does not dictate the maximum $\Delta p$ for a specified storage time, a minimum penalty weight $\Delta p$ (optimum) can be selected from Figures 29 and 30. For example, assuming a desired mission time of 400 hours, the optimum $\Delta p$'s for the $O_2/H_2$ and $F_2/H_2$ propellant combinations appear to be 10 and 15 psi respectively. For $O_2/H_2$, these conditions correspond to a fuel tank insulation thickness of 0.45 inches, an oxidizer tank insulation thickness of 0.0062 inches, and a storage penalty weight of 520 pounds. For $F_2/H_2$, the fuel tank insulation thickness would be 0.75 inches, the oxidizer

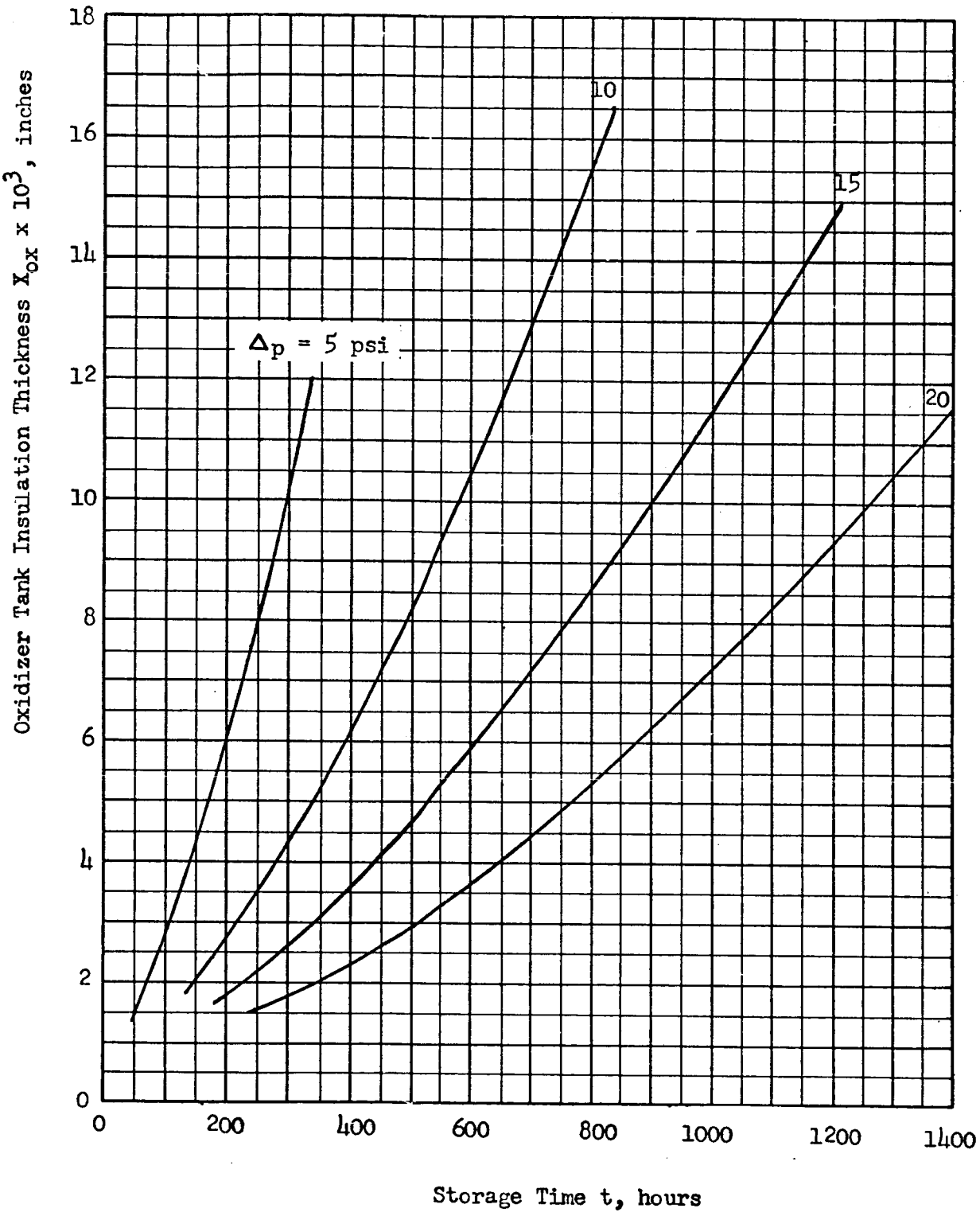


Figure 23 $O_2/H_2$ - Oxidizer Tank Insulation Thickness versus Storage Time for a 20-psi Range of Allowable Propellant Pressure Rises.



FORM 608-B (LEDGER) REV. 1-58

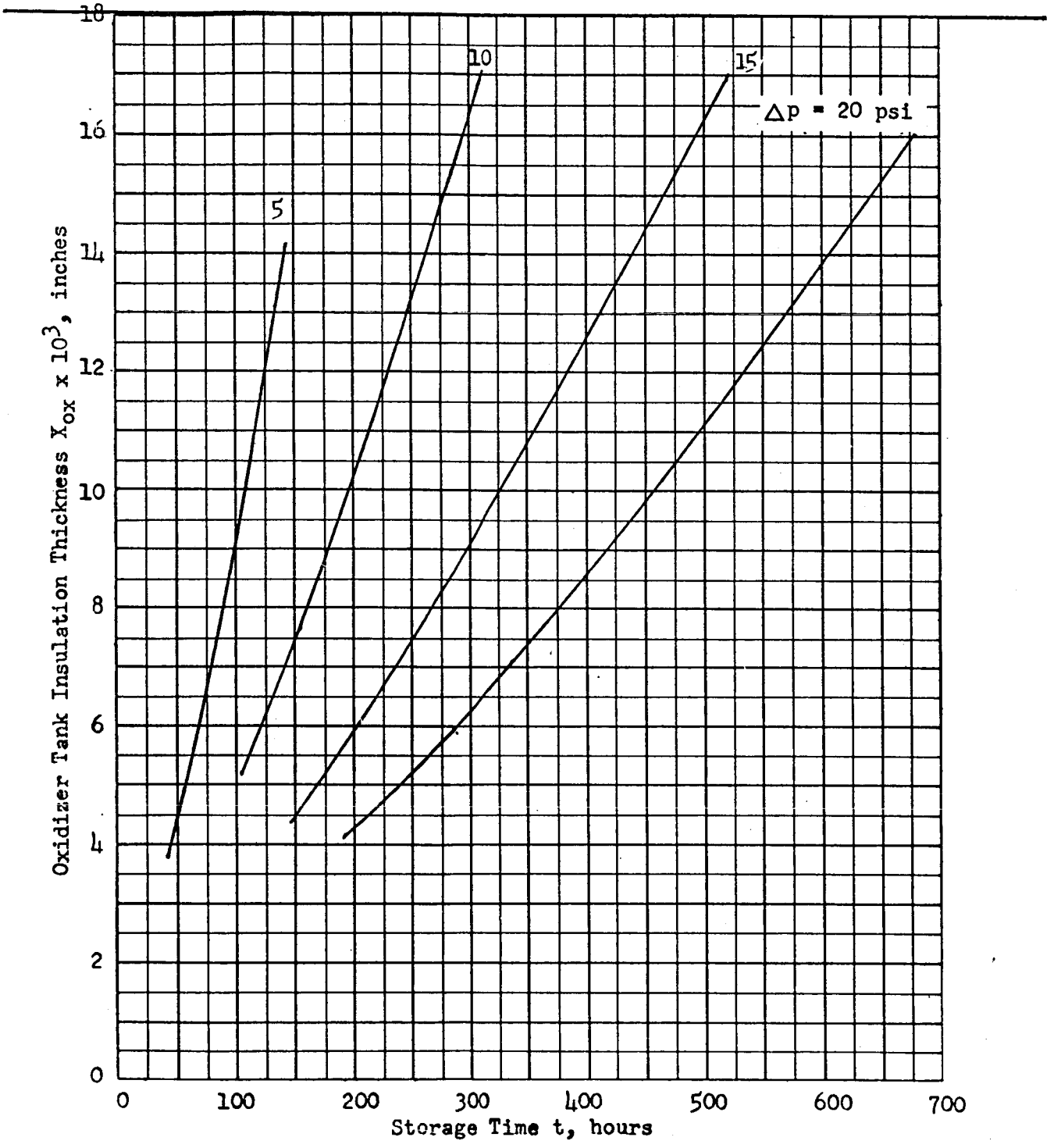


Figure 24 $F_2/H_2$ - Oxidizer Tank Insulation Thickness vs. Storage Time for a 20-psi range of allowable propellant pressure rises.



FORM 608-B (LEDGER) REV. 1 58

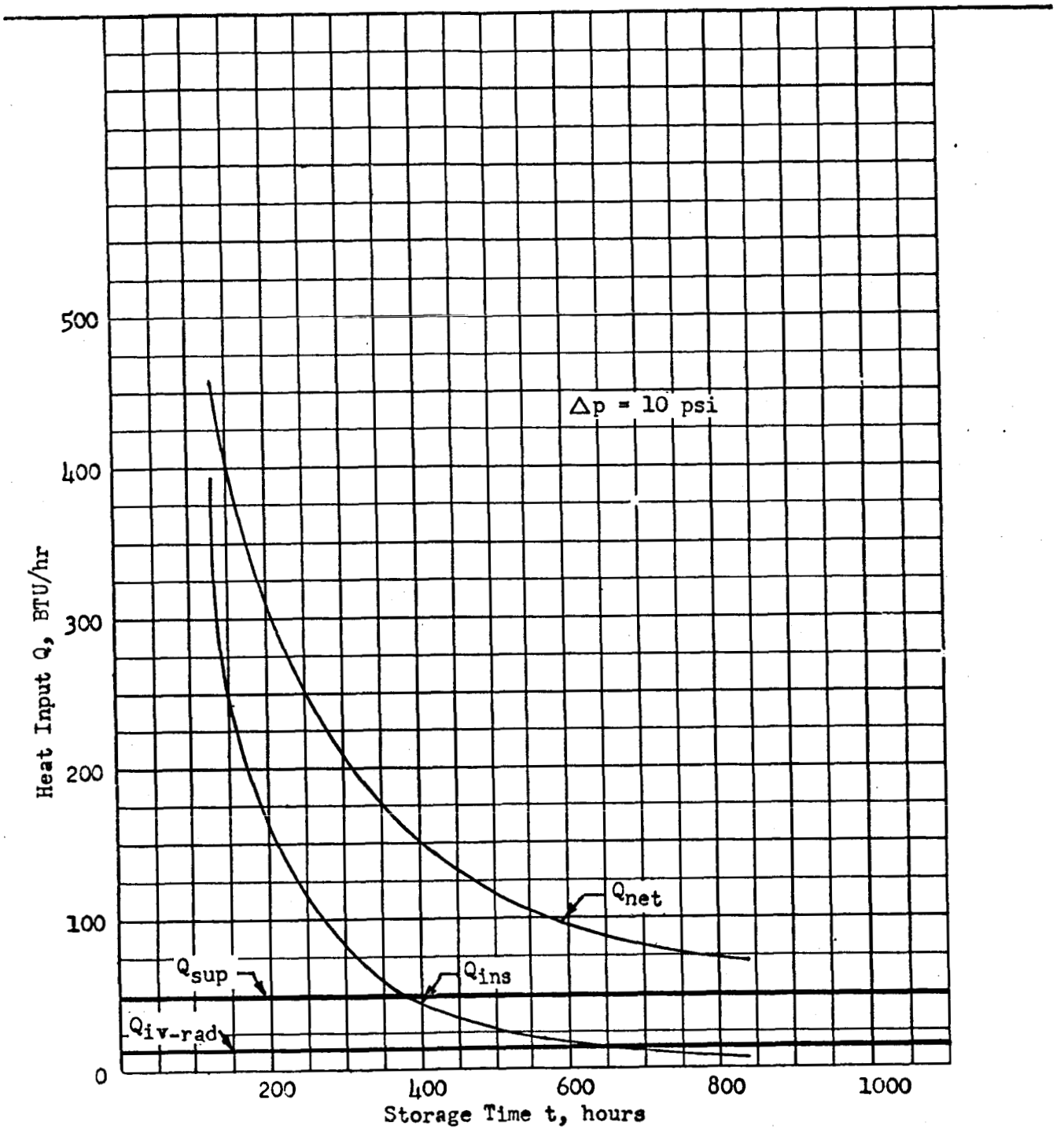


Figure 25 Heat Inputs to Fuel ($H_2$) vs. Storage Time for $O_2/H_2$ - propellant combination with $\Delta p$ = 10 psi.



FORM 608 B (LEDGER) REV. 1 58

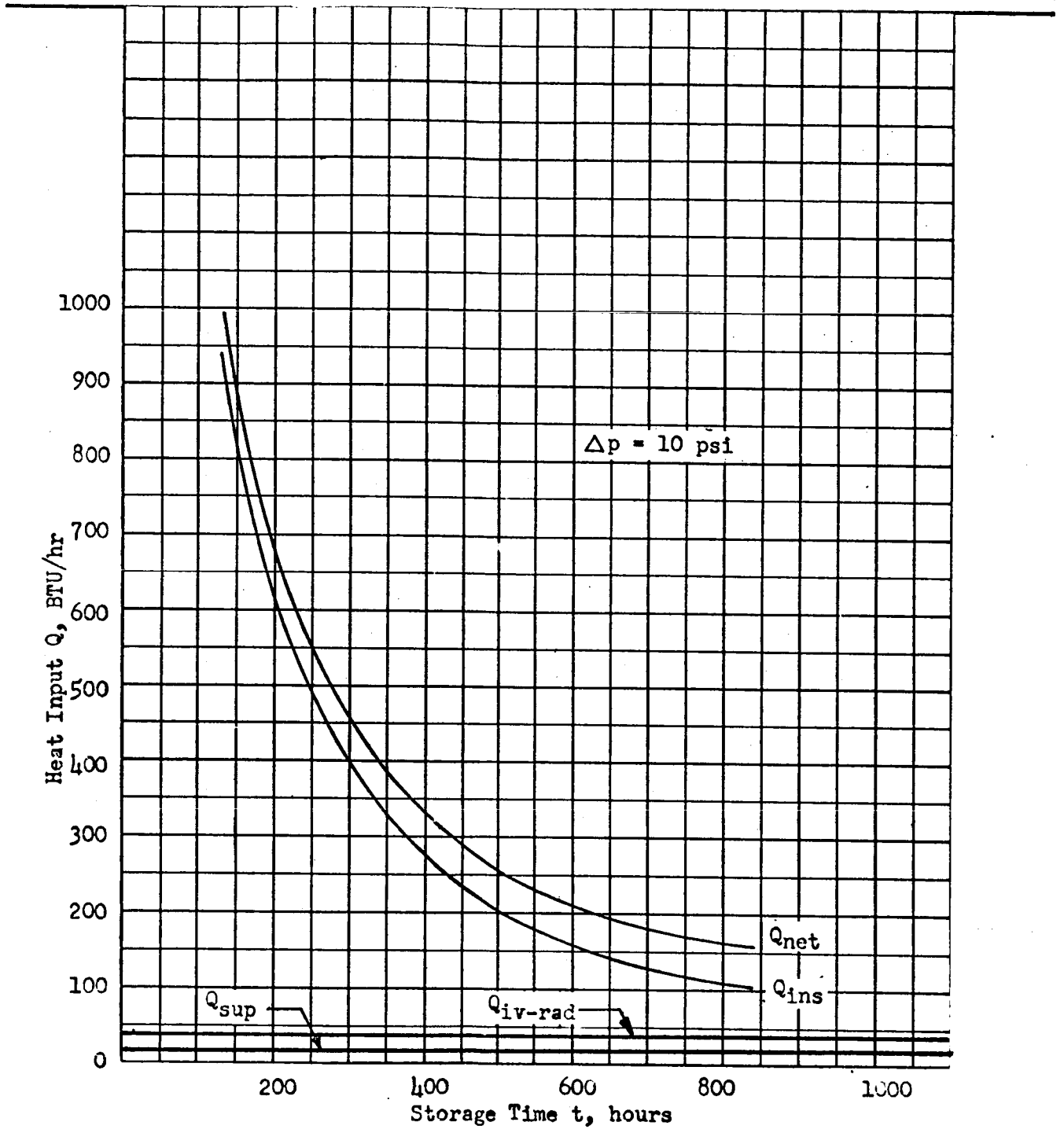


Figure 26 Heat Inputs to Oxidizer ($O_2$) vs. Storage Time for $O_2/H_2$-propellant combination with $\Delta p$ = 10 psi



FORM 608 B (LEDGER) REV. 1 58

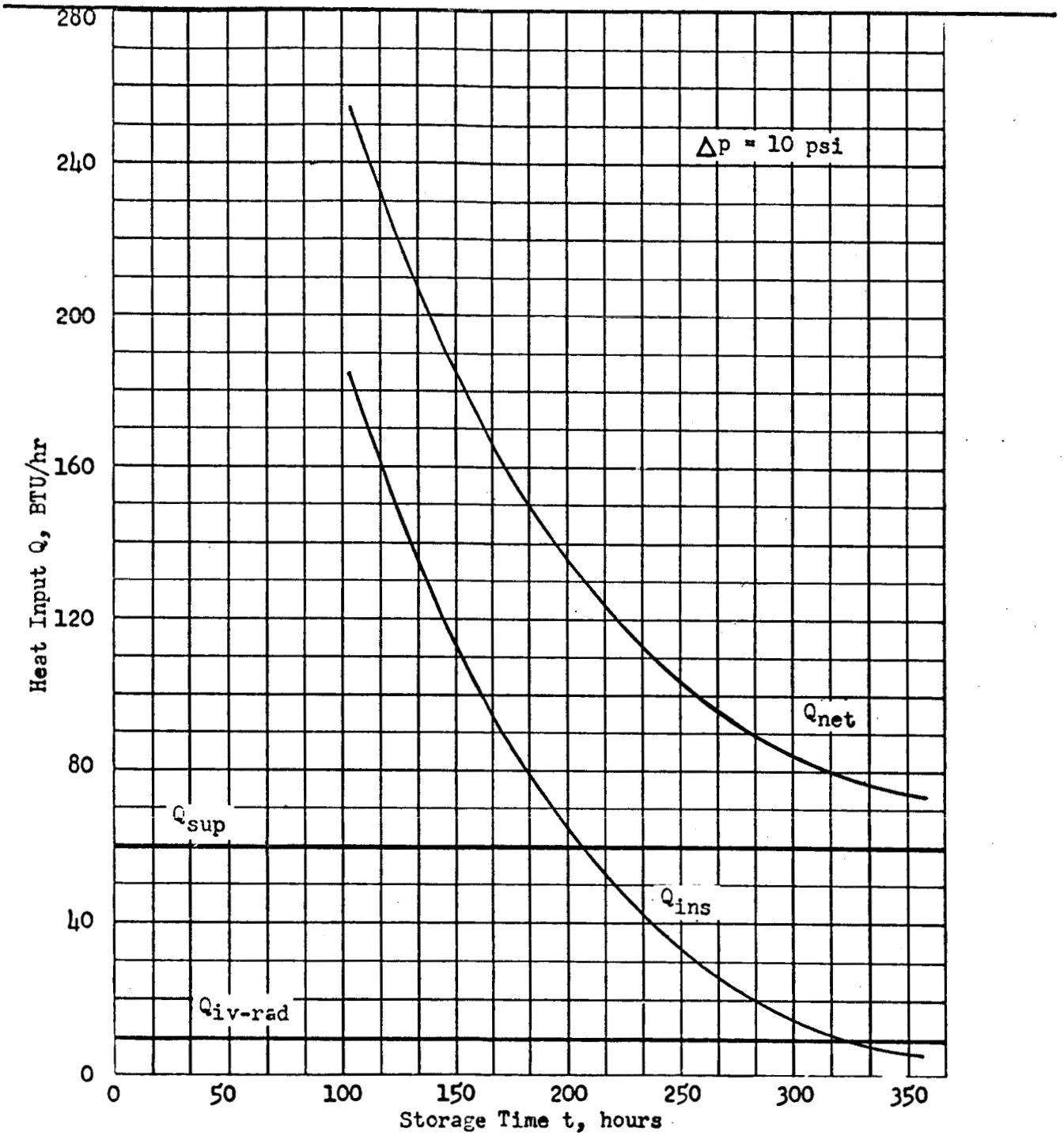


Figure 27 Heat Inputs to Fuel ($H_2$) vs. Storage Time for $F_2/H_2$ propellant combination with $\Delta p$ = 10 psi.



FORM 608 B (LEDGER) REV. 1 58

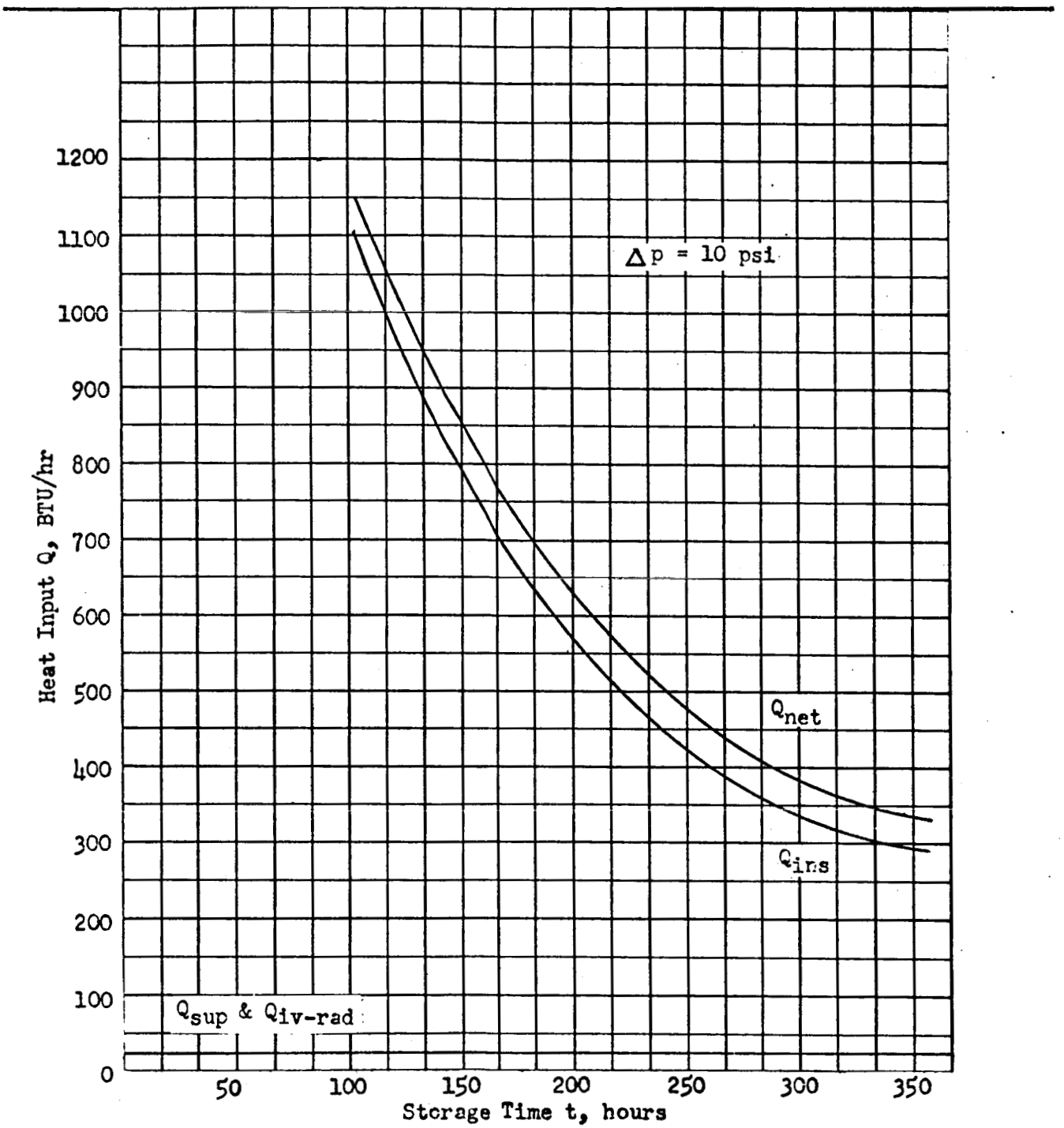


Figure 28 Heat Inputs to Oxidizer ($F_2$) versus Storage Time for $F_2/H_2$ propellant combination with $\Delta p$ = 10 psi.



FORM 608-B (LEDGER) REV. 1-58

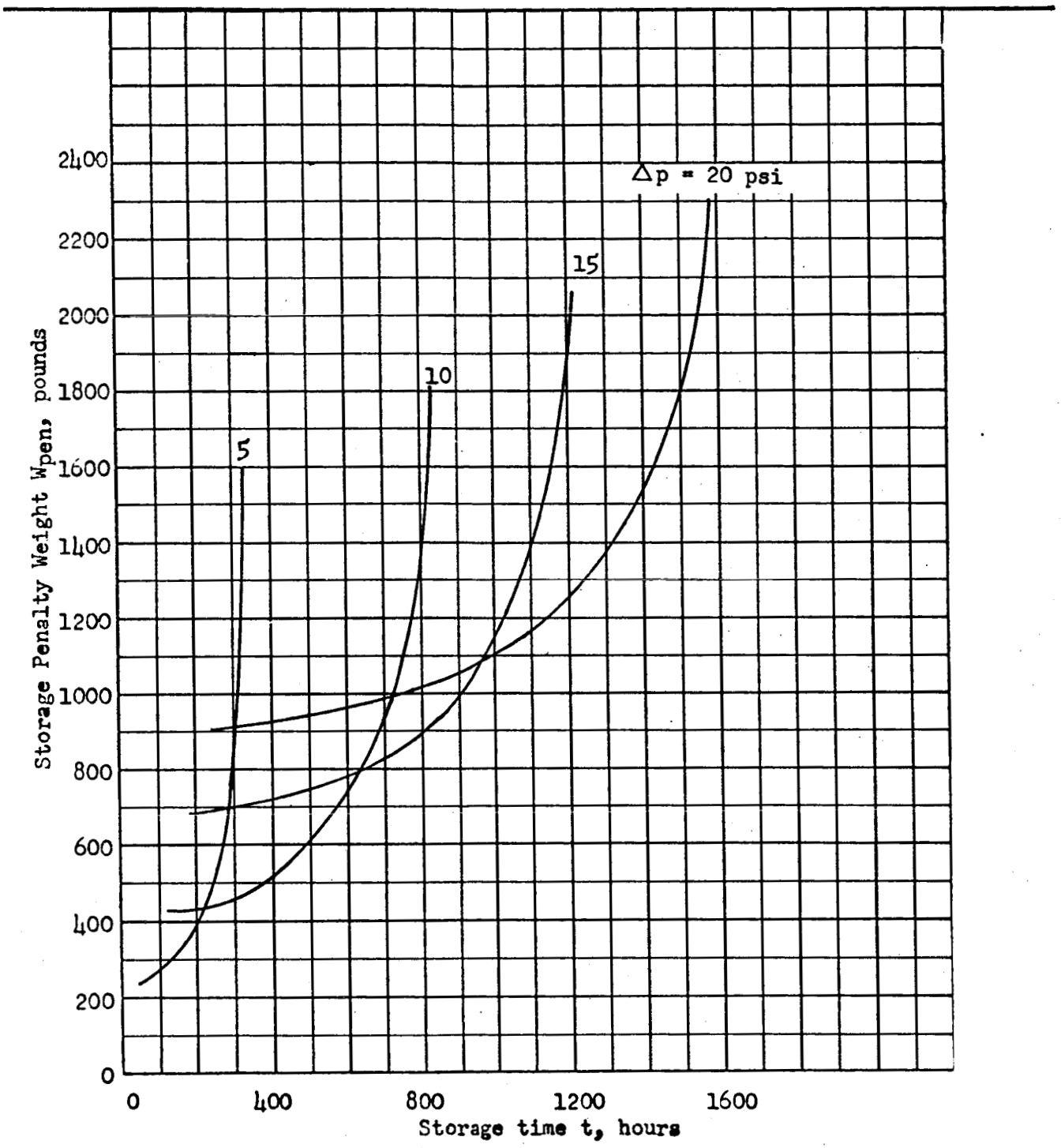


Figure 29 $O_2/H_2$ - Storage Penalty Weight vs. Storage Time for a 20-psi Range of Allowable Propellant Pressure Rises.



FORM 608-B (LEDGER) REV. 1-58

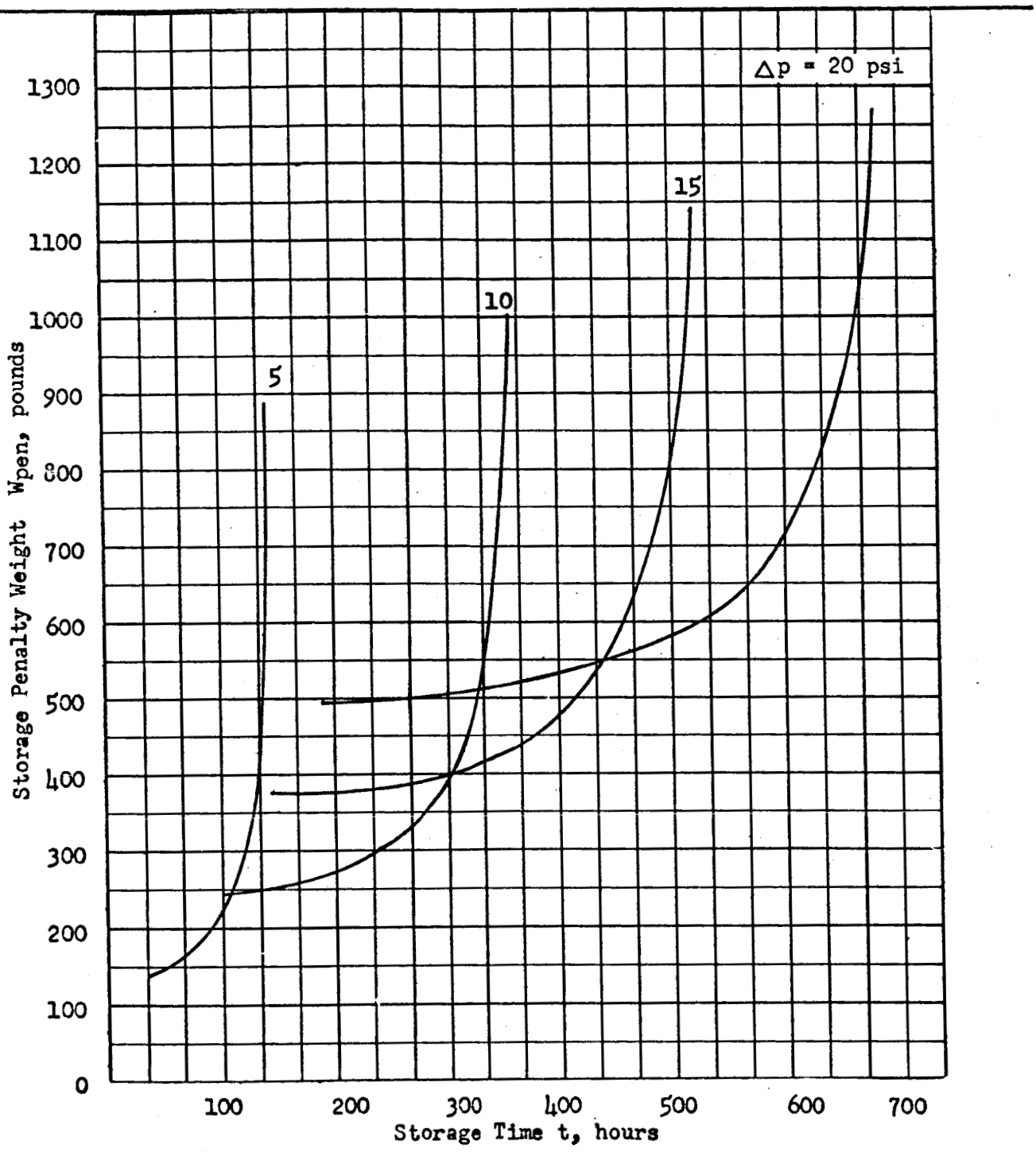


Figure 30 $F_2/H_2$ - Storage Penalty Weight vs. Storage Time for a 20-psi range of allowable propellant pressure rises.



FORM 608-B (LEDGER) REV. 1 58

tank insulation thickness 0.013 inches, and the storage penalty weight 475 pounds.

In conclusion, the $F_2/H_2$ propellant combination is more readily storable than $O_2/H_2$ (based on storage penalty weight) for the conditions assumed in this study. This is due mainly to the larger fuel tank dimensions (and therefore a greater tank insulation weight) for the $O_2/H_2$ system brought about by its lower mixture ratio.

The results presented are preliminary in nature and are intended to indicate trends of cryogenic propellant storage on the moon. Several of the basic assumptions significantly influenced the results obtained. For example, a less pessimistic assumption on the latitude location of the vehicle (assumed at the lunar equator), and some shadow shielding schemes could reduce the storage penalty weights of the cryogenic systems considerably. The heat transfer analysis is simplified; calculations are based on an average tank skin temperature; however, if instantaneous skin temperatures completely penetrate the insulation, a corresponding fluctuation in tank pressure rise would result. Storage time would then be decreased since the pressure peaks would dictate maximum allowable storage pressure instead of average pressure. Changes in assumptions of propellant pressure, vehicle design characteristics, and the lunar mission would also undoubtedly influence the results of the study. For different vehicle design concepts, tank weight factors may differ from those used in this analysis. Also, insulation may be required for local components (propellant lines, valves, etc.); however, compared to tank insulation, its weight should be negligible. The minute oxidizer tank insulation thickness obtained caused by small tank surface area-to-oxidizer weight ratio induced by high densities are obviously impractical. To employ a practical insulation thickness (e.g., 0.25-inch), a small (less than 35 pounds) weight increase would result.

The results indicate that the storage penalty weights range up to 2 percent of vehicle gross weight (or approximately 4.6 percent of payload weight), thus, the effect of lunar storage for 1 or 2 cycles (up to approximately 60 days) appears significant but does not prohibit use of high energy cryogenic liquid propellants or negate their performance advantage.



FORM 608 B (LEDGER) REV. 1 58

## SYMBOLS FOR THERMAL STORAGE ANALYSIS

$A_{sup}$ = cross sectional area of structural support members, square feet

$A_t$ = tank surface area, square feet

$A_m$ = moon surface area, square feet

Cp = propellant specific heat @ constant pressure, BTU/LB - Rankine

$d_{ins}$ = insulation density, $lbs/ft^3$

D = propellant tank diameter, feet

F = view factor

k = thermal conductivity, BTU/hr-ft-Rankine

K = tank weight factor

$\ell$ = length of longitudinal section of propellant tank, feet

L = total length of propellant tank, feet

N = number of reflective shields

NPSH = propellant pump net positive suction head, psi

$\Delta p$ = allowable propellant pressure rise, psi

Q = heat input, BTU/HR

S = solar intensity, 444 $BTU/HR\text{-}FT^2$

t = storage time, hours

T = temperature, Rankine

U = propellant tank ullage, percent

W = weight, pounds

$\Delta x$ = length of structural support members, feet

X = insulation thickness, inches



FORM 608-B (LEDGER) REV. 1-58

$\rho_m$ = lunar albedo (0.07)

$\tau$ = Sun rays angle or time angle, degrees

$\alpha$ = absorptivity

$\epsilon$ = emissivity

$\sigma$ = Stefan-Boltzmann's natural constant = $0.1714 \times 10^{-8}$ BTU/HR-FT$^2$ - R$^4$

Subscripts

ac = adjacent component

f = final

F = fuel

i = initial

ins = insulation

iv-rad = intravehicle radiation

m = moon

md = moon-daylight period

mm = moon-mean

mn = moon-night period

mt = moon to tank

net = net total

ox = oxidizer

p = propellant

pen = penalty

pf = propellant-final

pi = propellant-initial



FORM 608 B (LEDGER) REV. 1 58

rs = reflective shield

sm = sun to moon

st = sun to tank

sup = structural supports

t = vehicle skin

td = vehicle skin-daylight period

tm = vehicle skin-mean

tn = vehicle skin-night period

TE = tank-extra

$T_f$ = tank-final

$T_i$ = tank-initial



FORM 608 B (LEDGER) REV. 1-58

## VIEW FACTORS

The view factor from $A_1$ to $A_2$, written $F_{12}$ is defined as the fraction of the total radiant heat flux leaving $A_1$ that is incident upon $A_2$.

Sun to Moon

The ratio of the radiant flux leaving the Sun that is incident on the moon's surface to the total flux leaving the Sun can be expressed as

$$F_{sm} = \sin \tau \tag{12}$$

for an equatorial location (Reference 36)

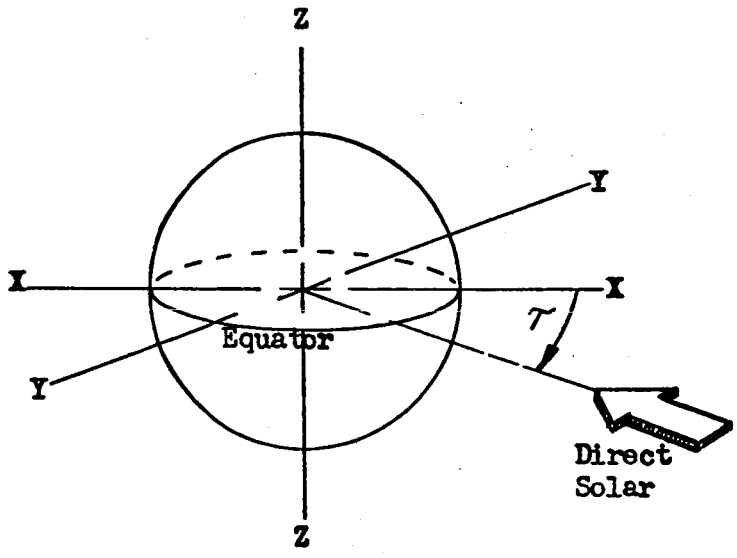


Sun to Tank

With axially aligned cylindrical propellant tanks, the solar view factor varies as the Sun passes overhead (projected tank surface areas exposed to the Sun's rays are altered).

$$F_{st} = \frac{\text{Projected longitudinal surface area}}{\text{Total longitudinal surface area}}$$

$$= \frac{D\ell|\cos\tau|}{\pi D\ell} = \frac{|\cos\tau|}{\pi} \tag{13}$$

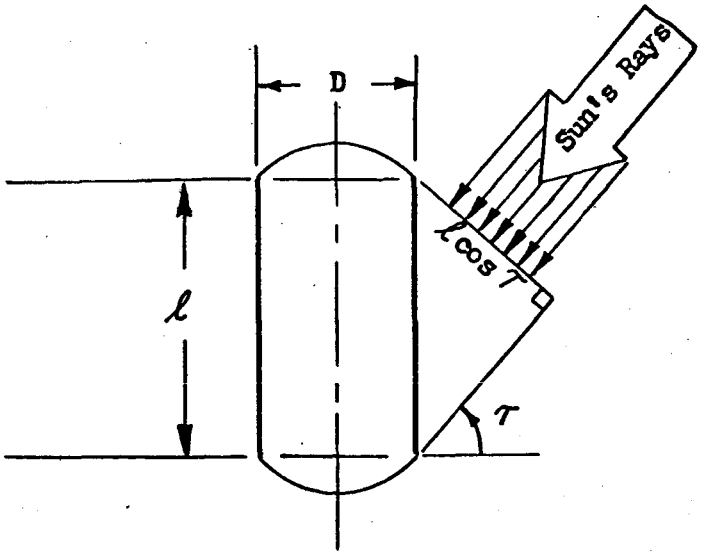


Moon to Tank

The moon to tanks view factor is considered at all times to be (Reference 36),

$$F_{mt} = 0.5 \tag{14}$$

## MOON SURFACE AND VEHICLE SKIN TEMPERATURE ANALYSIS

### MOON SURFACE TEMPERATURE

The lunar surface temperature is dependent upon the rate at which solar energy is absorbed and reradiated by the moon.

Assuming the moon to be perfectly insulated, and writing a heat balance for any time during the daylight period:

$$SF_{sm}\,\alpha_{sm}\,A_m - \sigma T_m^4\,\epsilon_m\,A_m = 0 \tag{15}$$

where $F_{sm} = \sin\tau$

Therefore, the surface temperature of the moon during the daylight period can be expressed as

$$T_{md} = \left[\frac{S}{\sigma}\,\frac{\alpha_{sm}}{\epsilon_m}\,\sin\tau\right]^{0.25} \qquad 0<\tau<\pi \tag{16}$$

During the lunar night period, the surface temperature of the moon is assumed to be constant:

$$T_{mn} = 220\ R \qquad \pi\leq\tau\leq 2\pi \tag{17}$$

For one complete lunar cycle, the mean (average) lunar surface temperature can be expressed as

$$T_{mm} = \frac{\int_0^{\pi} T_{md}\, d\tau + \pi T_{mn}}{2\pi} \tag{18}$$

VEHICLE SKIN TEMPERATURE

The skin temperature of insulation surrounding propellant storage tanks located on the lunar surface depends upon the rates at which the external radiant heat sources (direct solar, albedo, and infrared) are absorbed and reradiated by the surface.

Assuming that the heat transferred from the surface through the insulation to the propellant is only a small portion of the total amount of heat impinging upon the tank from external sources, a heat balance on the surface of the insulation can be written as

$$\text{Emitted Heat} = \text{Direct Solar Heat} + \text{Albedo Heat} + \text{Infrared Heat} \tag{2}$$

$$\sigma T_t^4 \epsilon_t A_t = SF_{st}\alpha_{st} A_t + SF_{sm}\rho_m F_{mt}\alpha_{st} A_t + \sigma T_m^4 \epsilon_m F_{mt}\alpha_{mt} A_t \tag{19}$$

where the view factors,

$$F_{st} = \frac{|\cos\tau|}{\pi},\ F_{sm} = \sin\tau,\ \text{and}\ F_{mt} = 0.5,$$

and the surface temperature of the moon ($T_m$) is given by Equation 16 for the daylight period and by Equation 17 for the night period.

After substituting and rearranging terms, the vehicle skin temperature during the lunar daylight period can be expressed as

$$T_{td} = \left[\frac{S}{\sigma}\ \frac{\alpha_{st}}{\epsilon_t}\ \frac{|\cos\tau|}{\pi} + \left(0.5\ \frac{S}{\sigma}\ \frac{\alpha_{st}}{\epsilon_t}\ \rho_m + 0.5\ \frac{S}{\sigma}\alpha_{sm}\ \frac{\alpha_{mt}}{\epsilon_t}\right)\sin\tau\right]^{0.25} \tag{20}$$

$$0 < \tau < \pi$$

By neglecting terms containing solar radiation (S) in Equation 19, the skin temperature of the vehicle during the lunar night period can be expressed as

$$T_{tn} = \left[T_{mn}^4\ \epsilon_m\ F_{mt}\right]^{0.25} \qquad \pi \le \tau \le 2\pi \tag{21}$$



FORM 608-B (LEDGER) REV. 1-58

where $T_{mn}$ = 220 R

The mean (average) vehicle skin temperature for one complete lunar cycle can be expressed as

$$T_{tm} = \frac{\int_c^{\pi} T_{td}\, d\tau + \pi T_{tn}}{2\pi} \tag{22}$$

The following assumptions contributed to the results obtained in this analysis: $\frac{\alpha_{mt}}{\epsilon_t} = 1.00$, $\alpha_{sm} = 0.93$, and $\epsilon_m = 1.00$.



FORM 608-B (LEDGER) REV. 1-58

## REFERENCES

1. Bobrovnikoff, N. T., Natural Environment of the Moon WADC Technical Note 847-3, Ohio State Univ. Research Foundation, AD 242177, June 1959

2. Salisbury, John W. and Charles F. Campen, Jr. Location of a Lunar Base, GRD Research Notes No. 70, Oct. 1961

3. Fielder, G., Structure of the Moon's Surface, Pergamon Press, 1961

4. Lang, H. A., Lunar Instrument Carrier - Landing Factors, Rand Corporation, RM-1725 AD 112403, 4 June 1956

5. Broner, M. A. and G. A. Lander, Jr., How Bad is the Moon Environment, Space/Aeronautics, Vol. 37 No. 4, April 1962

6. Moore, Patrick, "The Lunar Objective" Spaceflight, Vol. II No. 7, July 1960

7. Stewart, Peter A. E., "Surface Exploration of the Moon", Spaceflight, Vol. III No. 2, March 1961

8. Buwalda, P., The Lunar Environment, Jet Propulsion Laboratory, Technical Release No. 34-159, 28 Oct. 1960

9. Green, Jack, The Geology of the Lunar Base, SID 61-358 North American Aviation, Inc.

10. Hibbs, A. R., Exploration of the Moon, the Planets and Interplanetary Space, Report 30-1, Jet Propulsion Laboratory, 30 April 1959

11. Shaw, J. H., Natural Environment of the Planet Mars, WADC Phase Technical Note 847-1, Ohio State University Research Foundation, AD 242175, Feb 1959

12. Kiess, Carl C., and K. Lassovzsky The Known Physical Characteristics of the Moon and the Planets, ARDC TR-58-41, ASTIA Dec. No. AD 115-617

13. Briggs, Michael H.,"The Chemistry of Mars - II The Surface", Journal of the British Interplanetary Society, Vol. 17 No. 12, Nov., Dec. 1960

14. Arthur, Gilbert F., Physical and Positional Properties of the Planets, WADC Technical Note 58-347, ASTIA No. AD 206671

15. Shaw, J. H. and N. T. Bobrovnikoff, Natural Environment of the Planet Venus, WADC, Phase Technical Note 847-Z, Ohio State Univ. Research Foundation, AD 242176



FORM 608-B (LEDGER) REV. 1-58

16. Minitz, Yale, "Temperature and Circulation of the Venus Atmosphere", Planetary and Space Science, Vol. 5 No. 2 page 141-152

17. Kaplan, Lewis D. "A New Interpretation of the Structure and $CO_2$ Content of the Venus Atmosphere", Planetary and Space Science, Vol. 8 No. 1

18. Starr, S. V., The Atmosphere of Venus, Aero Dec. Mixc-004, General Dynamics/Convair, 12/5/61

19. Sagan, C., "The Planet Venus, Science, Vol. 133, page 849-858, 24 March 1961

20. Jones, C. D., et al, Preliminary Investigation of Interplanetary Lunar and Near Planet Environments and Methods of Simulation, ASD Technical Report 61-267, AD 268719, July 1961

21. PIBD-3C1, Space Facts Handbook, General Electric Co., 1960

22. Pocket Data for Rocket Designers - Bell Aircraft Corporation

23. Interaction of Highly Underexpanded Jets with Simulated Lunar Surfaces, NASA TND-1095, December 1961

24. R3923 Space Transfer Phase Propulsion System Study, Final Report, Rocketdyne, A Division of North American Aviation, Inc., Canoga Park, California, February 1963

25. A Survey and Evaluation of High Energy Liquid Chemical Propellant Systems, Stanford Research Institute SRI Project No. PRV-3652, Quarterly Report No. 4, April 4, 1962 and Quarterly Report No. 5, June 2, 1962

26. Development and Evaluation of Storable High Energy Bipropellant Systems, Summary Report, Report No. R-2767, AFFTC-TR-61-19, Contract AF 33 (616)-6768, Rocketdyne, A Division of North American Aviation, Inc., Canoga Park, California, April 1961

27. Straight, David M. and Edward M. Rottenberg, Ignition of LO/LH Rocket Engines with Fluorine, NASA TM-X.101, Lewis Research Center, Cleveland, Ohio, December 1959

28. Final Report on a Study of Controllable Thrust Liquid Propellant Rocket Engines Suitable for Spacecraft, Wright Aeronautical Division of Curtiss Wright Corporation, Report No. CTR 00-253 Contract NAS 5-1156, June 15, 1962



FORM 608 B (LEDGER) REV. 1-58

29. J-2 Quarterly Progress Report, Report No. R-2600-8, Contract NAS 8-19, Rocketdyne, A Division of North American Aviation, Inc., September 1962

30. Esgar, Jack B., Survey of Energy-Absorption Devices for Soft Landing of Space Vehicles, NASA Technical Memo, TND-1308, June 1962. (This reference also includes a bibliography on landing gear systems and high performance energy absorbers.)

31. Fisher, Jr., Lloyd J., Landing Impact Dissipation Systems, NASA TND-975, December 1961

32. O'Bryan, Thomas C. and Howard G. Hatch, Jr., Limited Investigation of Crushable Structures for Acceleration Protection of Occupants of Vehicles at Low Speeds, NASA TND-158, October 1959

33. McGhee, John R., A Preliminary Experimental Investigation of an Energy Absorption Process Using Frangible Metal Tubing, NASA TND-1477

34. Powell, R. L. and W. A. Blanpied, Thermal Conductivity of Metals and Alloys at Low Temperatures, National Bureau of Standards Circular 556, 1954

35. Smolak, G. R. and R. H. Knoll, Analysis of Thermal Protection Systems for Space-Vehicle Cryogenic Propellant Tanks, NASA TR R-130, 1962

36. Dempster, W. E., R. L. Evans and J. R. Oliver, Lunar Storage of Liquid Propellants, NASA TN D-1117, 1962